"Phytochemical Conjugated Gold Nanoparticles for the Treatment of Triple Negative Breast Cancer"

A thesis submitted for the degree of

Doctor of Philosophy

To

INDIAN INSTITUTE OF TECHNOLOGY GUWAHATI

By

JYOTHSNA UNNIKRISHNAN

Department of Biosciences and Bioengineering

Indian Institute of Technology Guwahati

Guwahati, Assam-781039, India

January, 2023

Dedicated to

My family, friends and teachers

For the love, support and encouragement

DEPARTMENT OF BIOSCIEENCES AND BIOENGINEERING

INDIAN INSTITUTE OF TECHNOLOGY GUWAHATI

GUWAHATI-781039

DECLARATION

I hereby declare that the contents of the research work described in this thesis titled **"Phytochemical Conjugated Gold Nanoparticles for the Treatment of Triple Negative Breast Cancer"** is a presentation of my original research work carried out in the Department of Biosciences and Bioengineering, Indian Institute of Technology Guwahati, India, under the supervision of Dr. Priyadarshi Satpati. Sincere efforts have been made to duly acknowledge the contributions from others for their ideas, technical help, references or any other help which may be involved in the completion of this thesis work.

January, 2023

Jyothsna Unnikrishnan

Roll No. 166106108

Department of Biosciences and Bioengineering

Indian Institute of Technology Guwahati

Guwahati, Assam-781039, India

DEPARTMENT OF BIOSCIEENCES AND BIOENGINEERING

INDIAN INSTITUTE OF TECHNOLOGY GUWAHATI

GUWAHATI-781039

CERTIFICATE

This is to certify that the work described in the thesis titled **"Phytochemical Conjugated Gold Nanoparticles for the Treatment of Triple Negative Breast Cancer** "submitted by Jyothsna Unnikrishnan (166106108) to Indian Institute of Technology Guwahati, India, for the award of the degree of Doctor of Philosophy is an authentic record of the research work carried out under my supervision in the Department of Biosciences and Bioengineering, Indian Institute of Technology Guwahati, Guwahati, India.

This thesis or any part thereof has not been submitted elsewhere for award of any other degree or diploma.

January 2023

Dr. Priyadarshi Satpati

Department of Biosciences and Bioengineering

Indian Institute of Technology Guwahati

Guwahati, Assam-781039, India

Acknowledgements

I am deeply indebted to many kind hearted people without their help and support the successful completion of my PhD would be impossible. I would like to take this opportunity to acknowledge each of them.

First and foremost, I would like to express my deepest gratitude to my thesis supervisor Dr. Priyadarshi Satpati for his constant support and inspiration throughout my PhD. His persistent support helped me a lot to overcome the hurdles came across this journey. I am extremely thankful to my doctoral committee members Dr. Selvaraju Narayanasamy, Prof. S. Kanagaraj, Prof. Kannan Pakshirajan for their valuable suggestions at relevant points, which helped me to think about different perspectives to improve the quality of my work. I am grateful to the Department of Biosciences and Bioengineering, IIT Guwahati for providing facilities and Ministry of Human Resource Development (MHRD) Gov. of India for financial support. I am thankful to the present and past HOD's of the Department of Biosciences and Bioengineering, Prof. Kannan Pakshirajan, Prof. Latha Rangan and Prof. Rakhi Chaturvedi for availing me the departmental facilities. I would like to express my gratitude towards the teaching and non-teaching staffs of the department and institute; and securities for their support during the course of my PhD.

I sincerely acknowledge the enormous help and support received from my fellow colleagues and friends Dr. J Monisha, Dr. G Padmavathi, Dr. NK Roy, Dr. Devivasha, Dr. Harsha C, Dr. Kishore, Dr.Amrita, Dr. Bethsebie, Krishan, Shabnam, Sosmitha, Dr. Babitha, Rajesh, Dr. Elina, Dr. Mangala, Anjana, Aviral, Mukesh, Viswa, Badri, Sujitha, Aswini, Anushka Uzini,Dr. Amit Kumar, Dr. Abhishek, Suvankar Ghosh, their contribution was phenomenal in my personal and academic progression. I also thank the present and past JRFs and trainees of the lab.

I am obliged to most important people in my life, my family Achan, Amma, my brother, Uthara, and my husband Ajai, who always stands by my side irrespective of the situation with lot of love and care. My kids Aavani and Aadharsh requires special mention here, who struggled their childhood for my carrier and still supported me with lot of energy and enthusiasm. I would also like to thank Chaina, Kalpana and Durga for their immense help and support during my Ph.D carrier.

I would like to express my gratitude to all my friends Uma, Emlin, Gayatri, Archana, Sirisha, Rajsree, Anuradha, Suganya, Meera who always helped and supported in my PhD carrier. I would express my gratitude to all my teachers who groomed me to the person I am now. Last but not the least; I thank Almighty God for providing good health and opportunities throughout the endeavour.

JYOTHSNA UNNIKRISHNAN

Table of contents

Abstract

Off late by 2020, breast cancer (BC) has superseded lung cancer incidences globally. Being the most aggressive subtype of BC, triple-negative breast cancer (TNBC) is difficult to tackle with conventional treatment approaches. Even though side effects restrain the use of contemporary methods; still, surgery, chemotherapy and radiation remain in the mainstream. At the beginning of the 19th century, improvements in organic chemistry unveiled active compounds from plants called phytochemicals, found to have excellent therapeutic efficacy against cancer. Nevertheless, low bioavailability and hydrophobicity limit the potential of these plant-derived compounds. It is well evident that nanotechnology tools could effectively bypass these limitations. Therefore, in the current study, phytochemical conjugated gold nanoparticles (AuNp) were prepared to target TNBC cells via EPR effect passively. Phytochemicals such as ethyl ferulate (EF), ellagic acid (EA), coronarin D (CD) and epoxy azadiradione (EAZD) were used to reduce gold chloride into AuNps. Formation of EF-AuNp, EA-AuNp, CD-AuNp and EAZD-AuNp were confirmed by UV-visible spectroscopy, XRD, EDX, TEM and FT-IR spectra. Our in-vitro analysis using MTT assay, colony-formation assay, PI-FACS and live and dead assay evidenced the anti-cancer potency of these phyo-nano complexes. Conclusively, EAZD-AuNp induced superior anti-proliferative and cytotoxic effects in MDA-MB-231 cells than other nanoparticles. Hence, it is worthwhile to proceed with *the in-vivo* studies and the molecular pathway analysis of this meritorious compound which would help this drug journey to the clinic.

CHAPTER 1

Introduction and review of literature

1.1 Introduction

In the recent past, breast cancer (BC), the most common malignancy afflicting women, has surpassed lung cancer and become the highest-diagnosed cancer globally (11.7%). It is also the fifth major cause of cancer related deaths among both sexes (Sung et al., 2021). The worldwide age-adjusted rate for BC incidence is 48/100000, while in developed countries, it goes up to 70/100000. In 2020, BC accounted for 685,000 deaths among women, worldwide. Two third of these are happening in economically backward regions. Interestingly, the 5-year survival rate for BC in developed countries is much above 80%. In India, it is less than 70% and in South Africa survival rate from BC is only 50% (Wilkinson and Gathani, 2022). Fortunately, western countries have been able to lower BC-related deaths in recent times owing to proper screening programs, early diagnosis and treatment methods (Igene, 2008; Sun et al., 2017). Moreover, the majority of BC reports in advanced countries are in stage I or II. On the contrary, in India, almost 47.5% of cases are in advanced stages, where the health care system is virtually inaccessible to most of the population (Kakarala et al., 2010). Bangalore ranks the topmost position in India for BC incidences (age-adjusted incidence rate or AAR per 100,000 is (36.6%). In North-East region, Aizawl recorded the maximum number of cases (30.3%) and Kamrup Urban district 22.8% (National Cancer Registry Programme, 2009-2011) (Sharma et al., 2014). These facts lead to the lack of proper diagnostic and treatment tools in India.

On account of heterogeneity and varied etiopathology, BC can be stratified into five subtypes such as luminal A, luminal B, estrogen receptor (ER) and progesterone receptor (PR) positive, human epidermal growth factor receptor 2 (HER2) positive,

and triple-negative breast cancers (Kumar et al., 2020; Thakur and Kutty, 2019). Triple-negative BC (TNBC) is one of the most aggressive subtypes of BC and accounts for more than 15-20% of the total BC incidences (Shen et al., 2020; Vagia et al., 2020).

Majority of TNBC's exhibits basal-like phenotype, accounting for 75% of the TNBC-reported cases (Jain et al., 2020). As the name suggests, TNBC lacks surface receptors and exhibits poor clinical outcomes with high tumor relapse, poor overall patient survival, and frequent metastasis to distant organs (Thakur et al., 2021).

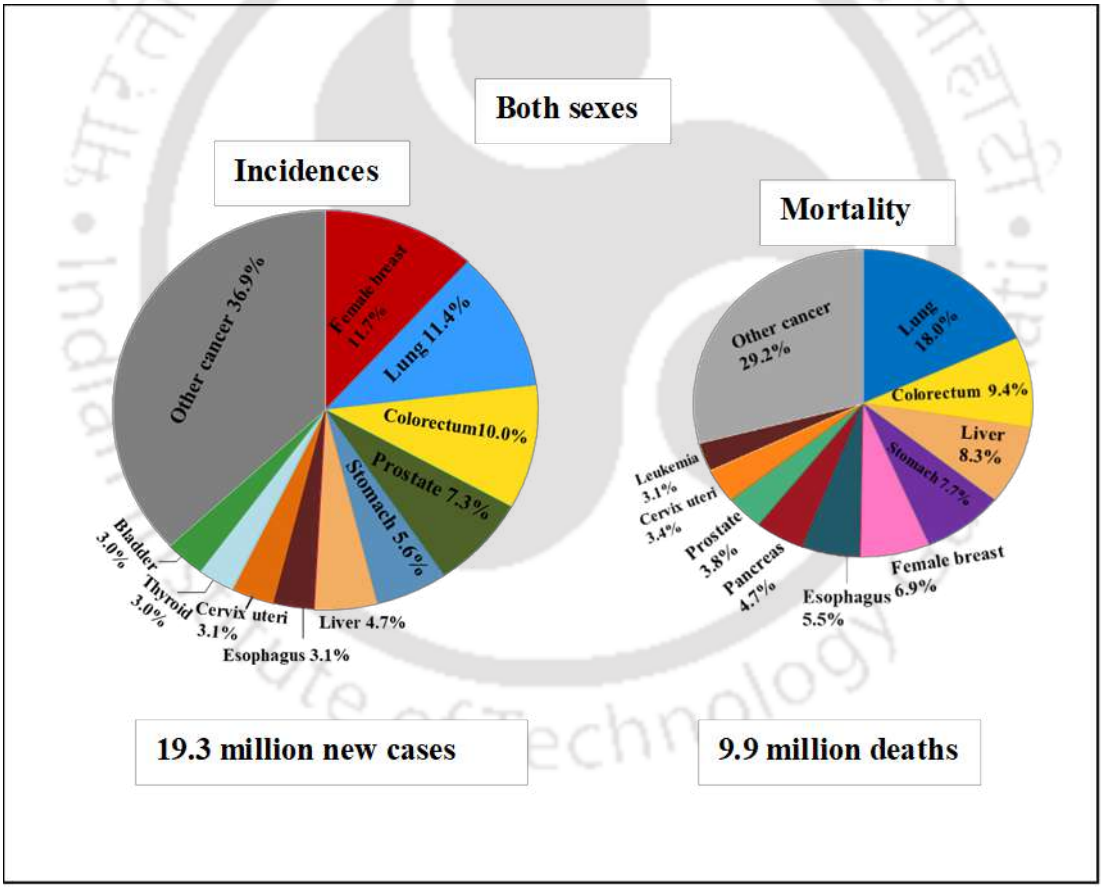

Figure 1.1 Estimated incidence and mortality of all cancers worldwide, both sexes, all ages (Source: GLOBOCAN 2020)

Additionally, its incidence is reported in premenopausal women of younger age

Due to the lack of receptors, most conventional hormonal therapies are ineffective in circumventing TNBC. Therefore, chemotherapy tools are prevalent in the current treatment regime, mainly in association with other treatment methods. Major concerns about chemo drugs are non-targeted nature, drug resistance, toxic effects and tumor recurrence. Treatment strategies for TNBC commonly include vascular endothelial growth factor A (VEGF-A) inhibitors, androgen receptor inhibitors, poly-ADP-ribose polymerase (PARP), mammalian target of rapamycin (mTOR) inhibitors, and immune checkpoint modulators (Bergin and Loi, 2019; Cao and Niu, 2020). Though these treatment strategies have increased the overall survival of TNBC patients, still the disease is lethal for advanced or late-stage patients. Hence, a lacuna exists in identifying novel therapeutic agents and integrating them with revolutionary technologies to develop novel therapeutic regimens combating TNBC.

As well documented, medicinal plants have been used since ancient times to treat various ailments (Ahmed et al., 2021; Amalraj et al., 2017; Buhrmann et al., 2021; Daimary et al., 2021; Girisa et al., 2019; Gupta et al., 2017; Kunnumakkara et al., 2017; Roy et al., 2019). Natural compounds isolated from these medicinal plants were reported to possess immunomodulatory, pleiotropic, pharmacological and anti-cancer properties (Choudhury et al., 2016; Girisa et al., 2021a; Girisa et al., 2021b; Kumar et al., 2021; Kunnumakkara et al., 2021; Nair et al., 2019; Verma et al., 2021). Interestingly, an estimate of 50% of approved anticancer drugs in 1981-2010 originated from natural products (Mushtaq et al., 2018). Allicin, gingerol, apigeninm, dicumarol, epigallocatechin, genistein are few phyto chemicals that are under preclinical trials; lycopene, resveratrol, sulforaphhane, epigallocalechin are some of

the phytochemicals evaluated in clinical trials (Choudhari et al., 2020). Vinca alkaloids, taxane diterpenoids, camptothecin derivatives, and epipodophyllotoxin. vinblastine, paclitaxel, docetaxel, topotecan, etopside are some of phytochemicals used for cancer treatment successfully (Choudhari et al., 2020). Therefore, phytochemicals still remain the crucial source for developing successful drugs for cancer treatment.

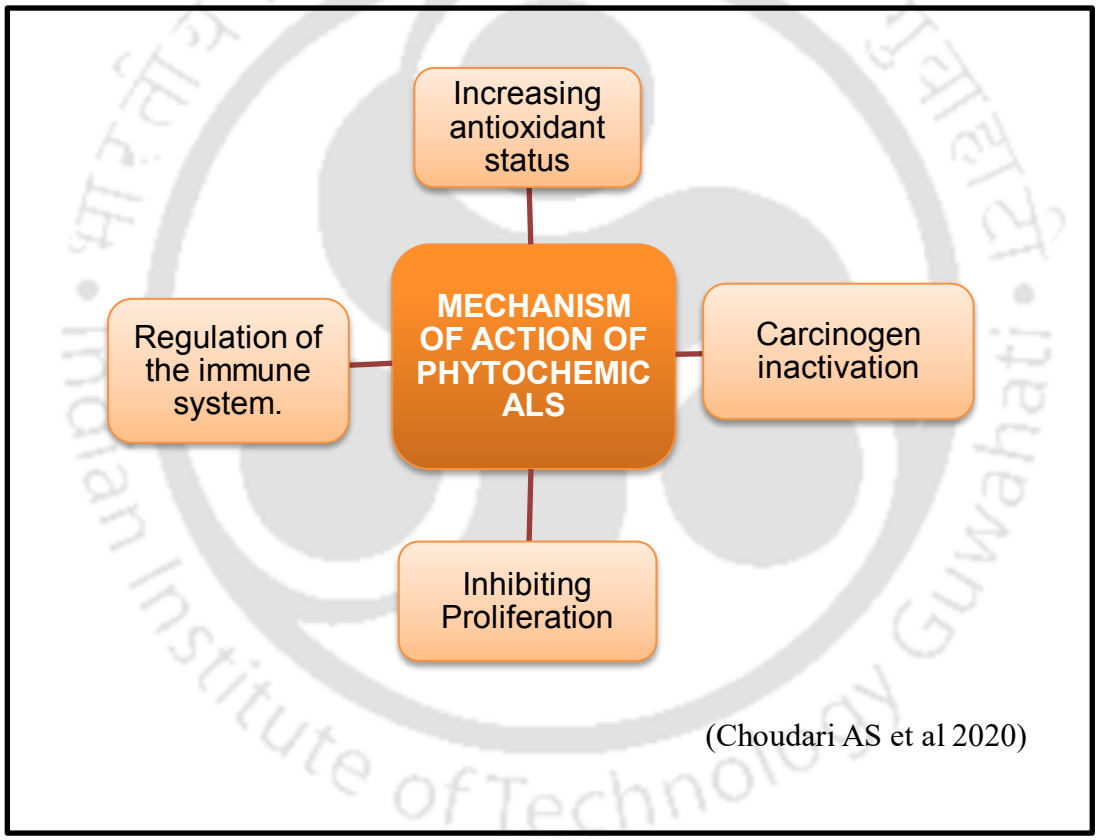

Figure 1.2 Mechanism of action of phytochemicals

It is broadly accepted that the anti-oxidant and anti-inflammatory activity of phytochemicals carries a vital role in their anticancer activity (Barbieri et al., 2017). However, the major limitations of these phytochemicals are their poor bioavailability

and rapid clearance and resistance to cancer cells (Aqil et al., 2013; Mazurakova et al., 2022). Nanotechnology tools can efficiently bypass these limitations of phytochemicals by improving the pharmacokinetics, bio-distribution and therapeutic index of these agents. Presently, gold nanoparticles (AuNps) have received greater attention in contemporary research due to their high biocompatibility, low toxicity, good surface plasmon resonance, uncomplicated synthesis approaches and easy to functionalise with different materials (Kalashgrani and Javanmardi, 2022). Therefore, the present study was aimed at synthesising, characterising and examining the anti-cancer properties of some of the known phytochemicals for TNBC treatment.

1.2 Breast cancer (BC)

BC is the abnormal growth of breast cells, which divide faster than healthy cells, pile up together and form a lump. Based on the location where it develops, BC can be classified as ductal carcinoma (carcinoma of milk ducts), lobular carcinoma (carcinoma of breast lobules), inflammatory BC (affects breast skin) and Paget disease (effects nipple and areola) (Watkins, 2019). Mammography and sonography are the primary diagnosis techniques; however, MRI is also used in particular if any abnormalities are suspected in first two techniques.

1.2 1 Different grades of BC

The histological grade of tumors is based on the degree of differentiation of tumor tissue. The grade is usually complementary to Lymph node status (LN) as well. Grading is generally determined by the morphological features suggested by Nottingham Grading System, which is based on (a) the degree of tubule or gland formation, (b) nuclear pleomorphism, and (c) mitotic count (Rakha et al., 2010).

Determining histological grade is a relatively simple, low-cost method that requires only hematoxylin-eosin-stained tumor tissue sections assessed by a trained pathologist using a standard protocol. Grade 1 tumors were found to be less than 2cm in size, showed good prognosis and have a 5-year survival rate of 99% (Henson et al., 1991). Only 4% of grade 1 tumor patients were found to be developed distant metastasis or died without developing a recurrence of higher-grade tumor (Henson et al., 1991). Grade 2 tumors are about 2-5cm in size, and LN involvement is comparatively low (Goldhirsch et al., 2009). In short-term follow-up, grade 2 tumors showed the intermediate outcome, recurrence and impaired outcome in the long term (Rakha et al., 2008a; Rakha et al., 2008b). Grade 2 tumors show intermediate risk, and this criterion hints toward the chemotherapy regime. Further, Grade 2 tumors are classified into the "grade 1 like" subgroup and "grade 3 like" subgroup. "Grade 1 like" shows very good outcome and usually gets treatment without chemotherapy, while grade 3 like are more aggressive subtype and requires systemic chemotherapy for treatment (Rakha et al., 2010). Grade 3 breast tumors are primarily found in larger size (Anderson et al., 2000). Most of the HER2 positive and triple negative tumors are higher grade (grade 3) and show poor prognosis (Desmedt et al., 2008; Wirapati et al., 2008). Grade III tumors need aggressive treatment methods and mostly exhibit nodal involvement.

1.2.2 Stages of BC

BC's stages are defined by the size of the tumor and the infiltration of tumor cells into the breast tissue (Heim et al., 1997).

Stage 0: In this stage, breast tumors are non-invasive, i.e., cancerous and non-cancerous cells are seen in the boundary of tumor. No evidence of invasion into the surrounding tissues of the breast. Ductal cell carcinoma in situ (DCIS) is an example of a stage 0 tumor (Akram et al., 2017). Usual treatment strategies are mastectomy or lumpectomy followed by radiation and/or hormone therapy to prevent the further development of cancer.

Stage 1: This particular subtype describes invasive breast carcinoma and includes two subtypes, stage 1A and 1B. Stage 1A describes 2cm tumors with no lymph node involvement, while stage 1B has smaller tumors (<2cm), and small clusters of cancer cells are of found in lymph nodes (0.2mm) (Akram et al., 2017). The major treatment option for this stage is surgery followed by radiation. Systemic therapy is also recommended for stage 1 tumors**.**

Stage 2: Stage 2 tumors are also divided into two distinct subgroups. Stage 2A represents tumors found in axillary lymph nodes or sentinel lymph nodes, but no tumor is found in the breast, and the tumour size is around 2cm. Stage 2B tumors are larger than 5cm but not seen in lymph nodes. Stage 2 tumors are generally treated with systemic therapy or hormone therapy before surgery and also recommended for radiation in case of nodal involvement (American Cancer Society).

Stage 3: Stage 3 BC has been subcategorized into Stage 3A, 3B and 3C. Stage 3A tumors are not found in breast tissues but develop in 4-9 axillary or sentinel lymph nodes. Stage 3B tumors are of variable size, can spread up to axillary or sentinel lymph nodes and also show swelling or ulcer on the skin of the breast. Hence, 3B is also

considered as inflammatory BC with red swollen breasts. Stage 3C includes more than 10 lymph node involvements and lymph nodes below or above the clavicle as well (Jacquillat et al., 1990). Surgery is the first option for stage 3 patients, followed by radiation; systemic neoadjuvant chemotherapy is also recommended. In case of hormone-positive tumors, targeted hormone therapies such as trastuzumab and pertuzumab are also recommended (American Cancer Society)

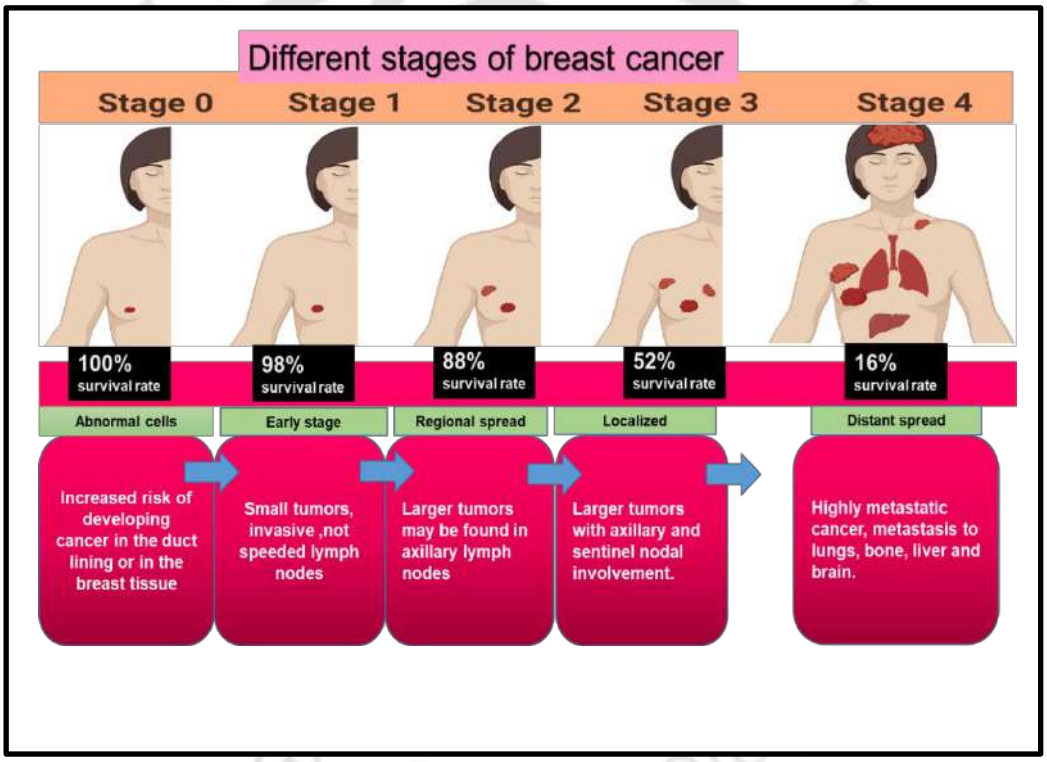

Figure 1.3 Different stages of breast cancer

Stage 4: Stage 4 is the advanced metastatic stage of cancer, characterised by metastasis towards the vital organs such as lungs, bones, liver and brain (Neuman et al., 2010). Chemotherapy, hormone therapy or immunotherapy combined or separately are used to treat or reduce the uneasiness of patients in Stage 4 (WebMD Editorial Contributors).

1.2.3 Subtypes of BC

BC, being a heterogeneous and complex disease, can be classified based on parameters such as tumor size, nodal involvement, histological grade, presence of various genes and proteins, intrinsic subtypes and extrinsic subtypes, etc. Since 2011 intrinsic subtypes of BC have been widely accepted for adjuvant systemic therapies in early stages (Goldhirsch et al., 2013). These intrinsic subtypes are further classified into luminal A, luminal B, HER2 enriched and basal-like tumors. Out of these, luminal A and luminal B are in ER positive branch; and HER2-enriched and basal-like tumors are in ER-negative branch (Yersal and Barutca, 2014). These molecular classifications help to predict the outcome of clinical practises and provide information regarding the patient-specific prognosis and risk factors (Malhotra et al., 2010).

Luminal A

Luminal A subtype is the most common subtype of BC and constitutes 50-60% of the total. These particular tumors are characterised by the expression of genes activated by ER factor commonly found in the luminal epithelial lining of the mammary duct (Eroles et al., 2012). The luminal subtype is defined by ER and/or PR positive and HER2 negative. Luminal A tumors are also defined by low Ki-67 labelling index (<14%) and/or nuclear grade 1 or 2 (Inic et al., 2014); low Ki-67 index correlates with better prognosis and late recurrence (Nishimura et al., 2010). Moreover, it is characterised by the expression of a high GATA3 marker. Nevertheless, patients with this subtype express good prognosis and relapse rate, significantly higher than other subtypes of BC (Kennecke et al., 2010) This disease has clear metastatic patterns with a higher incidence in bone, followed by lung, liver and brain (Guarneri and Conte,

2009). Treatment modalities for this particular subtype include third-generation hormonal aromatase inhibitors (AI) and selective estrogen receptor modulators (SERMs) like tamoxifen (Guarneri and Conte, 2009).

Luminal B

Luminal B tumors account for 10-20% of all BCs (Eroles et al., 2012). Luminal B tumors show aggressive relapse, poor prognosis, higher histological grade and proliferation index compared to luminal A. Even though the bone is the most common site for distant relapse, its recurrence pattern differs from other subtypes. It shows a higher recurrence rate at liver; also, the survival from relapse is lesser for this subtype than luminal A (Kennecke et al., 2010). The main biotic difference between this luminal A and luminal B is the expression of proliferative genes MKI67 (Marker of Proliferation Ki-67) and cyclin B1. Luminal B also often expresses GFR (Glomerular filtration rate) and HER2. Even though 6% of luminal tumors are ER- and HER2- , luminal B tumors are characterised by the expression of ER+, HER2+/- and high Ki67 (Eroles et al., 2012). Despite the fact that luminal B tumor shows worse prognosis towards tamoxifen and AI, its response towards neoadjuvant therapy is much better (Paik et al., 2004) with pathological complete response (pCR) 17%, which is higher than luminal A (7%), lower than HER2+ (36%) and basal-like (43%) (Parker et al., 2009). Hence, the treatment for this particular subtype is still challenging and many clinical trials are going on the inhibitory molecular pathways at different levels.

HER2 positive

Approximately, 20 to 30% of all BCs are HER2 positive (Ross et al., 2009). The main feature of these tumors is the overexpression of HER2 genes and the genes associated

with HER2 pathways. It also overexpresses proliferation-related genes, worse prognosis and poor disease-free survival (Ross and Fletcher, 1998). Though some HER2+ tumors are ER+, the immunohistochemistry (IHC) profile for this subtype shows ER-/HER2+ pattern. Since it is a challenging group of tumors, worldwide researchers have made a tremendous effort to discover targeted therapy for this particular disease. The first FDA-approved monoclonal antibody against HER2+ BC is trastuzumab.

Tastuzumab causes anti-tumor effect via different mechanisms such as inducing apoptosis, induction of cell cycle arrest, and antibody-dependent cell-mediated cytotoxicity (ADCC) (Baselga et al., 2001; Spector and Blackwell, 2009). Other monoclonal antibodies and their conjugates approved by FDA are pertuzumab, trastuzumab emtansine (T-DM1), and fam-trastuzumab deruxtecan. Eventhough these monoclonal antibodies successively diminish the effect of metastatic tumors, there is still a great demand for a more efficient treatment approach that can pull down the adverse impact of metastatic tumors.

Basal like

Basal-like subtype accounts for 10-20% of all BCs. The presence of high molecular weight cytokeratins, P-cadherin, caveolin 1 and 2, nestin, and epidermal growth factor (EGF) resembles basal-like tumors to normal breast myoepithelial cells. The most relevant feature of these tumors is the absence of crucial ER, PR and HER2 receptors. Another notable feature of basal-like tumors are mutations in TP53 and BRCA1/2 and deregulation in immune response (Schneider et al., 2008). Basal-like

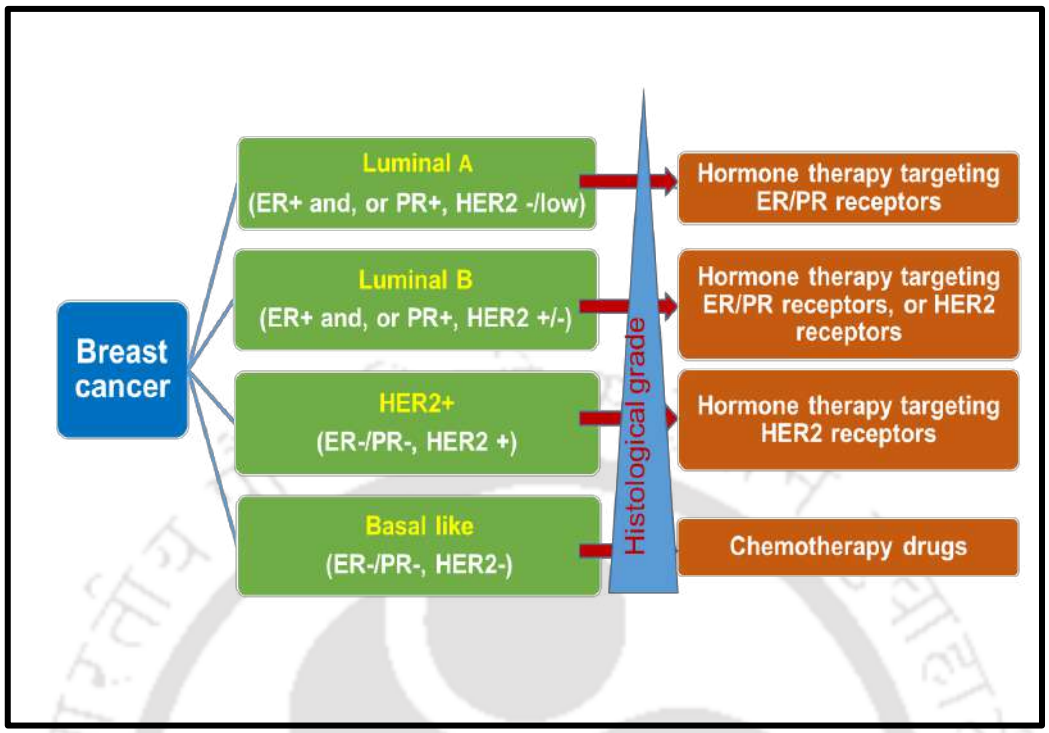

Figure 1.4 subtypes of breast cancer

tumors are usually seen in premenopausal women, especially African origin, mostly higher grade with nodal involvement (Bosch et al., 2010). Its metastatic pattern includes lung, brain and lymph nodes, also shows worse prognosis (Kennecke et al., 2010). TNBC and basal-like tumors are usually considered as surrogates, but all basal-like tumors are not TNBC. Because of the absence of receptors, this subtype is very difficult to target actively as HER2+. Even though targeting DNA response pathways is a reasonable approach for basal-like tumors. Luckily, these tumors are very much sensitive to platinum drugs and PARP inhibitors (Robson et al., 2017; Silver et al., 2010).

1.2.4 Triple negative breast cancer (TNBC)

TNBC accounts for 10-17% of all BCs, and it is the most aggressive subtype with poor clinical outcome, metastatic behaviour towards vital organs, and poor prognosis and mainly occurs in premenopausal women (Carey et al., 2007; Fulford et al., 2007; Van De Rijn et al., 2002). Recent advancements helped to properly understand intrinsic molecular and immunological heterogeneity in TNBC. Although PARP inhibitors and checkpoint inhibitors set new standards for treating TNBC, mainstream treatment still remains chemotherapy (Maqbool et al., 2022). According to gene expression profiles, Lehman et al (Lehmann et al., 2011) classified TNBC into six subtypes, including 2 basal-like (BL1 and BL2), immunomodulatory (IM), mesenchymal (M), mesenchymal stem-like (MSL), and luminal androgen receptor (LAR) subtype. Burstein MD et al also confirmed Lehmann's subtyping, as they identified four stable subtypes of TNBC luminal-AR (LAR), mesenchymal (MES), basal-like immune-suppressed (BLIS), and basal-like immune-activated (BLIA) (Burstein et al., 2015).

Basal like (BL1 and BL2)

BL1 subtype is characterised by high DNA damage pathways (ATR/BRCA), and high Ki67 mRNA expression indicates the highly proliferative nature of this subtype (Hubalek et al., 2017). BL2 subtype expresses growth factor signalling pathways, including glycolysis and gluconeogenesis. Growth factor receptors such as EGFR, MET (Mesenchymal Epithelial Transition), and EphA2 (hepatocellular receptor tyrosine kinase class A2) are peculiar to BL2 subtype as well (Lehmann et al., 2011).

In addition, nearly all BL subtypes are associated with BRCA1/2 gene mutation (Stefansson et al., 2009).

Immunomodulatory Subtype (IM)

IM subtype is closely related to immune regulation pathways. These regulatory functions depend on the interaction between cytokines and cytokine receptors (cytokine signalling pathways), T cell and B cell receptor pathways and Nuclear factor kappa B (NF-κB) signalling pathways (Yin et al., 2020). It also shows STAT signal transducer and activators transcription factor-mediated pathways. Despite its higher grade, this subtype shows a better prognosis than other subtypes of TNBC (Burstein et al., 2015).

Mesenchymal (M) and Mesenchymal Stem-Like Subtypes (MSL)

M and MSL subtype share some typical gene enrichments, such as cell motility, cellular differentiation, and growth pathways. MSL subtype also expresses some unique pathways, including growth factor signalling pathways, EGFR, PDGF Platelet-derived growth factor (PDGF), calcium signalling and G-protein coupled receptor (Hubalek et al., 2017).

Luminal Androgen Receptor Subtype (LAR)

LAR is the most peculiar subtype of TNBC, and these ER-negative tumors show molecular evidence of AR activation also. Androgen receptor mRNA is over-expressed in these subtypes, on an average nine-fold higher than other subtypes. Almost all studies suggested that the LAR subtype comprises AR overexpressed

tumors (Lehmann et al., 2011). Antiandrogen, enzalutamide has been tested effectively for advanced TNBC patients with AR positivity (Gucalp et al., 2013).

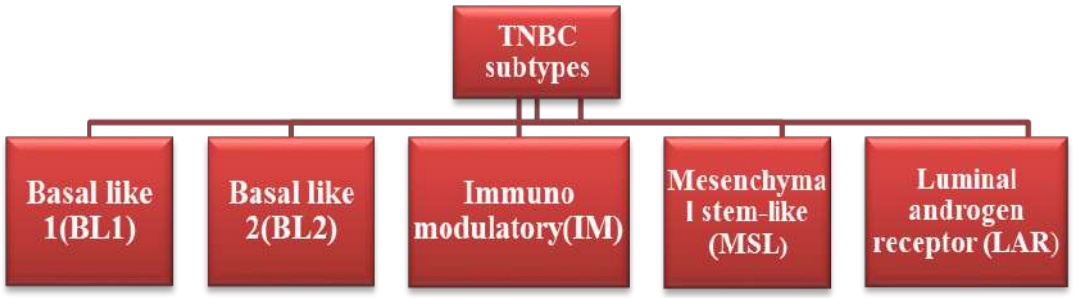

Figure 1.5 Different subtypes of TNBC

1.2.5 Risk factors of breast cancer

Approximate of 1 in 9 women develop BC by the age of 85 though the level of risk is not uniformly distributed across the population (Singletary, 2003). Some individuals are entirely out of danger, and some are at high risk of developing BC. Some of the main risk factors for BC are gender, age, physical activity, diet, weight, smoking, alcohol consumption, immoderate exposure to estrogen and oral contraceptives, family history and radiation exposure (Momenimovahed and Salehiniya, 2019; Ross et al., 2000; Thakur et al., 2017; Yousef, 2017). Various risk factors that effects BC are discussed below**:**

Gender

Major risk factor for BC is obviously being female. This particular malignancy is rare in men, almost less than 1% of all BC cases (Giordano et al., 2002). In men, it usually

occurs at an older age, who had hormonal imbalance, exposure to radiation and a family history of BC. Further, the most common risk factor for men to develop BC is BRCA gene mutation (Yousef, 2017).

Age

Next to gender, age is the most critical risk factor for BC (Thakur et al., 2017). The incidence rate for BC increases with age and reaches a maximum by the age of menopause, then decreases slowly and remains constant. Most BC incidences are reported after menopause (Seidman et al., 1985). Though the chances of developing BC in younger women is comparatively low (~2.5%), it develops at an advanced stage with positive lymph nodes also expresses weak prognosis and survival (Assi et al., 2013; Seidman et al., 1985).

Physical activity

Increased physical activity correlates with decreased incidence of BC in post-menopausal women. Most of the studies have reported an inverse relationship between BC and physical activity, while some studies stated that there is no relation between the two factors. Many studies have proven that calorie restriction could reduce mammary carcinogenesis development (Boissonneault et al., 1986; Cohen et al., 1988). Moreover, increased energy level stimulates the cumulative hormone level and enhances the risk of BC (Harlow and Matanoski, 1991). It is even verified that physical activity after diagnosis of BC can increase the survival time (Holmes et al., 2005; Momenimovahed and Salehiniya, 2019).

Diet and body mass index (BMI)

The correlation between BC and nutrition has been studied widely. It has been proved that carbohydrates, red meat and fat could significantly increase the risk of BC (Linos et al., 2010; Michels et al., 2007; Romieu, 2011). High carbohydrate intake causes constant insulin demand by increasing insulin levels in the body, which might increase the availability of insulin-like growth factor 1 (IGF-1) (Calle and Kaaks, 2004). The proliferative and anti-apoptotic effect of IGF-1 in breast tissues is already validated in many studies (Yanochko and Eckhart, 2006). Fat intake affects breast carcinogenesis via increasing sex hormone levels and weight gain. Though the exact molecular pathway that leads to carcinogenesis is unknown, experimental evidences have shown that low-fat diet reduces BC risk by about 9%. Red meat also increases the risk of carcinogens due to high bioavailable iron content, growth hormones used in animal growth and carcinogenic heterocyclic amines formed during the cooking processes (Romieu, 2011). However, some case-controlled studies have shown conflicting correlations between red meat and BC. Some recent studies suggest the relationship between red meat or processed meat with hormone receptors (ER and PR receptors) in BC (Cho et al., 2006). Fibre-containing food products such as fruits and vegetables are known to reduce the risk of BC. Many studies have proven the protective effect of fruit and vegetable, and their components including vitamin E and D on BC (Cui and Rohan, 2006; Pierce et al., 2007; Van Gils et al., 2005; Wang et al., 2018b).

Numerous studies were performed on the association of BMI and BC, which indicate that BMI greater than 30 elevate the BC risk in pre and post-menopausal

Figure 1.6 Risk factors for breast cancer

women (Sonnenschein et al., 1999; Tehard and Clavel-Chapelon, 2006; Tian et al., 2007). Though some studies suggest that high BMI reduces the risk of BC in premenopausal women and increases it in post-menopausal women, there is no clear evidence of the dependence of BMI in BC (Mathew et al., 2008; Montazeri et al., 2008; Palmer et al., 2007).

Alcohol consumption and smoking

Different studies have verified the positive correlation between alcohol consumption and smoking (Al-Sader et al., 2009; Reynolds, 2013). Daily alcohol consumption increases the risk of BC by about 30-40% compared to non-drinkers (Smith-Warner

et al., 1998). Alcohol-associated risk is more profound in postmenopausal women compared to premenopausal women (Feigelson et al., 2001). Even, moderate consumption of alcohol can increase the amount of oestrogen levels in the blood (Grant, 1997). BC cells depend on oestrogen and progesterone for growth. It has been reported that high level of oestrogen can trigger the growth of cancerous cells. Alcohol-related BC risk is almost same for premenopausal and post-menopausal women (Dorgan et al., 1994).

Tobacco increases the risk of almost all cancers, and the most eminent organ is the lung, where tobacco-induced cancer is more prevalent. Many research groups have studied involvement of tobacco in BC (Alberg et al., 2014; Band et al., 2002; Johnson et al., 2011; Kawai et al., 2014; Macacu et al., 2015; Rosenberg et al., 2013). Tobacco directly correlates with BC, as the breast tissue can take up tobacco carcinogens (Di Cello et al., 2013; Reynolds, 2013; Terry and Goodman, 2006). It is also evident that tobacco induces DNA damage and p53 gene mutations in breast tissues in smokers compared to non-smokers (Conway et al., 2002; Li et al., 1999). Smoking generally increases the premenopausal BC risk rather than the risk in postmenopausal women (Johnson, 2005).

Family history

Family history of BC is a significant risk factor, which has been verified in various studies (Lalloo et al., 2003; McPherson et al., 2000; Pharoah et al., 1997). Women having a first-degree relative (mother, daughter, sister) with BC are expected to have a 13-19% higher chance of getting BC than women without any family history (Shiyanbola et al., 2017). People with history of BRCA gene mutation showed 11

times more chance of getting BC (Metcalfe et al., 2009). Transformation in BRCA1/2 genes also plays an essential role in BC; 55%–65% of BRCA1 gene mutation carriers and 45% of BRCA 2 gene mutation carriers are prone to develop BC by the age of 70 (Godet and Gilkes, 2017).

Oral contraceptives

Oral contraceptives increase the risk of BC in premenopausal women below 45 years (Stadel et al., 1985). However, BC risk due to oral contraceptives is still in conflict among researchers, as it varies from no risk to 20-30% elevated risk. Kamani et al., showed that intake of oral contraceptives in individuals with high estrogen and progesterone levels increases BC risk as it can stimulate the proliferation of cells in the breast tissues (Kamani et al., 2022).

Exposure to radiation

Exposure to different types of radiation increases BC risk (Ronckers et al., 2004). Women who were exposed to radiation below 20 years are more prone to BC than those who have been exposed to radiation at an older age (Preston et al., 2002). Moreover, the patients who are monitored by X-ray for scoliosis or tuberculosis, received radiotherapy for benign disorders, treated with X-rays for BBD (Bladder & Bowel Dysfunction) or acute post-partum mastitis are at high risk for BC. In addition, childhood cancer survivors exposed to high dose chest radiation and adult cancer survivors treated with radiation therapy were also found to have significant radiation-related risk (Boice Jr et al., 1991; Howe and McLaughlin, 1996; Kenney et al., 2004; Lundell et al., 1999; Mattsson et al., 1993; Storm et al., 1992)

Other risk factors

Pregnancy, abortion (not natural abortion), breast density, benign breast diseases, obesity, overweight, vitamin D, air pollution and diabetes are other known risk factors for BC (Brasky et al., 2013; Byrne et al., 2017; Innes and Byers, 2004; Nazari and Mukherjee, 2018; Román et al., 2017; Wolf et al., 2005).

1.2.6 Warning Signs, symptoms and clinical features of BC

Early detection is very crucial in any cancer therapeutics, including BC. One of the most important signs of BC is painless lump in the breast or armpit (Hadi et al., 2010; Schettino et al., 2006). Another major sign of BC is nipple discharge and nipple retraction (Dimpled, inward pulling, sores and flaky skin) (Montazeri et al., 2008; Okobia et al., 2006). Discolouration of nipple skin and changes in breast skin (size, texture, contour or temperature) are also reported by women (Parsa et al., 2008).

1.2.7 Treatment modalities for TNBC

Even though, TNBC being the most aggressive and heterogeneous subtype of BC, no scientifically proven targeted therapy exists. The lack of ER, PR and HER2 receptors makes the discovery of better treatment approaches tiresome (Maqbool et al., 2022). TNBC subtype is associated mainly with BRCA1 mutation (Lakhani et al., 2002). Other major features of TNBC are younger age at diagnosis and nodal positivity (Dent et al., 2007). Even though TNBC patients respond to anthracycline and taxane-based neoadjuvant therapy, it shows a higher recurrence rate and worse prognosis than other subtypes (Dent et al., 2007). Fortunately, most TNBC tumors respond to neoadjuvant chemotherapy better than other subtypes.

Chemotherapy

TNBC has been evidenced for a very good response to chemotherapy regimens, including anthracyclines and taxanes (Carey et al., 2007; Esserman et al., 2009; Liedtke et al., 2008; Rouzier et al., 2005). Even though the initial response towards neoadjuvant therapy is good, it shows tumor recurrence and poor overall survival. This conflictual behaviour is called TNBC paradox (De Laurentiis et al., 2010). The subtypes of TNBC explain this paradox; more than 50-60% of TNBC's intrinsically resistant to chemotherapy. While the high pCR rate accounts for the remaining TNBC subtypes, these subtypes exhibit high chemosensitivity and better outcome (De Laurentiis et al., 2010). Various studies have reported the potency of platinum-based chemotherapy regimens against TNBC. Docetaxel and weekly carboplatin administration reported a pCR rate of 22%; weekly paclitaxel and carboplatin every 4 weeks showed a pCR rate of 67% as well (Byrski et al., 2010; Sikov et al., 2009). Further, cisplatin triweekly obtained a high pCR rate of 87% in premenopausal women with BRCA mutations (Byrski et al., 2010). Hence platinum-based neoadjuvant therapy is also considered effective for TNBC patients.

Surgery and radiation

Local control for any solid tumor including TNBC is surgery. Though breast conservation and sentinel node biopsy are considered the sensible treatment approaches for TNBC patients, mastectomy would be the better option for patients with BRCA gene mutations as the tumor recurrence chance is high in those patients (Wang et al., 2018a). Adjuvant radiation therapy is recommended after surgery to kill the remaining cancer cells.

Radiotherapy refers to the use high-energy radiation to constrain the growth and proliferation of malignant cells with minimal damage to normal cells. Breast conservation therapy and postoperative radiotherapy are recommended for patients with ≥4 axially nodal involvements to minimise the local recurrence risk. However, mastectomy and adjuvant radiation therapy are advisable for more than four axillary nodal involvement or stage III patients.

Novel targeted therapies for TNBC

In targeted therapy, ideally there is no damage to healthy cells in contrast to chemotherapy. Nevertheless, current targeted therapies (tamoxifen and AIs) are ineffective for TNBC. Novel targeted therapies under clinical are PI3K inhibitors, PARP inhibitors, EGFR inhibitors, VEGF inhibitors and androgen (AR) inhibitors (Lin et al., 2010).

Androgen receptor (AR) inhibitors: AR receptors are found in 30% of TNBC patients and 80% of invasive BCs (Rampurwala et al., 2016). Patients with positive AR profiles show better prognoses than those with negative AR profiles. High expression of AR is found in the luminal AR (LAR) subtype of TNBC. While *in-vitro* and *in-vivo* studies proved that AR inhibitors play critical role in the invasion and proliferation of non-LAR subtype of TNBC (Barton et al., 2015). Bicalutamide is an FDA-approved AR inhibitor that is orally bioavailable (Osguthorpe and Hagler, 2011), 2011). Further, enzalutamide is another androgen inhibitor under clinical trial (Phase II), and apalutamide and darolutamide are also promising AR inhibitors under phase III trials (Clegg et al., 2012).

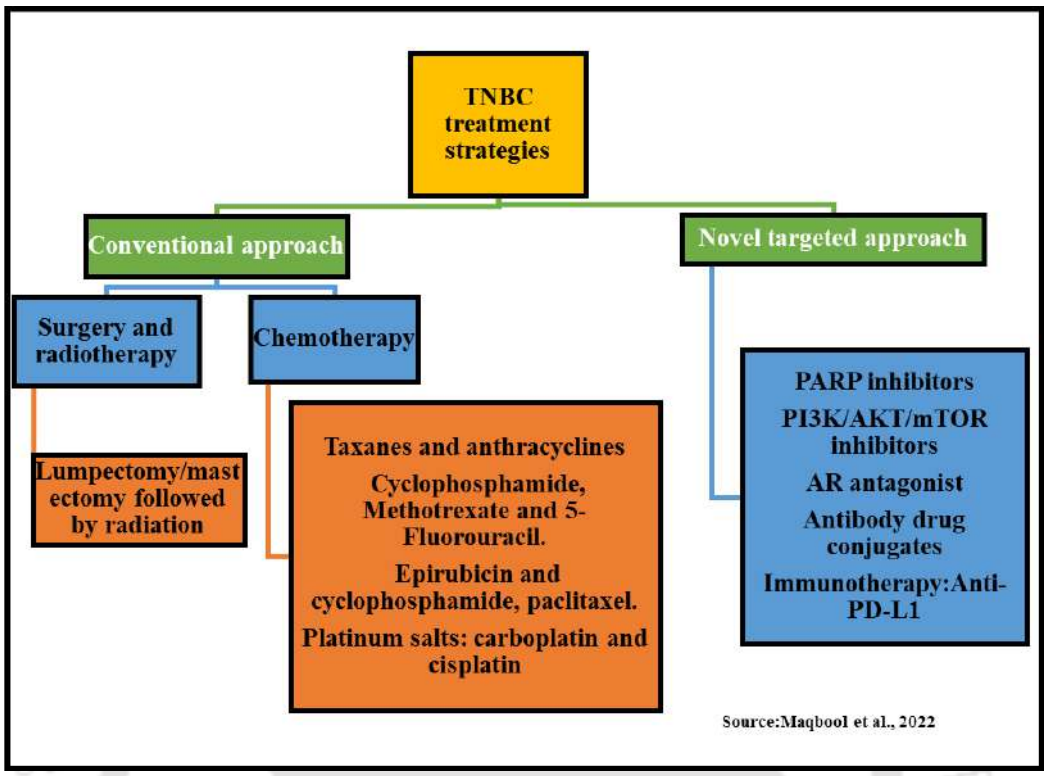

Figure 1.7 Treatment modalities for TNBC

Poly- (ADP) -Ribose polymerase (PARP) inhibitors: PARP inhibitors are DNA repairing enzymes which promote the repair of single stranded DNA (Gunn et al., 2016). PARP inhibitors suppress DNA repair through homologous recombination pathway, which induces cytotoxicity. In effect, PARP inhibitors can make a great outcome in TNBC patients with a BRCA1/2 mutation. FDA-approved PARP inhibitors are olaparib and talazoparib (Han et al., 2020). The other two PARP inhibitors rucaparib and niraparib are under clinical trials.

Epidermal growth factor receptor (EGFR) inhibitors and Vascular endothelial growth factor receptor (VEGFR) inhibitors: A large number of TNBC tumors overexpresses EGFR and VEGFR; hence these are important targeting tools for

TNBC (Rakha et al., 2009). The only FDA-approved EGFR inhibitor is lapatinib, which is recommended in combination with chemotherapy or hormone therapy (Iancu et al., 2022). The first FDA-approved EGFR-targeted antibody is cetuximab, proposed in combination with chemotherapy (Chen et al., 2019). Apatinib and lenvatinib are novel VEGFR inhibitors, and camrelizumab is another VEGFR inhibitor under Phase II clinical trial (Chen et al., 2019; Fan et al., 2014; Lo et al., 2020).

Phosphoinositide 3-kinase/ Ak strain transforming/ Mammalian target of rapamycin (PI3K/AKT/mTOR) pathway inhibitors: PI3K/AKT/mTOR pathway contributes crucially for the chemo resistance and survival of TNBC (Khan et al., 2019). 25% of the TNBC tumors carry abnormalities in PI3K/PTEN/AKT pathways, hence targeting this pathway is a good strategy for TNBC treatment (Chin et al., 2014; Pascual and Turner, 2019; Shah et al., 2012). The efficacy of gedatolisib as a PI3K and mTOR inhibitor is under phase II clinical trial (NCT03911973). In addition, other PI3K/AKT/mTOR inhibitors under clinical trial are ipatasertib (an AKT inhibitor), buparlisib (a PI3K inhibitor), everolimus (an mTOR inhibitor), and capivasertib (an AKT inhibitor) (Li et al., 2022).

Immunotherapy

TNBC is suited for immunotherapy due to its high-level expression of immune markers, such as Programmed death-ligand 1 (PD-L1) and programmed cell death protein-1 (PD-1), that are firmly related to tumor response and overall outcome (Li et al., 2022). Atezolizumab is an FDA-approved drug for PD-L1 against TNBC; FDA also proved pembrolizumab in combination with chemotherapy. Other immune

checkpoint inhibitors under clinical trial are pembrolizumab or atezolizumab monotherapy (Emens et al., 2019; Nanda et al., 2016).

Being highly heterogeneous, combinational therapies are highly recommended to ameliorate TNBC patients, including targeted therapy and immunotherapy regimes.

Other treatment options for TNBC

Other contemporary research areas for TNBC therapeutics are adoptive cell therapy (ACT), antibody-drug conjugates, cancer stem cell-related strategy, epigenetic modifications inhibitors, fibroblast growth factor receptor inhibitor (FGFR) etc (Charafe-Jauffret et al., 2009; Corti et al., 2022; Pearson et al., 2016; Su et al., 2021; Turner et al., 2010; Yang et al., 2001).

1.2.8 Challenges with TNBC therapies

Owing to its high mortality rate TNBC is the point of convergence in BC research. The occurrence rate for TNBC is only 12.7%, while its mortality rate is over 40% (Doval et al., 2015; Haffty et al., 2006). Also, almost 50% of TNBC patients are below 40 years, and the 5-year survival rate of TNBC patients is below 30% even after being treated with chemotherapy tools (Sharma et al., 2013; Sparano et al., 2015). Tumor recurrence and chemo resistance are the pre-eminent snags that prevent TNBC treatment outcomes.

Tumor recurrence

Tumor recurrence risk is maximum in TNBC patients, 1 to 3 years after surgery; metastasis to vital organs within five years after the first diagnosis is also seen in TNBC patients (Dent et al., 2009). Further, the recurrence rate is high in stage III

patients and is found to be lesser in older patients (Bayraktar et al., 2011). The possibility of recurrence is also disparate in TNBC. Surprisingly, TNBC shows high distant metastatic rate within four years of surgery, and then the rate declined for another eight years of follow-ups. Most of the recurrent or metastatic tumors are found to be chemo resistant; in effect, it increases the mortality rate (Khan et al., 2019). Hence the invention of targeted therapy for TNBC is in high demand in contemporary cancer therapeutics.

Chemo resistance

An alarming fact in cancer treatment is that, almost 90% of the currently available drugs are ineffective in metastatic cancer owing to chemo resistance (Longley and Johnston, 2005). Chemo resistance is meant by the ability of cells to maintain their viability through different cellular fates even after being treated with chemotherapeutic agents. Tumor microenvironment and cellular fates play a vital role in the chemo resistance of TNBC cells. Six known mechanisms for the chemo resistance of TNBC cells are 1) APC (Amino acid, polyamine and organic cation) transporters, 2) β-tubulin III, 3) mutations in DNA repair enzymes such as topoisomerase II and DNA mismatch repair enzymes, 4) alter-actions in genes involved in apoptosis, 5) ALDH1 (Aldehyde dehydrogenase 1) and glutathione (GSH)/Glutathione-S-transferase (GST) and 6) NF-κB signalling pathways (O'Reilly et al., 2015).

1.3 Phytochemicals for cancer treatment

At the beginning of the 19th century, improvements in organic chemistry unveiled a non-traditional route of extraction and characterization of active compounds from

plants. Between 1981 and 2014, more than half of the approved drugs were derived directly or indirectly from plants (Newman and Cragg, 2016). Moreover, almost 50% of the approved anticancer drugs from 1940 to 2014 originated from natural products or were directly isolated from plants (Newman and Cragg, 2016). Flavonoids, polyphenols, terpenoids, alkaloids, saponins, coumarins are some of the phytochemicals, identified for their anticancer effect in various tumors (Zheng et al., 2022). Most of the phytochemicals exhibit anti-cancer activity by targeting multiple pathways. They induce programmed cell death by modulating different pathways/proteins that are dysregulated in cancer cells (Zheng et al., 2022)).

1.3.1 Barriers limits the therapeutic potential of phytochemicals

In contemporary research, various phytochemicals are thoroughly scrutinised for their medicinal properties. Despite its potency in cancer therapy, certain limitations of these compounds need to be addressed before administrating into the physical system. Major constraints are poor solubility, adverse pharmacokinetic properties and rapid uptake by normal cells (Son et al., 2019; Xie et al., 2016).

Generally, phytochemicals exhibit poor water solubility, including paclitaxel, docetaxel and cabazitaxel (Ali et al., 1997; Hamada et al., 2006; Mastropaolo et al., 1995; Song et al., 2014). These drugs need the help of surfactants for parental infusion. However, these surfactants also show various side effects (Fjällskog et al., 1993; Kubis, 1979). Further, taxol and taxotere have hypersensitivity reactions such as neutropenia, gastrointestinal toxicity etc. (Eisenhauer et al., 1994; Grem et al., 1987; Ho and Mackey, 2014; Piccart et al., 1995; Weiss et al., 1990). Additionally, being small-molecule drugs, phytochemicals show low pharmacokinetic parameters. For

example, vincristine a backbone for treating solid tumors and hematologic malignancies exhibits a poor distribution half-life, (Escobar et al., 2003; Silverman and Deitcher, 2013).

1.4 Nanotechnology tools to overcome the hurdles in phytochemical therapy

Contemporary research on phytochemicals focuses on targeted delivery with nanotechnology gadgets. Nanoparticles can increase the solubility of phytochemicals and improve the pharmacokinetic index. The primary mechanism of targeting cancer cells by nanoparticles is the EPR effect (Maeda H et al., 2003). By the EPR effect, nanoparticles can preferentially leak into the tumor cells and remain there as the tumor lacks lymphatic clearance. The particle size is a critical factor in EPR effect; nanoparticles in the size range 5-50nm are suitable for this effect as they overcome the renal clearance range of 40KDa (Xie j et al., 2016). Therefore, nanoparticles can improve the circulation time of low molecular weight phytochemicals, enhancing efficacy. Other approaches to improve therapeutic potential of phytochemicals are antibody-drug conjugates and nano vehicles to subdue the multidrug resistance in cancer cells (Chari et al., 2014; Patel et al., 2013; Peetla et al., 2013).

1.4.1 AuNps in cancer therapy

Tunable size and shape

Gold is a biocompatible metal, well utilised for many biomedical applications. While discussing about nanogold, its physical and chemical properties are extremely different from the bulk counterpart, since it obeys quantum mechanics, not classical mechanics. The foremost feature of nanogold that makes it a suitable commodity for cancer treatment is tunable size and shape (Dreaden et al., 2012). The size of AuNps

varies in different preparation methods. In Turkevich's citrate-mediated chemical reduction method produced monodisperse spherical AuNps of 16–150 nm (Turkevich et al., 1951). After that, many studies have reported on the size-controlled synthesis of AuNps. Since the chemical route for synthesizing nanoparticles often produces toxic byproducts. Contemporary research is focused on the green synthesis of AuNps for biomedical applications.

Shape-controlled synthesis of nanoparticles attracted attention in the early 90s; since then, different nanoparticle structures have been successfully synthesized such as spherical, triangular, hexagonal, cubical and rode-shaped etc. The shape of the nanoparticles is also crucial in cancer treatment as they exhibit distinct therapeutic parameters (Chithrani et al., 2006; Elbialy et al., 2010; Suarasan et al., 2022; Sun et al., 2011).

Toxicity and cellular uptake

Essential parameters of AuNps that need to be addressed before administrating into the physical system are cellular uptake and toxicity. Just like any pharmaceutical agent, AuNps are also anticipated to have adverse effects upon administration to the biological system. The toxicity of AuNps has been studied extensively *in-vitro* and *in-vivo* (Alkilany and Murphy, 2010a; Khlebtsov and Dykman, 2011; Lewinska et al., 2017; Nel et al., 2006). Generally, gold nano particles at low concentrations (320–3200 µg/kg/day) are found to be non-toxic *in vivo* system in the size range 10-100nm. Studies showed that gold core is generally biologically inert; even though, it is not valid for all sizes. Being very small-sized nanoparticles (>2nm), it is showing exceptional chemical reactivity. Due to the very high surface to volume ratio, less than

2 nm AuNps act as chemical catalysts, leading to unwanted chemical reactions and side effects (Alkilany and Murphy, 2010a; Turner et al., 2008). For example, researchers have already proved the catalytic property of 1.4nm (50 gold atoms in a cluster) AuNps (Pan et al., 2009). Usually, AuNps used for anticancer properties are above 10nm, and their core is found benign (Longmire et al., 2008); above 10nm particles can also exclude the renal clearance limit. Nonetheless, most toxicity studies on AuNps are *in-vitro*; more size and shape-dependent *in-vivo* studies should be performed before moving to clinical use.

The cellular uptake of AuNps has been thoroughly investigated so far, and it is widely accepted that size, shape and surface charge are the main criteria that determine the cellular uptake. Also, the cellular level, enhanced uptake of AuNps are explained by the adsorption of media /plasma proteins on the surface of nanoparticles to reduce the surface free energy of nanoparticles (Cedervall et al., 2007). As a result, these growth media/plasma proteins (protein corona) can mediate the uptake of the nanoparticles through receptor mediated endocytosis (Connor et al., 2005). In the biological system, it has shown that, gold nanoparticles can accumulate in tumor tissue micro environment via EPR effect. Further, adsorption of plasma proteins on the surface of gold nanoparticles helps in the increased internalization of AuNp. According to Jiang et al., the cellular uptake of AuNps is maximum at 40-50nm size than smaller-sized particles (Jiang et al., 2008). In a particular study, triangular nanoparticles showed three times more cellular uptake than spherical nanoparticles with a similar surface area (RAW264.7 cells). For HeLa cells, triangular nanoparticles expressed 20 times more effective internalization than spherical nanoparticles (Nambara et al., 2016).

Another study reported the high mass internalisation of hexagonal AuNps in the Calu-3 cells, compared with spherical and triangular gold nanoparticles (Tian et al., 2015). The "angle of attack concept explains this", when the nanoparticles interact with the cellular surface, total parallel component of the kinetic energy produced gets accumulate to the cutting wear (Buzea et al., 2007; Neilson and Gilchrist, 1968). Hexagonal nanoparticles could involve in small angle attack on the cell surface and results in greater internalisation. The surface chemistry of AuNps also significantly affects cellular uptake; various studies have shown that cationic nanoparticles could internalise more easily than anionic nanoparticles (Alkilany and Murphy, 2010a; Hauck et al., 2008).

1.4.2 Phytofabricated AuNps for anticancer therapy

Present studies focus on phyto-nanoto concomitant therapy to improve the disadvantages of phytochemicals in cancer therapy. Recently, AuNp-conjugated phytochemicals acquired remarkable space in cancer research. Resveratrol conjugated nanoparticle shows anticancer properties in BC (Thipe et al., 2019). Moreover, AuNp conjugates of curcumin, turmeric, quercetin, and paclitaxel were tested in BC cells (MCF7 and MDA-MB-231), show significant anticancer effects (Vemuri et al., 2019).

In the current work, we aim to prepare phytochemical conjugated AuNps. After a thorough literature survey of phytochemicals, we selected ethyl ferulate (ethyl 4-hydroxy-3-methoxycinnamate) (EF), ellagic acid (EA), coronarin D (CD) and epoxy azadiradione (EAZD) based on their anticancer activity, availability and structural properties such as the presence of carbonyl and enol group (Sreelakshmi et al., 2013).

While administrating phyto-nano complexes in to the biological system, nanoparticles in the size range 10-50nm can exclude the limit of renal clearance limit (40KDa) (Iyer et al., 2006). It increases the circulation time of nanoparticles. Hence these nanoparticles can easily accumulate in the tumor microenvironment via EPR effect and retain there as the tumor lacks lymphatic clearance. Further, the "protein corona" adsorbed in the surface of AuNp helps in the faster internalisation of phyto-nano complexes inside the tumor cells.

1.5 Importance of the study

Accumulating evidence has established the promising potential of phytochemicals as anti-cancer agents. A few factors that limit its efficacy are hydrophobicity and rapid clearance due to low molecular weight (Aqil et al., 2013; Mazurakova et al., 2022). Therapeutic use of phytochemicals along with nanoparticles can bypass the constraints of phytochemicals. Nanoparticles in size range of 10-50 nm exceed the limit for renal clearance (40KDa), thus improving the circulation time and target site accumulation. Owing to the EPR effect, the gap in the tumor vasculature is 100nm-2µm, enabling nanoparticles to easily permeate through these gaps and retain in the tumour site, as it lacks lymphatic clearance (Lee et al., 2014).

With this background, ethyl ferulate (EF), ellagic acid (EA), coronarin D (CD) and epoxy azadiradione (EAZD) were used as a precursor (reducing agent) for the preparation of Au nanoparticles. Moreover, ethyl ferulate AuNp complex (EF-AuNp), ellagic acid AuNp complex (EA-AuNp), coronarin D AuNp complex (CD-AuNp) and epoxy azadiradione AuNp complex (EAZD- AuNp) were used to target the TNBC cells passively via EPR. This is the first report on the synthesis and characterization

of EF, EA, CD and EAZD based nanoparticle systems for the treatment of TNBC. Our results demonstrated that the EF-AuNp, EA-AuNp, CD-AuNp and EAZD-AuNp exhibited anti-tumorigenic effects by reducing cell growth and survival, and inducing cell death of TNBC cell lines.

Objectives:

- To prepare AuNps using plant-derived phytochemicals Epoxy azadiradion, Coronarin D, Ellagic acid, and Ethyl ferulate.
- To characterize Phyto-nano complexes by various methods.
- To determine the biological activity of Phyto-nano complex in TNBC cancer cells.

CHAPTER 2

Synthesis, Characterization and Biological Activities of EF-AuNp

2.1 Introduction

Ethyl ferulate (EF) (ethyl 4-hydroxy-3-methoxycinnamate) is an alkyl ester derivative of ferulic acid, usually found in forage crops such as rice, maize and other grains (Cunha et al., 2019). It is already identified for its antioxidant, anti-inflammatory and neuroprotective activities (Pang et al., 2022). EF has been found to inhibit acute lung injury by regulating inflammatory pathways (Wu et al., 2021). EF was also studied for its suppressive effect in diabetes-induced oxidative stress and inflammation (Kaikini et al., 2021). It also has protective effects on oxidative and neurodegenerative conditions in brain cells and age-related macular degeneration by regulating retinal degeneration (Kohno et al., 2020; Scapagnini et al., 2004). Moreover, EF was shown anticancer effect in patient-derived oesophagal tumor growth by inhibiting the mTOR/AKT/p70S6K signalling pathway and on the growth of HepG2 cells mainly by inducing cellular apoptosis (Pang et al., 2022).

As it is well known that natural compounds have lower bioavailability and pharmacokinetics, we aimed to develop nanoparticles to improve the performance of EF as an anticancer agent. Accumulating evidence has established the promising potential of nanoparticles as effective therapeutics because of their high surface area, EPR, surface modifications, high accumulations, and targeted delivery (Chaturvedi et al., 2019; Ding et al., 2020; Kourani et al., 2022; Kumar et al., 2022; Shi et al., 2017; Swaminathan et al., 2021). The conventional chemotherapeutic drugs are primarily low molecular weight (less than 1KDa). It create adverse pharmacokinetics, suboptimal biodistribution, and non-targeted accumulation in various vital organs (Golombek et al., 2018). Nanoparticles in size range 10-50 nm exceed the limit for

renal clearance (40KDa), thus improving the circulation time and target site accumulation. Owing to the EPR effect, the gap in the vasculature of tumors is 100nm-2µm, enabling nanoparticles to easily permeate through these gaps and retain in the tumour site as it lacks lymphatic clearance (Lee et al., 2014). AuNps are being developed as prospective cancer therapeutic agents, with applications including drug transporters, contrast agents, photothermal agents, and radio sensitizers (Jain et al., 2012; Lim et al., 2011).

With this background, EF is used as a precursor (reducing agent) for preparing Au nanoparticles. In the present study, EF AuNp complex (EF-AuNp) was used to target the TNBC cells passively via EPR. This is the first report of using EF based nanoparticulate system for the treatment of TNBC. Our results demonstrated that the EF-AuNp exhibited anti-tumorigenic effects by reducing cell growth, and survival and inducing cell death of TNBC cell lines.

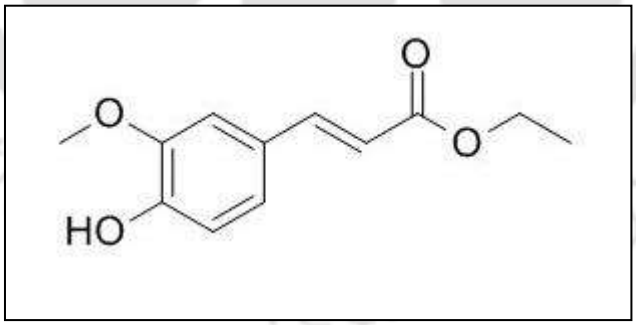

Figure 2.1 chemical structure of ethyl ferulate

2.2 Materials Used:

Gold (III) chloride trihydrate obtained from ($HAuCl_4$. $3H_2O$) Himedia, India. Dimethyl sulphoxide was purchased from Merck (Cat No. 1.16743.0521, Darmstadt, Germany) and trypsin from Gibson 2500-1072. 3-(4, 5-dimethylthiazol-2-yl)-2, 5-diphenyl tetrazolium bromide (MTT), and propidium iodide (PI) was obtained from Sigma-Aldrich, Missouri, USA). Crystal violet was purchased from SRL Pt. Ltd Cat No: 548-6209, Mumbai, India. MDA-MB-231 cells were procured from National Centre for Cell Sciences (NCCS), Pune, India. The cells were maintained in Dulbecco's Modified Eagle Medium (DMEM; Gibco™; Life Technologies, NY, USA), supplemented with 10% fetal bovine serum (FBS; Gibco®, NY, USA) and 1× Pen-Strep (Invitrogen, CA, USA) at 37 °C, 5% CO_2 and 95% humidity. Ethyl 4-hydroxy-3-methoxycinnamate (EF, $C_{12}H_{14}O_4$) was purchased from Tokyo chemical industry CO.LTD, Tokyo, Japan).

2.3 Method of preparation

As previously mentioned, the direct reduction method was used to prepare AuNps. In this chemical reduction method, EF is the reducing agent to reduce gold chloride into AuNps.

A stock solution of 5mM gold chloride was prepared in Milli Q water, and 0.01Methyl ferulate was also made in DMSO separately. Further, 1ml EF was added dropwise into 10ml gold chloride while stirring and heating (40^{o}C). This solution was heated for 10 minutes, then diluted with 30ml water. This was again heated for 10 minutes,

which resulted in a change in colour to purple. The obtained colloidal solution was kept at -80ºC for 24hrs and lyophilised for two days to obtain powdered nanoparticles.

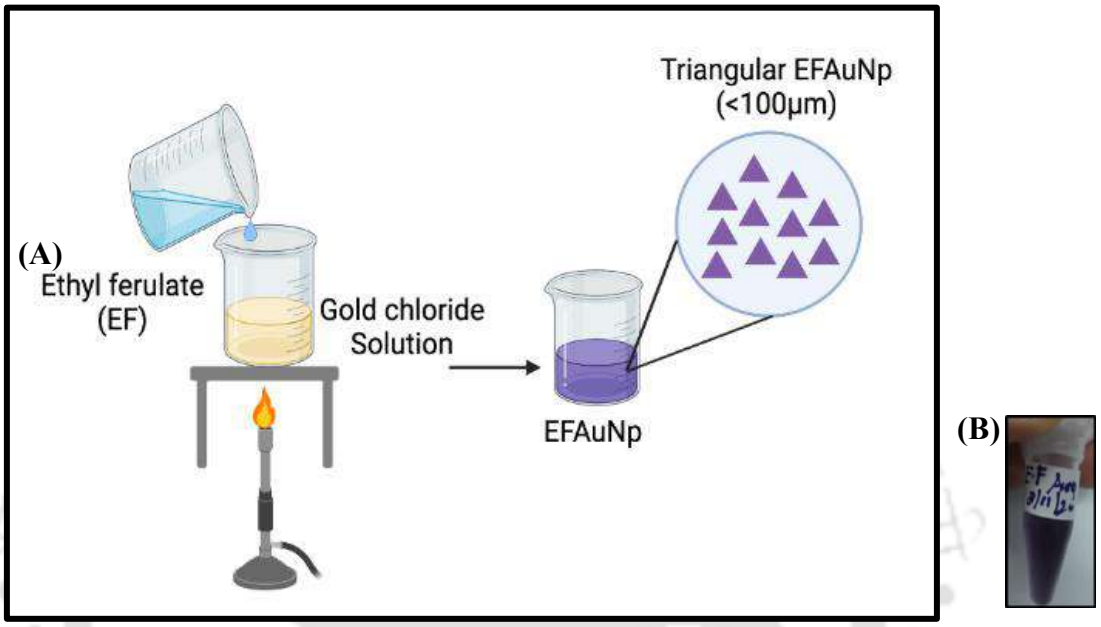

Figure 2.2: Method of preparation of EF-AuNps

2.4 Characterization of AuNps

The prepared nanoparticles were further processed for characterization and morphology analysis. The formation of AuNps was confirmed by UV-visible spectroscopy, X-ray diffraction spectroscopy, Energy dispersive X-ray analysis (EDX), and Selective area diffraction pattern (SAED) studies. Morphology studies were done using Transmission electron spectroscopy (TEM). Fourier Transform Infrared- Spectroscopy (FT-IR) analysed the formation mechanism of AuNps. The biological effect of EF-AuNps on the MDA-MB-231 was analysed using MTT assay,

colony formation assay, PI, fluorescence-activated cell sorting (FACS) assay, and live/ dead assay.

2.4.1 UV-visible spectroscopy

UV-Visible spectroscopy was performed to analyze the surface plasmon peak for AuNps (Tecan Infinite 200 PRO multimode reader (Switzerland), within the wavelength range 400-800nm. Upon irradiation with the visible spectrum, the oscillating electric field induces the oscillation of conduction band electrons. As the conduction band electrons get displaced from the nuclei, a restoring columbic attraction arises to pull it back. Depending upon the size, shape, and the surrounding medium a resonance oscillating condition generates in the electron cloud. This oscillation is called localized surface plasmon resonance (LSPR) (Alkilany and Murphy, 2010b; Eustis and el-Sayed, 2006; Kelly et al., 2003).

2.4.2 X-Ray Diffraction Spectroscopy (XRD) and selective area diffraction pattern (SAED)

XRD is a very powerful tool to characterize AuNps. XRD data confirms the formation of AuNps as it matches with the JCPDS (Joint Committee on Powder Diffraction Standards) file no No.00-004-0784 for AuNps. XRD patterns were recorded on a powder X-ray diffractometer (Rigaku, Japan Model: Micromax-007HF) with Cu Kα1 radiation (λ = 1.54060 Å) with the instrument being operated at 40kV and 40 mA. SAED pattern shows bright circular rings corresponding to the crystalline planes of AuNps. SAED was performed in Model: JEM 2100 Jeol, Peabody, MA, USA. XRD and SAED pattern confirms the crystalline nature of the prepared AuNp without phase impurity.

2.4.3 Energy dispersive X-ray analysis (EDX)

EDX was performed using JEOL, Model: JEM 2100, Peabody, MA, USA. to confirm the formation of EF-AuNps.

2.4.4 Transmission electron microscopy (TEM)

TEM image was acquired to study the size and surface morphology of the prepared AuNps using JEOL, Model: JEM 2100, Peabody, MA, USA, which was operating at a maximum accelerating voltage of 200keV. For the transmission electron microscopy (TEM) analysis, 10µL of the sample was drop-cast to a carbon-coated copper grid and air-dried overnight.

2.4.5 Fourier Transform Infrared- Spectroscopy (FT-IR)

FT-IR patterns of EF and EF-AuNp were recorded to analyze the mechanism of formation of AuNps. FT-IR measurements were taken from 400 to 4000 cm^{-1} with a Perkin Elmer spectrum 2 device.

2.4.6 Cell proliferation assay

The cell viability of MDA-MB-231 cells on treatment with EF and EF-AuNp was determined using MTT assay. In short, 2,000 cells per well were seeded in 96 well plates and incubated for 24 hours and added different concentrations of EF and EF-AuNp (10, 50, and 100µg/ml). The MTT assay was performed fort 24 hours and 72 hours. After incubation, 10µl of 5mg/ml of MTT solution was added to each well and again incubated for 2 hours. Subsequently, culture medium was removed and 100µl of DMSO was added to all the wells and incubated at ambient temperature for one hour to liquefy the MTT-formazan product. Finally, the absorbance of the colour

solution was measured with Molecular Devices Spinco Biotech Plate reader at 570nm. The inhibition induced by EF and EF-AuNp on the growth of MDA-MB-231cells represented as the percentage of viability.

2.4.7 Colony-forming assay

The clonogenic potential of MDA-MB-231 cells was analysed with the help of a colony formation assay. Briefly, a 6 well plate was seeded with MDA-MB-231 cells cultured in DMEM media (500cells/well). The cells were treated with EF and EF-AuNp in two different concentrations 5µg and 15µg each. Untreated wells were considered as control and monitored for colony formation for 7 days. After the formation of colonies, the media was discarded and given a gentle wash with PBS (1X). Ethanol fixation was done for two hours. Afterwards, crystal violet stain was added to each well and incubated for 2 hours. The extra stain was removed by washing with PBS (1X), and the photograph was taken. The plating efficiency was calculated as follows:

PE, Plating efficiency = (Number of colonies counted/ Number of cells plated) × 100

SF, Survival fraction = (PE of treated sample/ PE of control) × 100 (Bordoloi et al., 2020)

2.4.8 PI-FACS assay

To verify the efficacy of EF and EF-AuNp on cytotoxicity of MDA-MB-231 BC cells, PI-FACS assay was performed. Precisely, 6-well plate was seeded with 5X 10^4 cells and incubated for 24 hours, and subsequently treated with EF and EF-AuNp in two different concentrations (25 and 75µg/ml) for 72 hours. Next to incubation, the cells

were washed with 1X PBS, trypisinised, and then collected. Further, the cell suspension was centrifuged at 4000 rpm for 10 minutes at 40ºC. The supernatant was discarded, and the pellet was washed with 1mL 1X PBS and centrifuged again, and the step was repeated twice. Final pellet was resuspended in 495 µl of PBS, and 5 µl of PI dye was added. The cells were then analysed in the flow cytometer (BD FACS Celesta™, Becton-Dickinson, New Jersey, USA) (Aswathy et al., 2021).

2.4.9 Live and dead assay

To further confirm the effect of EF and EF-AuNp on cell death of MDA-MB-231 BC cells, the live and dead assay was performed using an inverted fluorescence microscope. Approximately, $2x10^3$ cells were seeded in a 96-well plate and incubated for 24 hours, followed by treatment with EF (75µg/ml) and EF-AuNp (75 µg/ml) for 72 hours at 37°C. After the incubation time, the cells were stained with the live and dead reagent (5 µM ethidium homodimer and 5 µM calcein-AM) and incubated at 37°C for 20 minutes. Cells were then analysed, and images were captured using an inverted fluorescence microscope (Olympus, Japan) (Aswathy et al., 2021).

2.4.10 Statistical analysis

Graph pad prism (version 9.2) was used for statistical analysis. Experiments were carried out in triplicates, with data reported as mean ± standard deviation. Statistical significance was denoted as * $p<0.05$, ** $p<0.01$, *** $p<0.001$.

2.5 Results

2.5.1 Synthesis and characterization of EF-AuNp complex

EF has been reported to possess wide pleiotropic and pharmacological properties. However, its high hydrophobic nature and poor bioavailability limit its potential as an anti-cancer drug. In the present study, we synthesized EF AuNps using green synthesis approach by mixing 0.01M EF with gold chloride solution and continuous stirring and heating at 40^0C. The shift in colour of the solution from pale yellow to purple indicates the reduction of Au^{3+} to Au°. The UV-visible spectrum of EF-AuNps validated this result, showing the characteristic absorption peak at 560nm (Figure 2.3A).

To confirm the formation of AuNps and their crystal structure, XRD was performed, which reported distinct peaks at 38.18°, 44.39°, 64.58°, 77.55°, 81.7° corresponding to face-centred cubic AuNps as shown in Figure 2.3B. The diffraction peak at 38.1° indicates the preferred growth of Au^0 gold was preferred in the (111) direction. Notably, one intense unassigned peak at 58° corresponded with the crystallization of the bio-organic phase on the surface of nanoparticles (Juibari et al., 2015; Kumari and Philip, 2013).

SAED pattern of EF-AuNp showed (Figure 2.3B) four diffraction rings corresponding to four different crystal planes in the face-centred cubic structure. Rings from inner to outside correspond to the standard Braggs reflection of (111), (200), (220), and (311) lattices. The TEM images and the HR-TEM of EF-AuNp are represented in Figures 2.3D and E.

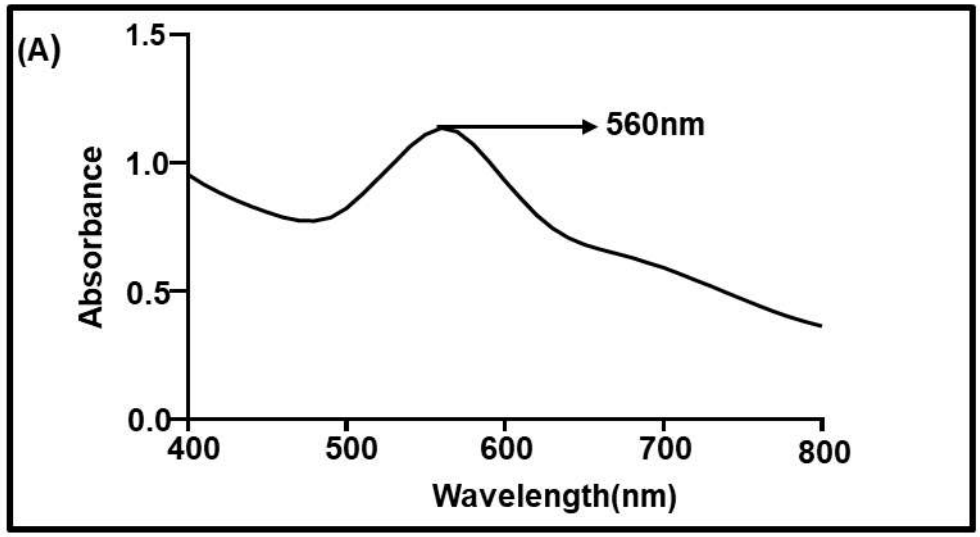

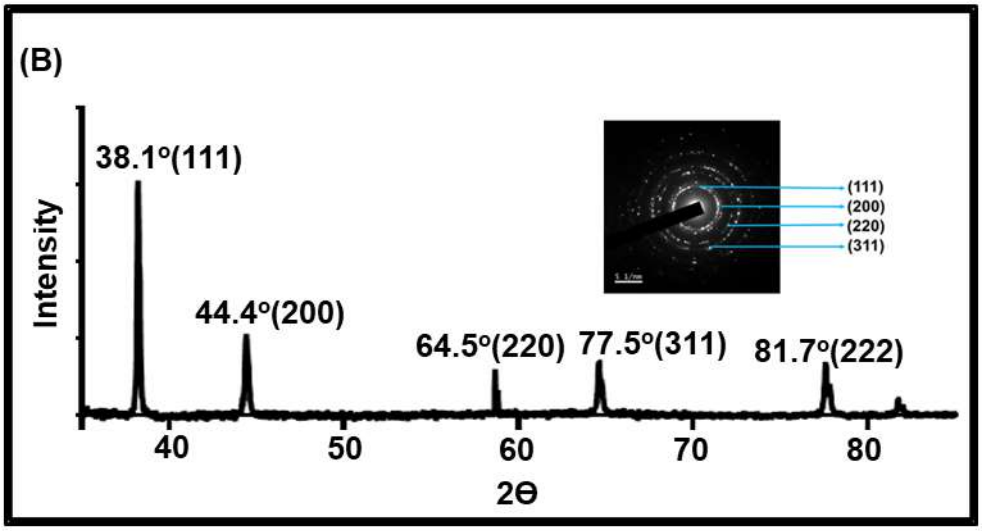

Figure 2.3: Characterization of EF-AuNp. (A) UV–vis spectrometric analysis of the EF-AuNp which exhibited the absorbance at 560nm, (B) XRD analysis of EF-AuNp, where nanoparticles are represented by five characteristic peaks corresponding to standard face centers cubic lattice. The intense peak at 38.1 and the unidentified peak at 58° show the synthesis of the EF-AuNp in the (111) direction. In addition, the SAED pattern of EF-AuNp shows four diffraction rings corresponding to four different crystal planes

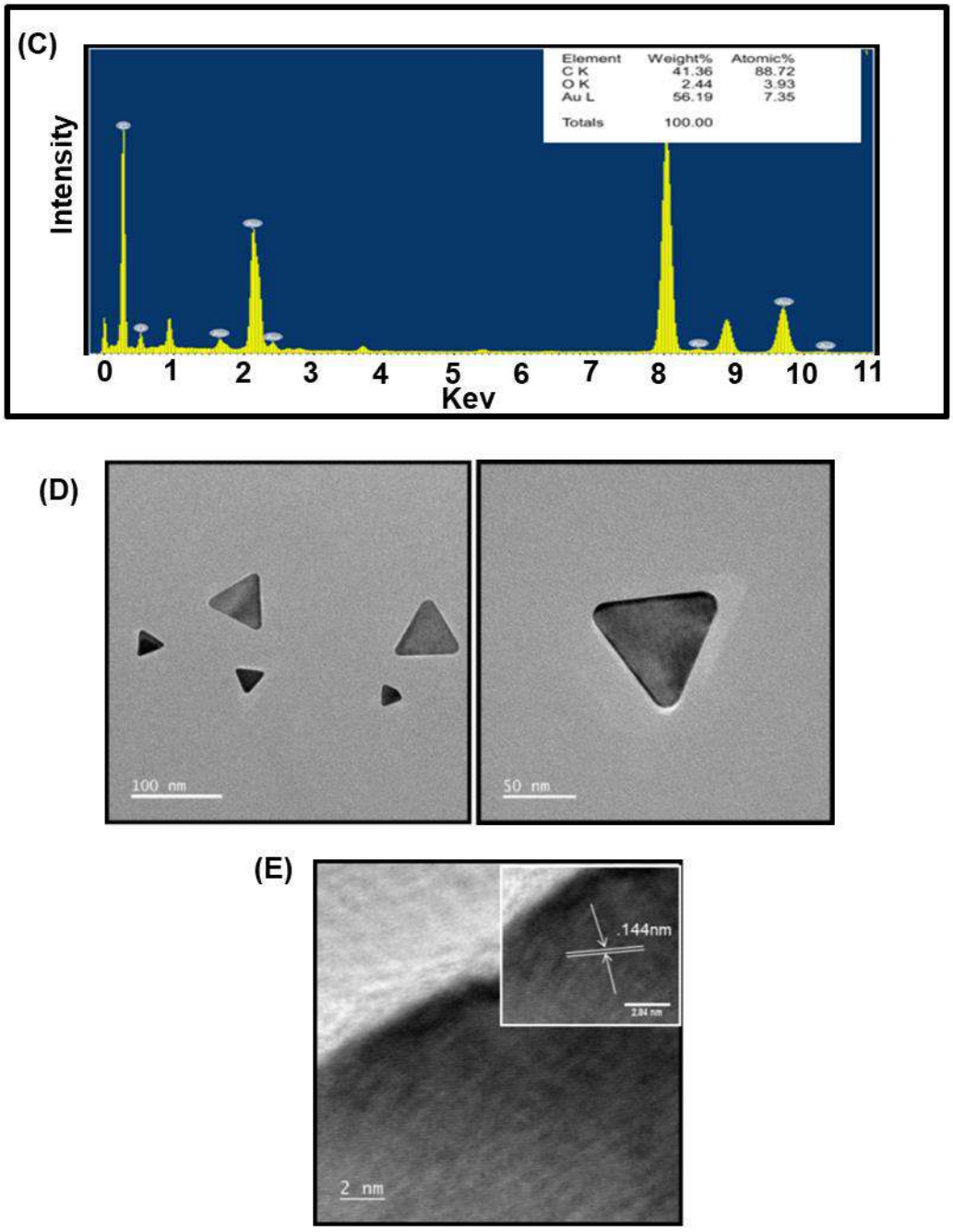

Figure 2.3: (C) Elemental analysis using EDX of the EF-AuNp depicting varied peaks for C, O, and Au. TEM images of EF-AuNp which exhibited a triangular-like morphology at (D) 100 nm, (E) 50 nm, (F) the HR-TEM images of the EF-AuNp with the fringe spacing shown around 0.144 nm.

TEM images indicated that most of the particles had triangular morphology. Though the particles are polydispersed, all are below 100nm. The fringe spacing measured from the HR-TEM image was around 0.144 nm, corresponding to the (220) plane of the face-centered cubic (FCC) (Figure 2.3 D-F).

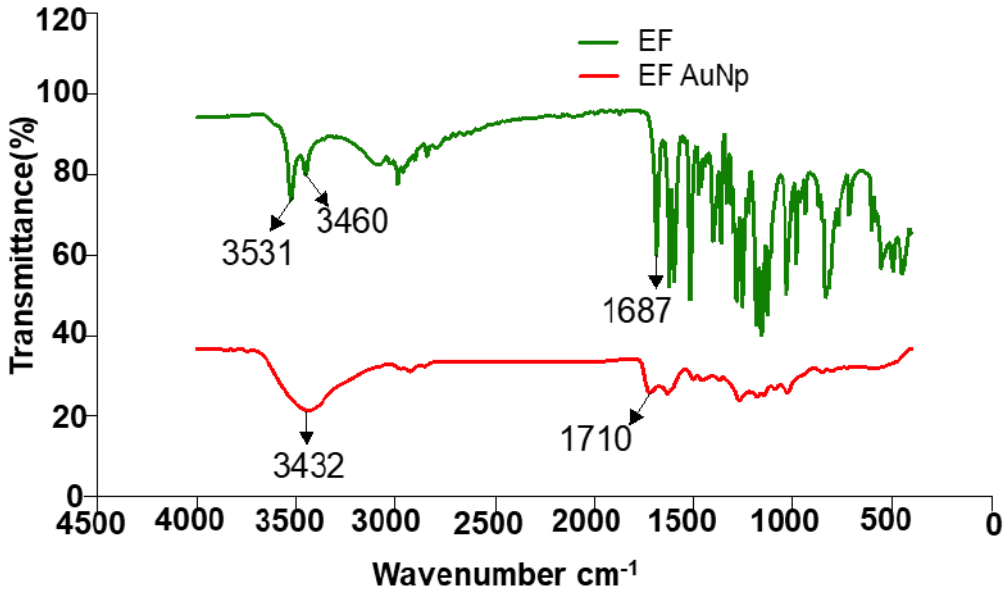

Figure 2.4: FTIR analysis of bare EF and EF-AuNp. FTIR graphs of EF-AuNp revealed the peak broadening at 3432 cm^{-1} nm and shifter carbonyl group peak at 1710 cm^{-1} confirming the formation of EF-AuNp systems.

The FT-IR spectrum of EF showed a carbonyl group stretching peak at 1687 cm^{-1}. In contrast, the FT-IR spectrum of EF-AuNp showed a suppressed carbonyl peak at 1710 cm^{-1} and a O-H broadened peak at 3432cm^{-1} as in Figure 2.4, validating the successful synthesis of the nanoparticle systems. The shift in the carbonyl group peak in a wide band indicates the shift in the frequency of the group after the oxidization of the carbonyl group into the hydroxyl group during the bio reduction of Au^{3+} to Au° (Basha et al., 2010; Kasthuri et al., 2009b; Sreelakshmi et al., 2013).

2.5.2 Anti-proliferation effect of EF-AuNp complex,

Following the successful synthesis of AuNp, we tested the antiproliferative effect of EF-AuNp on aggressive triple-negative BC cell line MDA-MB-231. MTT assay revealed that treatment with increasing concentrations of EF and EF-AuNp reduced the proliferation rate of MDA-MB-231 cells as indicated in Figure 4A. Interestingly, a drastic reduction of cell proliferation rate with increasing drug concentration (30% greater reduction at 10 µg, 75% at 50µg and 80% at 100 µg/ml) were observed with the treatment of EF-AuNp compared to EF treatment. The IC_{50} for EF-AuNp complex was found to be 18µg/ml in MDA-MB-231 cells (Figure 2.5A).

Further, we determined the effect of EF and EF-AuNp on the clonogenic potential of MDA-MB-231 cells. Colony formation assay revealed that both EF and EF-AuNp treatment at 5µg/ml concentration reduced clonogenicity of MDA-MB 231 cells to 40% while treatment at 15 µg/ml concentration showed 50% reduction in EF treated MDA-MB-231 cells and 90% in EF-AuNp treated MDA-MB-231 cells (Figure 2.5B-4). This indicates that EF-AuNp systems have higher anti-clonogenic potential that bare EF treatments. These results showed that the EF-AuNp complex inhibits the proliferation and survival of TNBC cells.

2.5.3. Effect of EF AuNp complex on cell viability

Subsequently, we performed PI-FACS to determine the effect of EF-AuNp complex on MDA-MB-231 cells viability. Our analysis showed EF at 25µg/ml concentration induced ~10% cell death whereas EF-AuNp at the same concentration showed 35% cell death.

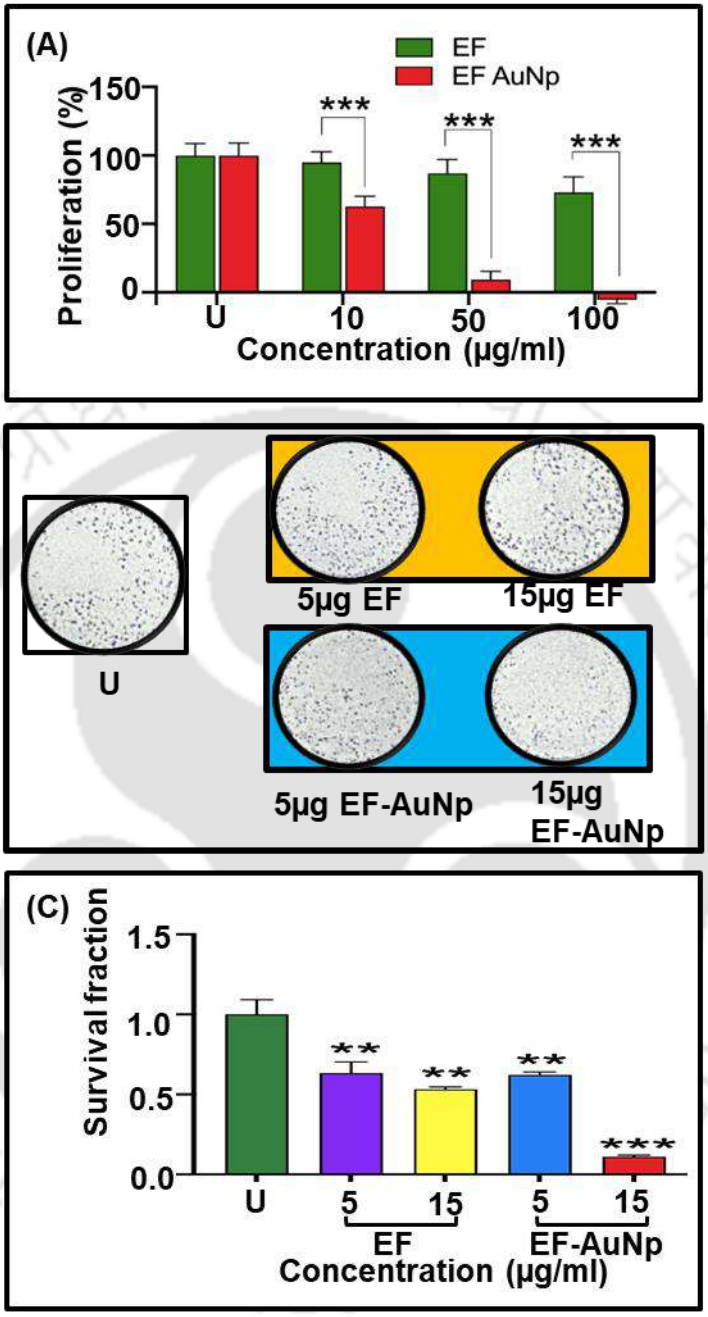

Figure 4: *In vitro* cellular studies of EF and EF-AuNp as anti-proliferative and anti-clonogenic agents on MDA-MB-231 breast cancer cell line. (A) Cytotoxic assay analysis depicting anti-proliferative attributes of EF and EF-AuNp treatment in MDA-MB-231 cells in response to increasing concentrations of drug-treated for 24 and 72 hours, (B) Colony formation assay revealed the anti-clonogenic potential of EF and EF-AuNp with increasing drug concentrations (5 and 15 µg), (C) Quantification of the colony formation assay using the Image J software for both EF and EF-AuNp treatments.

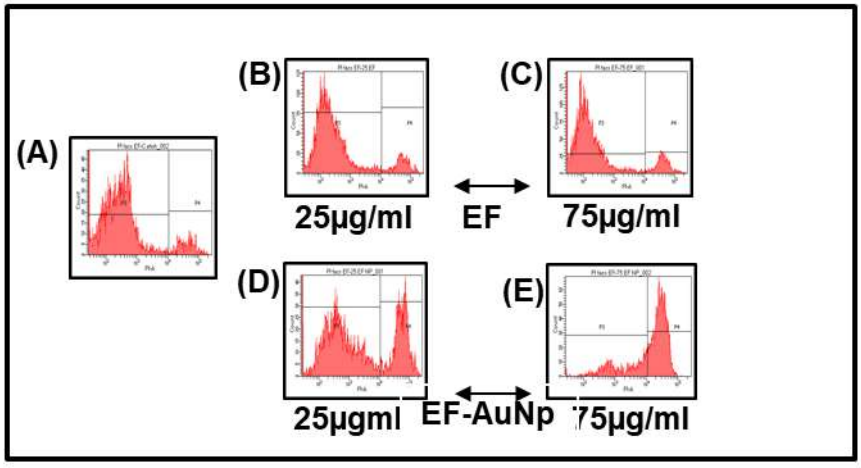

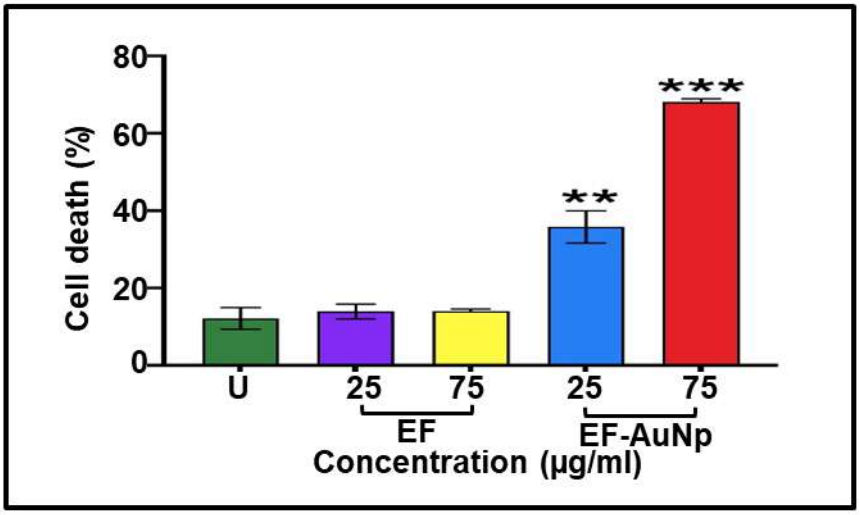

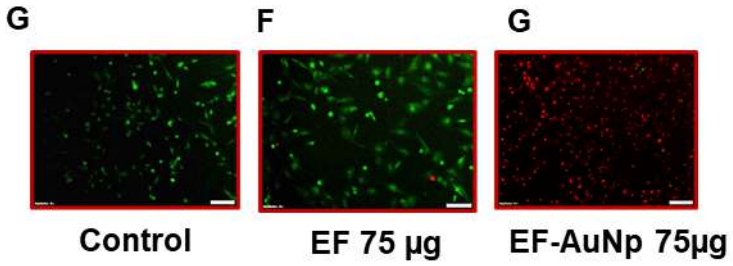

Figure 5.6: *In vitro* cellular studies of EF-AuNp on cell death in MDA-MB-231 breast cancer cell line. (A-E) PI-FACS assay following the treatments of EF and EF-AuNp at different concentrations (25 and 75µg) for 72 hours, **(F)** Quantification of the PI-FACS assay revealed the induction of cell death by the treatment of EF and EF-AuNp, (**G-I**) Live dead assay to assess cell death of MDA-MB-231 breast cancer after treatment with EF and EF-AuNp at 75µg treatment. Images were taken at 10X magnification.

The increase in the concentration of EF-AuNp to 75µg induced 70% of cell death while EF at this high concentration was able to induce only 10% cell death (Figure 6A-F). Hence, this flow cytometry analysis revealed that EF-AuNp induced around 3.5-7-fold greater cell death compared to the phytochemical EF alone. Furthermore, live/dead cell assay revealed EF AuNp induced greater cell death compared to EF at 75 µg/ml concentration as represented in Figure 6G-I. Taken together, our results demonstrated that the EF-AuNp complex possesses a significant cytotoxic effect compared to EF alone on the MDA-MB-231 cell line.

2.6. Discussion

This is the first report on the use of EF as a reducing agent in the synthesis of AuNps. The completion of synthesis of EF-AuNp in the solution was indicated initially by the transformation from yellow to purple colour. This color shift is due to the surface plasma resonance (SPR) exhibited by the formation of AuNps (He and Lu, 2014). Moreover, the UV-visible spectroscopy showed that the characteristic SPR band was located at 560 nm. The SPR band is reported to occur in the 510-560 nm region for the aqueous synthesis of AuNps (Shankar et al., 2004). These results obtained were comparable to the typical reports on AuNps synthesis (Basha et al., 2010; Kasthuri et al., 2009a). The XRD spectra revealed intense peaks indexed to (111), (200), and (220) planes at 2θ = 38.18°, 44.39°, 64.58°, 77.55°, and 81.7° confirming their crystalline structure. The SAED pattern for these nanoparticles revealed prominent rings corresponding to (111), (200), and (220) planes which in turn confirmed the crystalline feature of biosynthesized AuNps and is in line with the results obtained from other XRD studies of the AuNps (Krishnamurthy et al., 2014). EDX profile of

this synthesized compound revealed strong signals for gold atoms with a prominent absorption peak at 2-3KeV. These results concurred with the previous investigations (KS et al., 2016; Shankar et al., 2004; Uzma et al., 2020). TEM images confirmed the triangular morphology of nanoparticles and the crystalline structure of AuNps was further confirmed by the distinct lattice fringes that emerged in HR-TEM images.

Furthermore, the FT-IR spectra obtained from the synthesized complex showed carbonyl group stretching peak at 1710 cm^{-1} and a broadened OH peak at 3432 cm^{-1}. Moreover, the carbonyl group stretching of EF at 1687 cm^{-1} showed a shift and broadening of the peak at 1710 cm^{-1} in EF-AuNp, indicating the successful reduction and stabilization of AuNps with the carbonyl groups of the EF. The additional EF characteristic peaks are also present in FT-IR spectrum of AuNps, showing that the phenolic compounds from EF are capped on the surface of the produced nanoparticles (Clichici et al., 2020b).

In order to evaluate the therapeutic efficacy of the nano-bio drug, we tested the cytotoxicity and cell viability of EF-AuNp on triple-negative BC cell line MDA-MB231 cells. The MTT assay showed treatment of EF-AuNp induced nearly 80% reduction in cell proliferation of MDA-MB-231 cells compared to EF alone. Additionally, EF-AuNp-treated MDA-MB-231 cells' clonogenic potential was 5 times lesser than EF-treated cells. Propidium iodide-based flow cytometry analysis and live and dead cell assay revealed that EF-AuNp induced cell death of MDA-MB-231 cells which is in accordance with our MTT and colony formation assays. These results indicated that biosynthesized EF-AuNp with a size of less than 100nm are potent anti-cancer agents compared to EF alone. Thus, this demonstration of a proof of concept

enumerates the way for a promising alliance of natural compounds and nanotechnology as next-generation cancer therapeutics.

2.7 Conclusion

In the current study, we have reported the preparation of AuNps using EF as a reducing agent and investigated its anticancer activities in MDA-MB-231 cells. In this study, we prepared a triangular EF-AuNp complex (<100nm) by direct reduction method with mild reaction conditions using a green synthesis approach. Structural characterization by XRD, EDX, and FT-IR confirmed the formation of highly crystalline and extremely pure AuNps. In addition, our *in-vitro* studies demonstrated that triangular EF-AuNp complex inhibited the growth of MDA-MB-231 cells by inducing a reduction in proliferation, clonogenic potential, and by inducing cell death compared to the phytochemical EF alone. The EF-AuNp developed in this study has significant potential to be used in various therapeutic applications. However, studies examining molecular pathways and the *in-vivo* parameters of EF-AuNp treatments such as transport, bioavailability, intoxication, or inactivation and accumulation of AuNps in the biological system need to be conducted for further validation of these findings.

CHAPTER 3

Synthesis, Characterization and Biological Activities of EA-AuNp

3.1 Introduction

Ellagic acid (EA) was discovered by a French chemist Henri Braconnot in 1831 and named it “acide ellagique” (Law, 1922). EA is a naturally origin bioactive compound, polyphenolic, mainly found among eudicotyledons (Evtyugin et al., 2020; Lorenzo et al., 2019; Ríos et al., 2018). The main sources of EA are berries such as, strawberries, cranberries, blackberries, raspberries and goji berries. It is also present in grapes, pomegranates, nuts and green tea. So far, EA has been tested for many bio medical applications, including neuroprotective, cardio protective, anticancer, anti-inflammatory effects (Ahmed et al., 2016; Cozza et al., 2006; Lin and Yin, 2013; Liu et al., 2017; Liu et al., 2020; Neamatallah et al., 2020; Yüce et al., 2007). EA has been widely examined for its efficacy as anti-cancer agent in different cancers. *In-vitro* studies carried out in Caco-2, breast, and human prostatic cancer cells revealed the anti-proliferative effect of EA, though the best performance was found in Caco-2 cells (Losso et al., 2004). Another study proved the efficacy of EA against colon cancer, increased apoptosis and decreased proliferation of HCT-15 cells. Moreover, EA induces apoptosis, inhibition of cell growth and decreased cell viability in the BC cells (Jaman and Sayeed, 2018).

As the main concerns with phytochemicals are their poor bioavailability and poor solubility, nanoparticles based formulation has been synthesised to improve the efficacy of phytochemical. The anti-cancer properties of AuNps are evident as they can be engineered in different size, shape and structures (Ghosh et al., 2008; Sztandera et al., 2018). AuNps of 10-100mn can easily permeate into the cells through EPR effect and remain in the tumor due to the lack of lymphatic clearance and disordered

extracellular matrix (Lee et al., 2014). EPR effect was discussed in detail in chapter 2, this effect was used to target TNBC cells passively using EA-AuNp phytochemical complex.

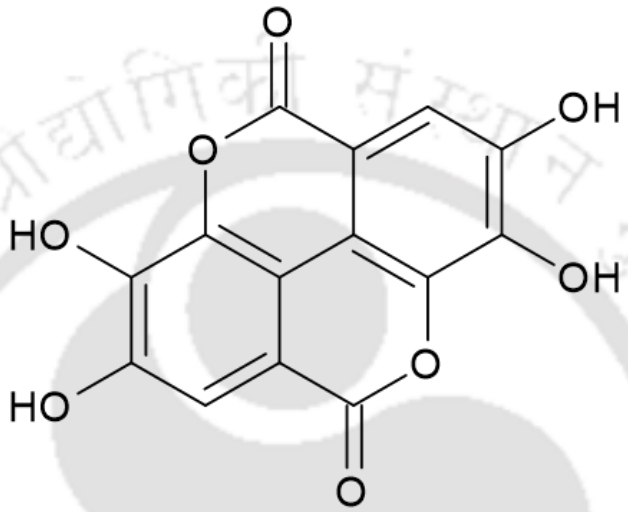

Figure 3.1 Chemical structure of EA

Within this framework, we prepared AuNps using EA as a precursor through a single-step direct reduction method. The resultant EA-AuNp complex was used to target TNBC cells passively. Our *in-vitro* studies revealed that EA-AuNp exhibited anti-proliferative effect by reducing cell growth and induced cell death in TNBC cells.

3.2 Materials used

EA ($C_{14}H_6O_8$) was purchased from Tokyo chemical industry CO.LTD, Tokyo, Japan. All other cell culture materials were same as discussed in chapter 2.

3.3 Method of preparations

For the preparation of AuNps 10ml of 5mM stock solution of gold chloride was prepared in Milli Q water, and 2ml stock solution of 0.01M EA was prepared in DMSO. 5mM gold chloride was heated at 40°C with vigorous stirring for 10 minutes followed by the addition of 0.01M EA drop wise. Subsequently, this solution was diluted with 30ml distilled water. Again heated at 40°C and stirred for 10 minutes to complete the chemical reduction process, which resulted in a colour change from light yellow to purple, the characteristic colour of AuNps.

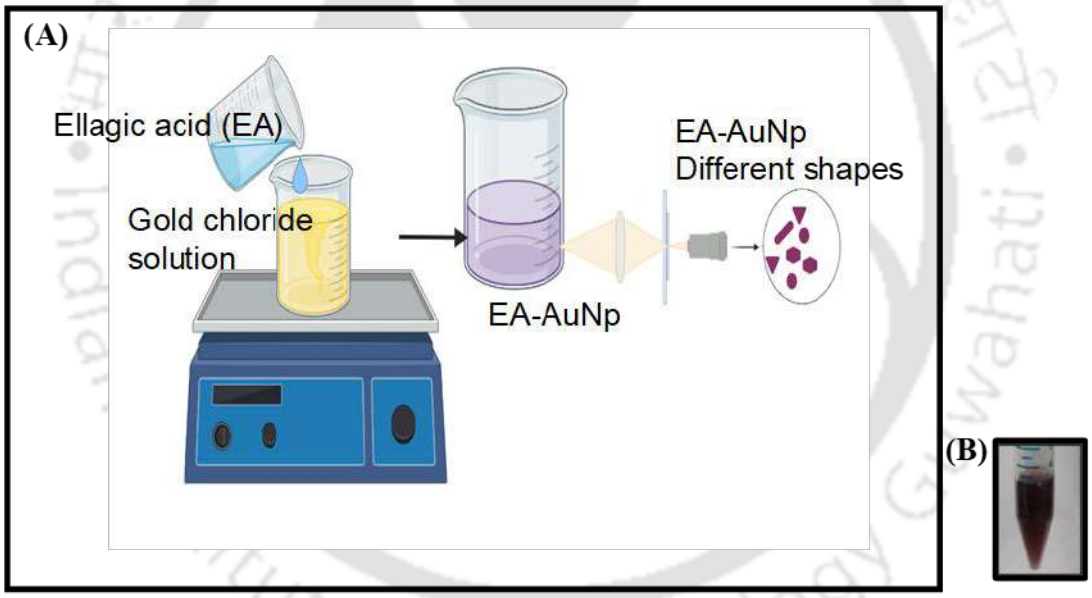

Figure 3.2 Method of preparation of EA-AuNp

3.4 Characterization of EA-AuNp

AuNps were further processed for the characterization and morphology analysis. The formation of AuNps was confirmed by UV-visible spectroscopy, XRD, EDX, and SAED studies. Morphology studies were carried out by TEM. The mechanism of

formation of AuNps was analysed by FT-IR. Further, biological effect of EA-AuNps in the MDA-MB-231 was assay, and live and dead assay.

3.4.1 Structural characterization of EA-AuNp

Structural characterization of EA-AuNps was performed using the same characteristic tools as in chapter 2. XRD, EDX, UV-visible spectroscopy, TEM and FT-IR were performed using the same machine and under the identical operating conditions.

3.4.2 *In-vitro* studies of EA-AuNp on MDA-MB-231 cells

In-vitro assays, such as MTT, colony formation assay, PI-FACS, and live and dead assay were carried using the same protocol and instrumental conditions as stated in Chapter 2 using different concentrations of EA-AuNPs. For MTT assay MDA-MB-231 cells were treated with different concentrations of EA and EA-AuNps (0 to 50µg/ml).

3.5 Statistical analysis

As discussed in chapter 2, graph pad prism (version 9.2) was used for statistical analysis.

3.6 Results

3.6.1 Synthesis and characterization of EA-AuNp complex

Formation of AuNps was confirmed initially by UV-Visible peak. Surface plasmon absorption peak for AuNps were obtained at 530nm in the visible range of electromagnetic spectrum (Figure 3.3A). XRD pattern further confirms the formation and crystallinity of the sample. XRD reflection peaks were obtained at 38.2°, 44.4°, 64.6°,77.6°,81.6°, corresponds to FCC AuNps (Bindhu and Umadevi, 2014). High

intense peak at 38.2^{o} indicates the growth of nanoparticles predominantly in (111) direction. Absence of additional peaks in the spectrum underlined the high purity of the material (Figure 3.3B). SAED pattern showed four diffraction rings corresponds to (111), (200), (220), (311) planes from inner to outer, respectively, characteristic of polycrystalline structure. To further verify presence of EA along with the AuNp quantitatively, EDX profile was studied. EDX spectrum showed distinct peaks for Au, C, and O elements, presence of carbon and oxygen peak along with AuNps verified the presence of phytochemical in the sample. Very intense peak at 6KeV was from copper, arises from copper grid. Absorption peaks at ~2 KeV is typical for the absorption of metallic AuNps in agreement with previously reports (Fayaz et al., 2011) (Figure 3.3C). Shape and size of the nanoparticle are crucial factors before administrating them in to cells, hence TEM analysis was performed to analyse the surface morphology of nanoparticles (Figure 3.3D and E).

TEM images revealed nanoparticles were in different shapes, including rod, triangular, hexagonal and spherical. Nano rods are nontoxic and cellular uptake is more efficient than spherical, triangular and hexagonal AuNps were also known for anticancer properties (Chithrani et al., 2006; Sztandera et al., 2018). Fringe spacing measured from HR-TEM image 0.235 nm, corresponding to the (111) plane of the FCC, indicated the preferential growth of AuNps in (111) plane (Figure 3.3F).

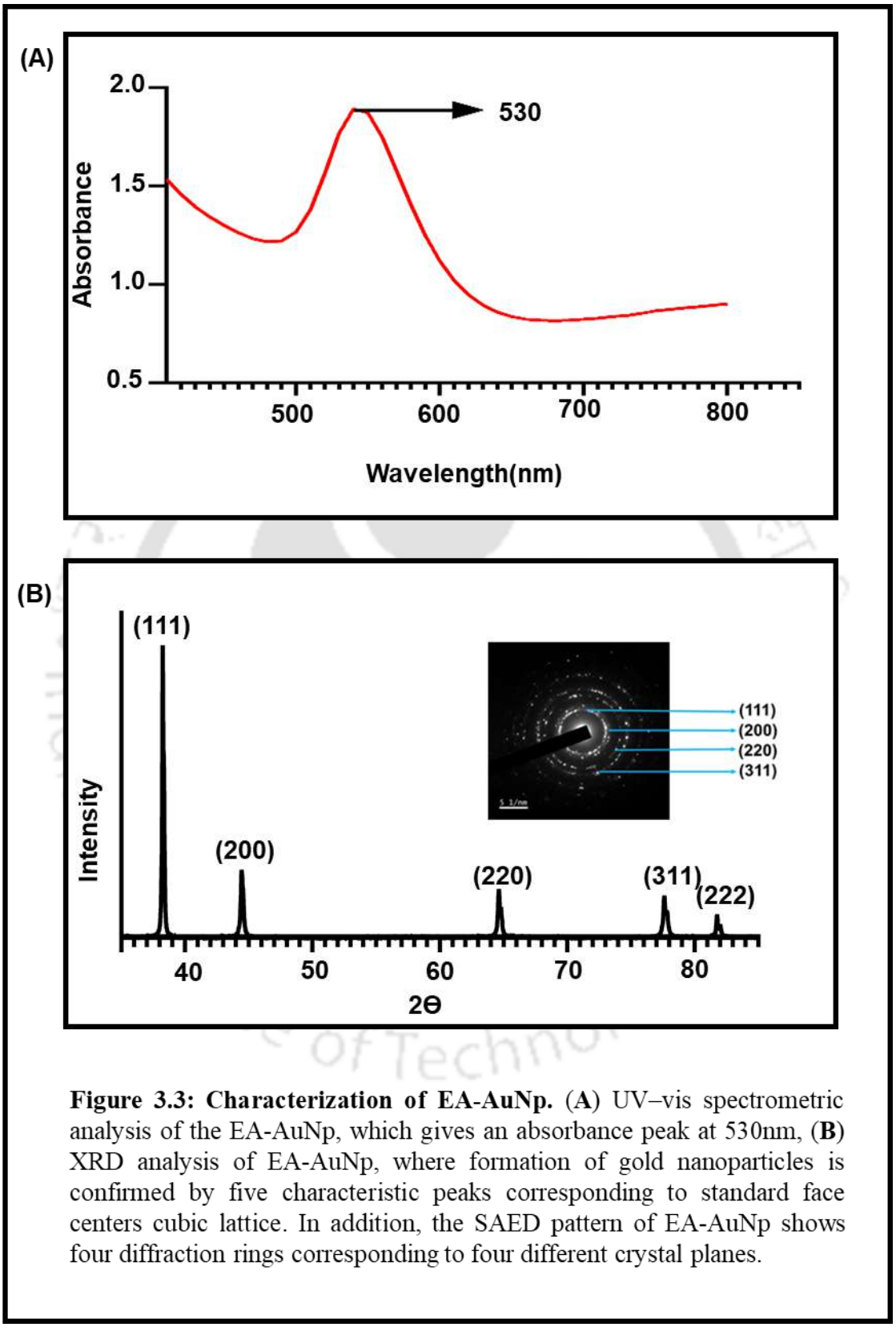

Figure 3.3: Characterization of EA-AuNp. (**A**) UV–vis spectrometric analysis of the EA-AuNp, which gives an absorbance peak at 530nm, (**B**) XRD analysis of EA-AuNp, where formation of gold nanoparticles is confirmed by five characteristic peaks corresponding to standard face centers cubic lattice. In addition, the SAED pattern of EA-AuNp shows four diffraction rings corresponding to four different crystal planes.

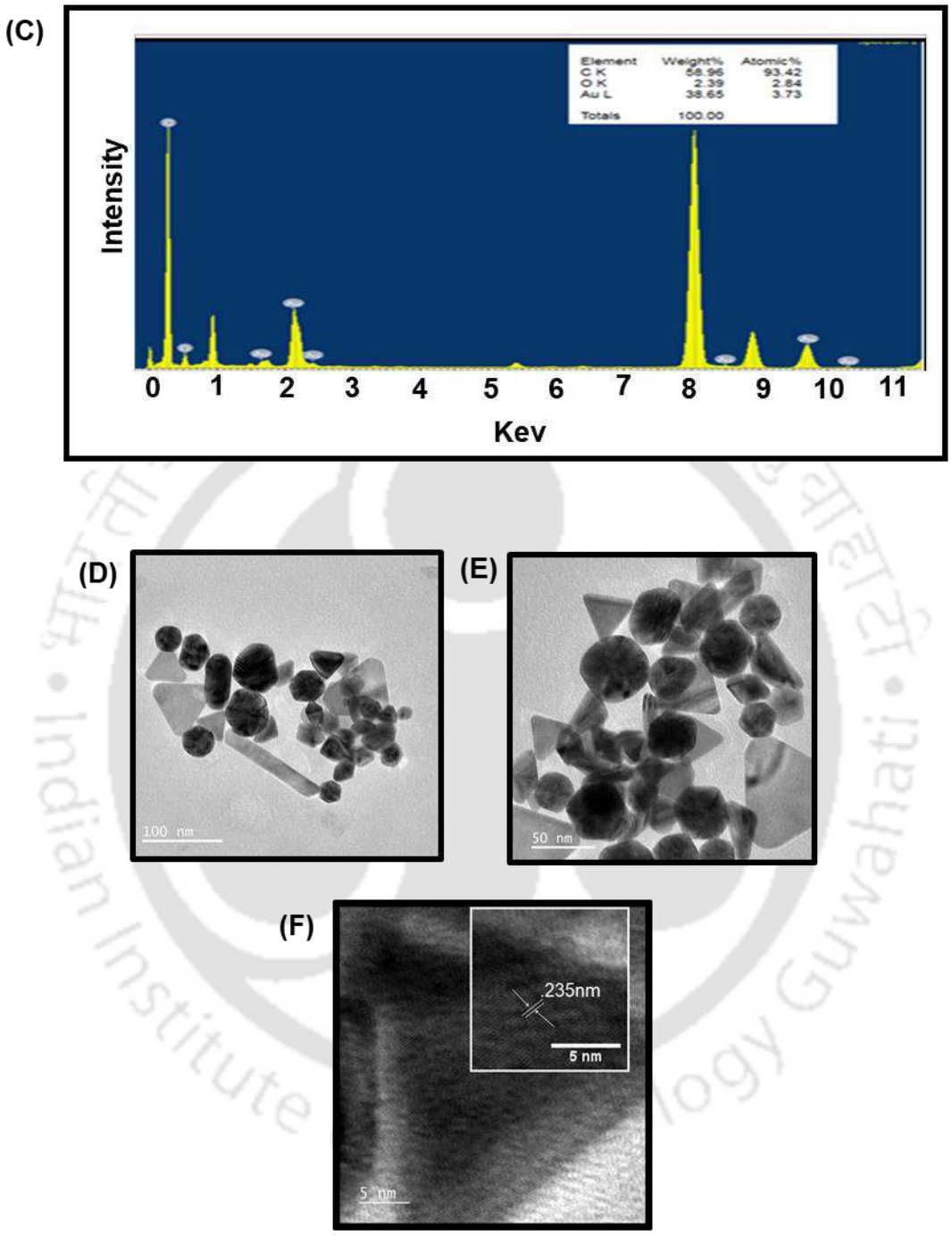

Figure 3.3 (**C**) Elemental analysis using EDX of the EA-AuNp revealing varied peaks for C, O, and Au. TEM images of EA-AuNp exhibited a triangular-like morphology at (**D**) 100 nm scale, (**E**) 50 nm scale, (**F**) the HR-TEM images of the EA-AuNp with the fringe spacing shown around 0.235nm

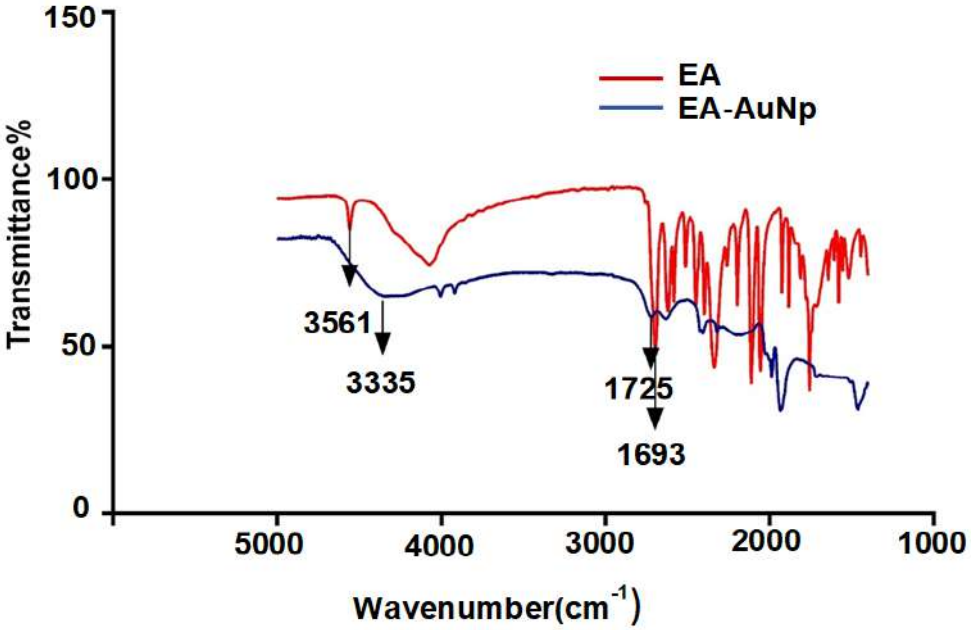

Figure 3.4: FT-IR analysis of bare EA and EA-AuNp. FT-IR graphs of EA-AuNp revealed peak broadening at 3335 cm^{-1} (OH group) and a suppressed carbonyl group peak at 1693 cm^{-1} confirming the formation of EA-AuNp systems

FT-IR spectra showed OH stretching peaks at 3561cm^{-1} for EA, while the peak got shifted and broadened to 3335cm^{-1} for EA-AuNps. It was also demonstrated that carbonyl group stretching peak for EA was obtained at 1725 cm^{-1}, whereas, the same group was suppressed and shifted to lower frequency (1693cm^{-1}) in EA-AuNp complex, signifying the successful reduction and stabilization of AuNps by carbonyl groups of the EA (Clichici et al., 2020a) (Figure 3.4).

3.6.2 Anti-proliferation effect of EA-AuNp complex

Next to structural characterization, we tested the anti-proliferative effect of EA-AuNp complex on TNBC cells. MTT assay on MDA-MB-231 cell line unveiled the anti-proliferative effect of EA-AuNp over EA, as shown in Figure 3.5.

EA-AuNp have shown a remarkable reduction in proliferation in comparison with EA, 38% more reduction at 20µg/ml and 29% higher reduction at 50µg/ml. IC_{50} obtained for EA was found to be 27µg/ml and for EA-AuNp IC_{50} was 15µg/ml. In cancer research, it is important to analyse the clonogenic potential of cells, since it is a standard tool to analyse the cellular growth and cytotoxic effect of a drug in cancer cells. EA and EA-AuNp make substantial reduction in the clonogenic potential at 5µg/ml and 10µg/ml. However, EA-AuNp induces 20% more reduction in survival fraction at 10µg/ml against EA (Figure 12B and C).

3.6.3 Effect of EA-AuNp complex on cell viability

Further, PI-FACS was performed to evaluate the effect of EA-AuNp complex on the cell viability of TNBC cell line. EA induced 35% cell death while EA-AuNp induced 66% cell death compared to control. Our studies revealed that EA-AuNps induced 30% more cell death in comparison with the phytochemical EA (figure 3.6A-D). In addition, live and dead assay revealed that at 25µg/ml EA-AuNps induced more cell death than EA at the same concentration. Overall, EA-AuNp exhibited significant cytotoxic effect compared to EA on MDA-MB-231 TNBC cell line (Figure 3.6E-G).

3.7 Discussion

In the present study, we prepared AuNps using EA as a reducing agent. This is the first report on the preparation of AuNps using EA as a precursor. Formation of AuNps was first indicated by the colour change of colloidal suspension from yellow to purple, due to the localised surface plasmon absorption peak exhibited by AuNps depending on the size and shape (Kelly et al., 2003). Experimentally, the LSPR peak

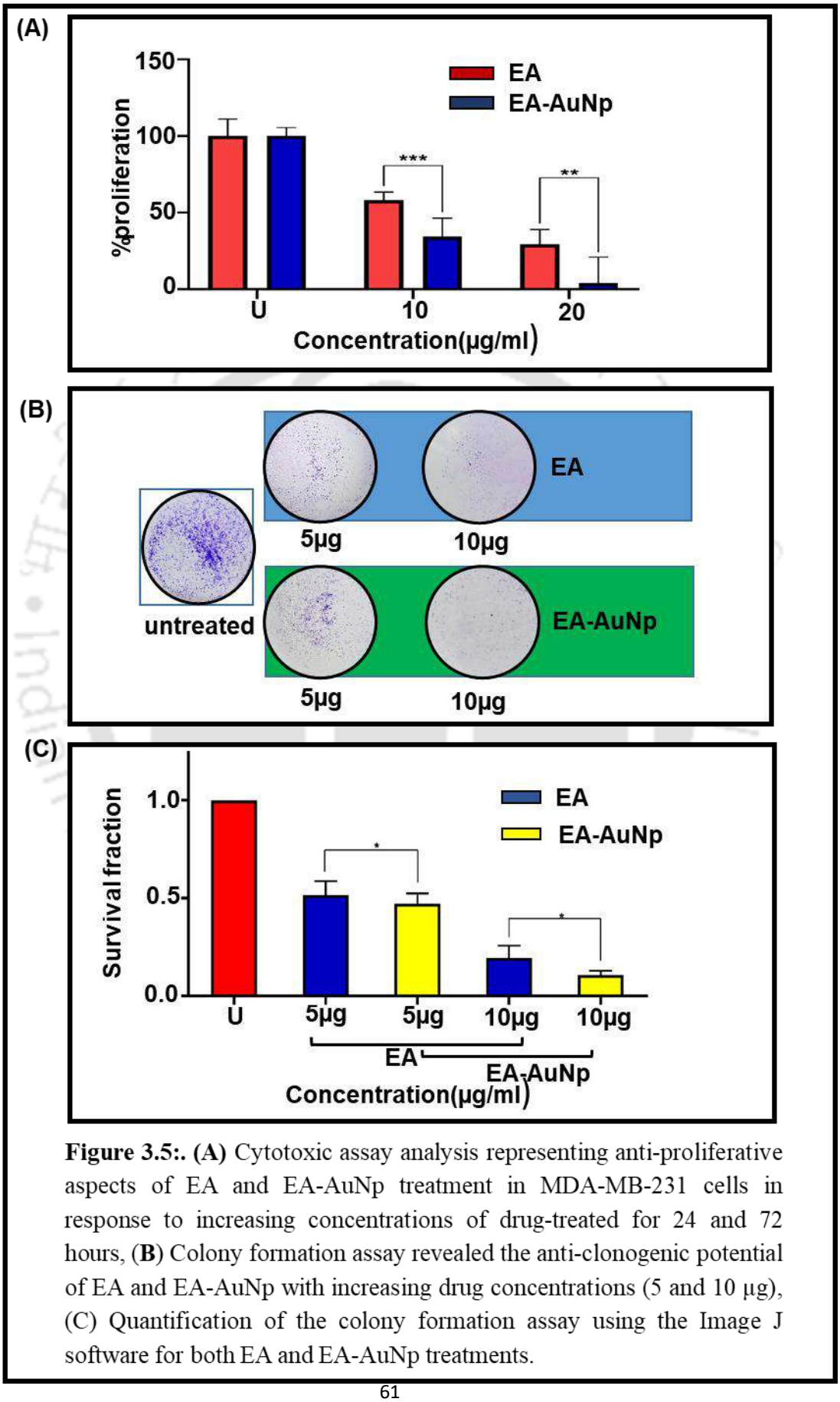

Figure 3.5:. (A) Cytotoxic assay analysis representing anti-proliferative aspects of EA and EA-AuNp treatment in MDA-MB-231 cells in response to increasing concentrations of drug-treated for 24 and 72 hours, (**B**) Colony formation assay revealed the anti-clonogenic potential of EA and EA-AuNp with increasing drug concentrations (5 and 10 µg), (C) Quantification of the colony formation assay using the Image J software for both EA and EA-AuNp treatments.

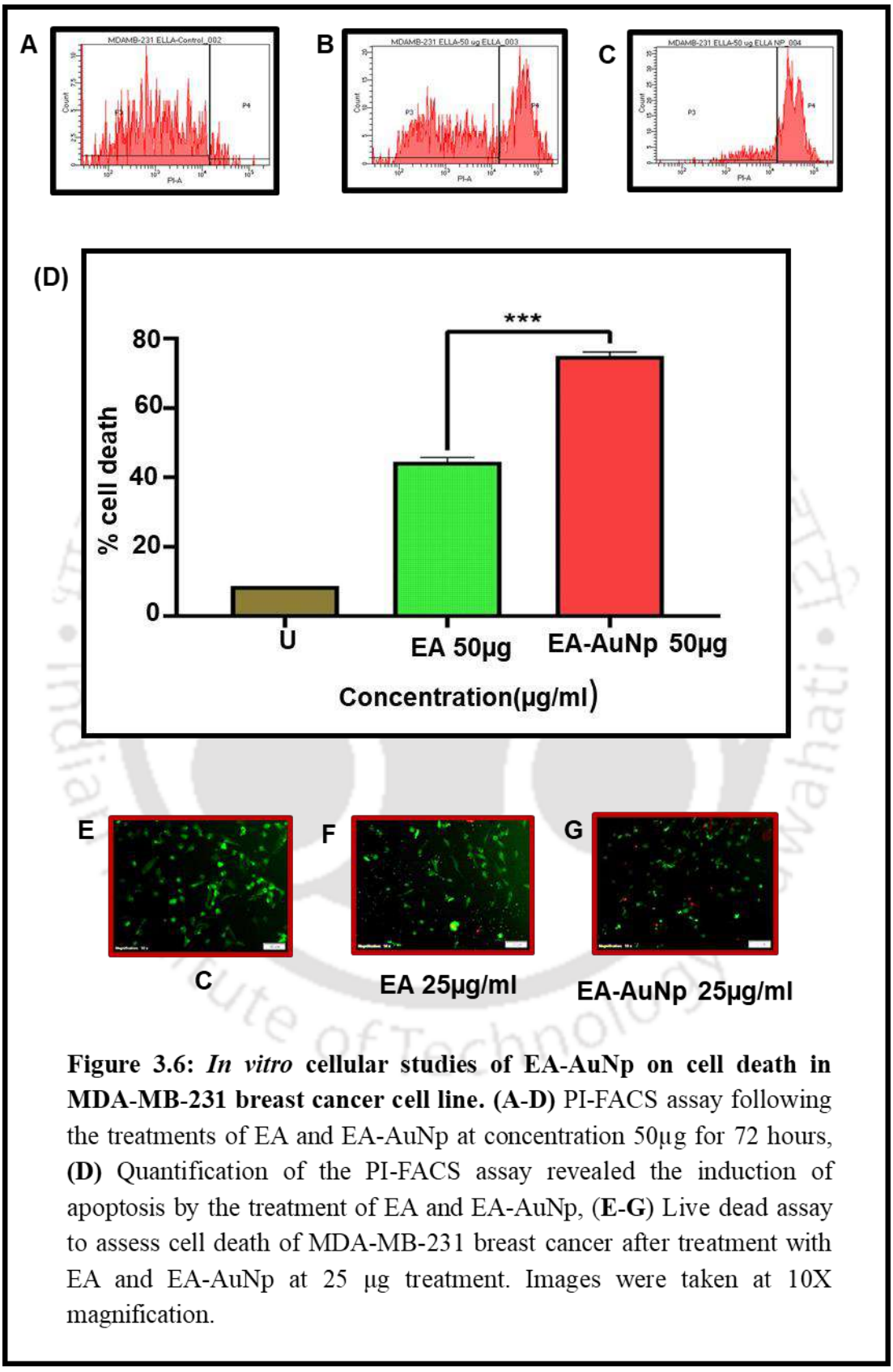

Figure 3.6: ***In vitro*** **cellular studies of EA-AuNp on cell death in MDA-MB-231 breast cancer cell line. (A-D)** PI-FACS assay following the treatments of EA and EA-AuNp at concentration 50µg for 72 hours, **(D)** Quantification of the PI-FACS assay revealed the induction of apoptosis by the treatment of EA and EA-AuNp, (**E-G**) Live dead assay to assess cell death of MDA-MB-231 breast cancer after treatment with EA and EA-AuNp at 25 µg treatment. Images were taken at 10X magnification.

was confirmed by UV-Visible absorption spectra, which showed an absorption peak at 530nm which is in agreement with previous reports (Figure 2A) (Alkilany and Murphy, 2010a; Sreelakshmi et al., 2013). XRD showed characteristic AuNp peaks at 38.2°, 44.4 °, 64.6 °, 77.6°, and 81.7 ° corresponding to (111), (200), (220), (311) and (222) planes, respectively (Figure 2B). These XRD patterns are the finger print peaks for AuNps at 2Θ angle (Baruah et al., 2018; Philip, 2010). In addition, the SAED pattern with a single set of diffraction spots indicated the same lattice orientation running across the whole nanoparticle. These patterns were indexed according to (111), (200), (220), (311) and (222) reflections of FCC gold. In this study, SAED pattern revealed four diffraction rings, implied the formation of polycrystalline AuNps. The rings (111), (200), (220), (311) corresponds to FCC gold from inner to outer respectively (Philip, 2010; Smitha et al., 2009). Additionally, EDX spectrum showed peaks for C, O and Au; carbon and oxygen peaks along with gold was a clear indication of the presence of phytochemical in the sample (Kumar et al., 2012) (Figure 2C). Further, TEM imaging was carried out to obtain highly magnified images for the synthesized AuNps. The TEM image revealed that nanoparticles were in dissimilar shapes such as triangular, spherical, hexagonal, and rod shaped. Such morphologies were previously known for their anticancer activity in different cancer cell lines (Govindachari et al., 2000). Furthermore, HR-TEM image confirmed the crystalline nature of AuNps by distinct lattice fringes with spacing of 0.235nm (111) (Figure2D-F). FT-IR spectra showed OH stretching peaks at 3561cm^{-1} for EA, while the peak got shifted and broadened to 3335cm^{-1} for EA-AuNps. It was also shown that the stretching peak for carbonyl group for EA was obtained at 1725 cm^{-1}, whereas,

the same group was suppressed and shifted to lower frequency (1693cm^{-1}) in EA-AuNp complex, signifying the successful reduction and stabilization of AuNps by carbonyl groups of the EA (Clichici et al., 2020a) (Figure 3).

In order to evaluate the anti-cancer efficacy of this nano-bio combination drug, we performed an *in-vitro* analysis in MDA-MB-231 TNBC cell line. MTT assay showed that EA-AuNp induced 38% more reduction at 10µg/ml and 29% more reduction in proliferation at 50µg/ml compared to EA (Figure 4A). In addition, clonogenic potential of the cells significantly diminished by both EA and EA-AuNp. However, EA-AuNp showed ~20% decrease in survival fraction compared to EA at 10µg/ml (Figure 4B and 4C). PI-FACS analysis also revealed that, EA-AuNp induced 30% more cell death compared to phytochemical counterpart (Figure 5A-D). Cytotoxicity effect was further confirmed by live and dead assay (Figure 5E-G) which showed similar cytotoxicity effect as in PI-FACS assay. Therefore, *in-vitro* analysis of EA-AuNps on TNBC cells verified the superior anti-cancer potential of EA-AuNp in comparison with EA. Thus EA-AuNp complex in association with conventional therapies could be used for the effective passive targeting of TNBC cells through EPR effect; however, further mechanistic studies are required to validate these effects.

3.8 Conclusion

In this study, we reported a facile, simple and biosynthetic route for the preparation of AuNps using EA as a precursor and examined its anti-cancer potential in intractable in MDA-MB-231 cells. AuNps of different shapes were synthesised using EA as a reducing agent by direct reduction method. Structural characterization using XRD, UV-visible spectroscopy, EDX, TEM and FT-IR confirmed the formation of highly

crystalline and pure AuNps along with the phytochemical EA. Our *in-vitro* studies verified the potential of EA-AuNp in reduction of proliferation, clonogenic potential and in cytotoxicity compared to EA. Thus EA-AuNp could be used as a potential anti-cancer agent in combination with TNBC therapies. However, *in-vivo* studies are critical to verify the transport, bioavailability, intoxication, and accumulation of EA-AuNps in the biological system.

CHAPTER 4

Synthesis, Characterization and Biological Activities of CD-AuNp

4.1 Coronarin D

Coronarin D (CD) was first isolated in 1988 along with coronarin A-F. These bioactive labdane diterpene structures were isolated from the rhizomes of *Hedychium coronarium*, a flowering plant of Zingiberaceae (ginger) family, commonly known as butterfly flower or butterfly ginger (Chimnoi et al., 2008; ITOKAWA et al., 1988). CD has been already identified for its antimicrobial, anti-inflammatory, anti-fungal and anti-cancer properties (Kaomongkolgit et al., 2012; Reuk-ngam et al., 2014; Van Kiem et al., 2011). Various studies have been carried out on the anticancer efficacy of CD and it is evidenced that suppressed cancer cell growth in various cell lines, such as cell cycle arrest in osteosarcoma cells (HOS and MG-63), induction of apoptosis and autophagy in nasopharyngeal carcinoma cells (NPC-BM and NPC-039), induction of apoptosis and autophagy in hepatocellular carcinoma cells (Huh7 and Sk-hep-1), induction of apoptosis in oral carcinoma cell line (SCC-9 and SAS) and induction of DNA damages and apoptosis in glioblastoma cells (U-251) (Chen et al., 2017; Hsu et al., 2018; Lin et al., 2018; Liu et al., 2019; Zhou et al., 2020). So far, there is no clear authentication for the mechanism of action of CD. Yet, it is widely accepted as a modulator of JNK (Jun N-terminal Kinase) pathway (Hsieh et al., 2020).

As a continuation of the previous chapter, to overcome the adverse pharmacokinetics and solubility issues of phytochemicals, we incorporate AuNp along with the phytochemical. Here, we used CD as reducing agent to produce AuNp from $HAuCl_4$. In the present chapter, we are hypothesising that CD-AuNp could effectively target TNBC cells through EPR effect and produce superior anticancer properties than CD.

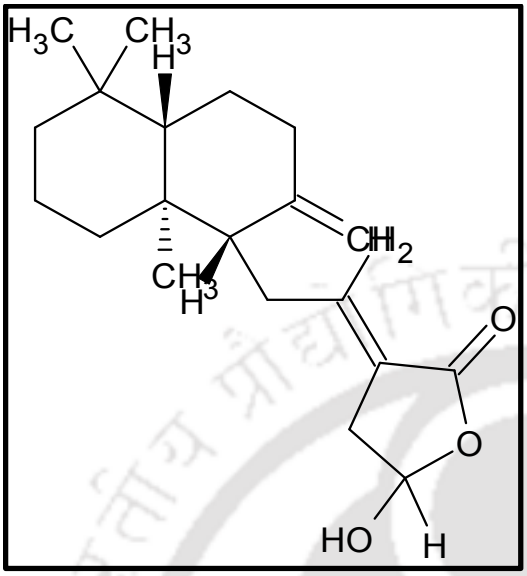

Fig 4.1 (A) chemical structure of coronarin D

Fig 4.1 (B) *Hedychium coronarium* (White ginger lily)

4.2 Materials used

CD was kindly provided by Dr. Mangalam S. Nair (Chemical Sciences and Technology Division, CSIR- National Institute for Interdisciplinary Science and Technology (CSIR-NIIST), Thiruvananthapuram, Kerala, India. All other cell culture materials used in this study were same as in chapter 2.

4.3 Method of preparation

Briefly a stock solution of 2mM CD was prepared in DMSO and 0.41mM gold chlorde was prepared in milli Q water separately. Then 1ml of CD was added dropwise in to 1ml of gold chloride solution with simultaneous stirring and heating at 40^{o}C. When CD was added to the gold chloride solution, white turbidity appeared.

The solution was again heated for 30 minutes while stirring. Slowly colour of the solution changed to purple as the reduction reaction completed.

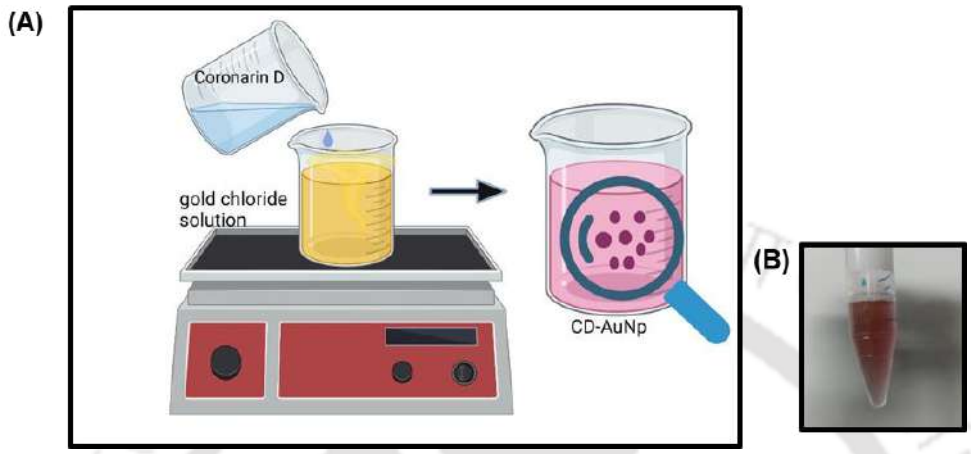

Fig 4.2 Method of preparation of CD-AuNp

4.4 Characterization of CD-AuNp

4.4.1 Structural characterization of CD-AuNp

Structural characterization of CD-AuNp complex was performed using UV-visible spectroscopy, XRD, EDX, TEM and FT-IR. All instruments and instrumental conditions are the same as in chapter 2.

4.4.2 *In-vitro* studies of CD-AuNp on MDA-MB-231 cells.

MTT assay, colony formation assay, PI-FACS and live/assay were carried out using the identical protocol, experimental conditions and instruments as in chapter 2. However, the concentration of drug was different in each experiment.

4.5 Statistical Analysis

Statistical analysis was performed as discussed in the previous chapter, with the software.

4.6 Results

A

4.6.1 Synthesis and characterization of CD-AuNp

Formation of nanoparticles was confirmed primarily by UV-visible spectroscopy and XRD. UV-Visible spectroscopy showed a narrow and high absorbance surface plasmon resonance peak at 560nm (Figure 4.3A). XRD patterns were recorded on a powder X-ray with CuKα radiation (λ=0.15418 nm) in the 2θ range of 30° to 90°. XRD the peaks at 38.53°, 44.89°, 64.76° and 77.81° corresponded to the (111), (200), (220), and (311) crystal planes of FCC AuNps, respectively (Figure 4.3B). The SAED pattern showed the diffraction ring from inner to outer which can be indexed as (111), (200), and (220), reflections, respectively of FCC gold (Figure 4.3B). EDX analysis showed the presence of a strong signal from gold atom. The presence of sharp optical absorption peak in the range of 2–3 keV is typical for the absorption of metallic gold nanocrystallites. The peaks from C and O indicate the presence of phytochemical coronarin D along with nanoparticles. However, the very high weight percentage for C is because of the presence of C in copper grid (Figure 4.3C). TEM was performed to analyse the morphology and size of the AuNps. TEM revealed that AuNps were less than 50nm and the HR-TEM displays a single particle image. The fringe spacing measured from the HR-TEM image was 0.240 nm, corresponding to the (111) plane of the FCC, which indicated that the growth of AuNps occurred preferentially on the (111) plane (Figure 4.3D-F).

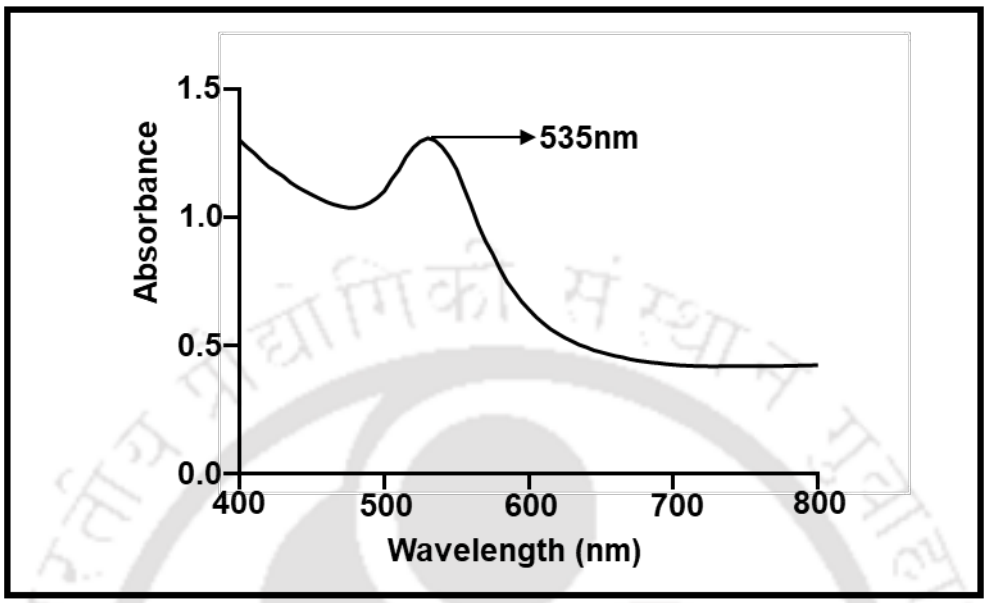

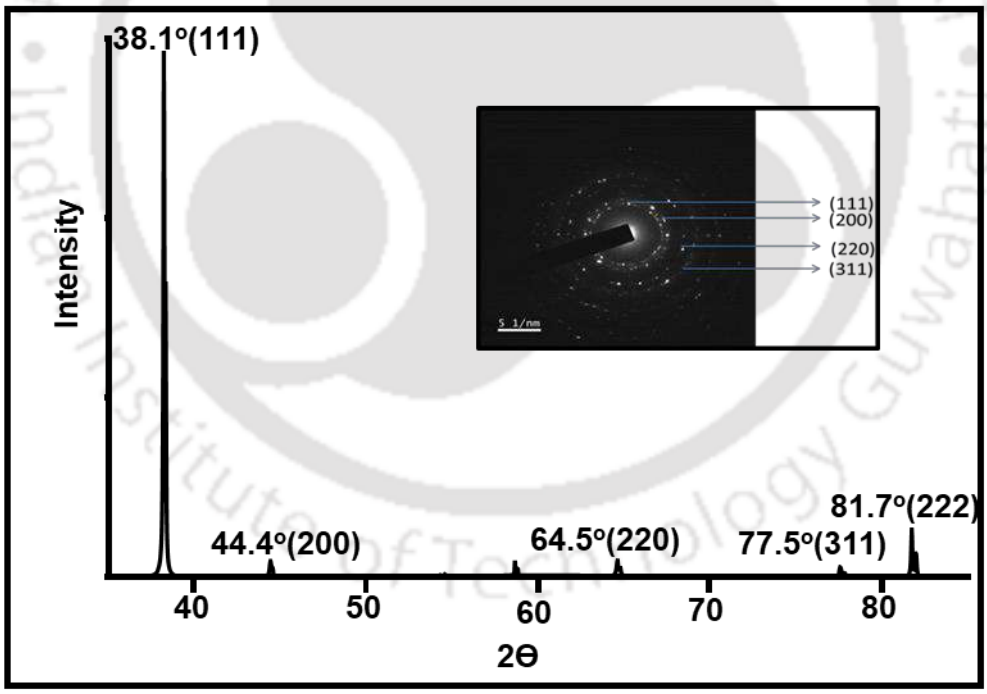

Figure 4.3: Characterization of CD-AuNp. (A) UV–vis spectrometric analysis of the CD-AuNp which exhibited the absorbance at 535nm, (B) XRD analysis of CD-AuNp, where nanoparticles are represented by five characteristic peaks corresponding to standard face centers cubic lattice. The intense peak at 38.1 and the unidentified peak at 58° show the synthesis of the CD-AuNp in the (111) direction. In addition, the SAED pattern of CD-AuNp shows four diffraction rings corresponding to four different crystal planes

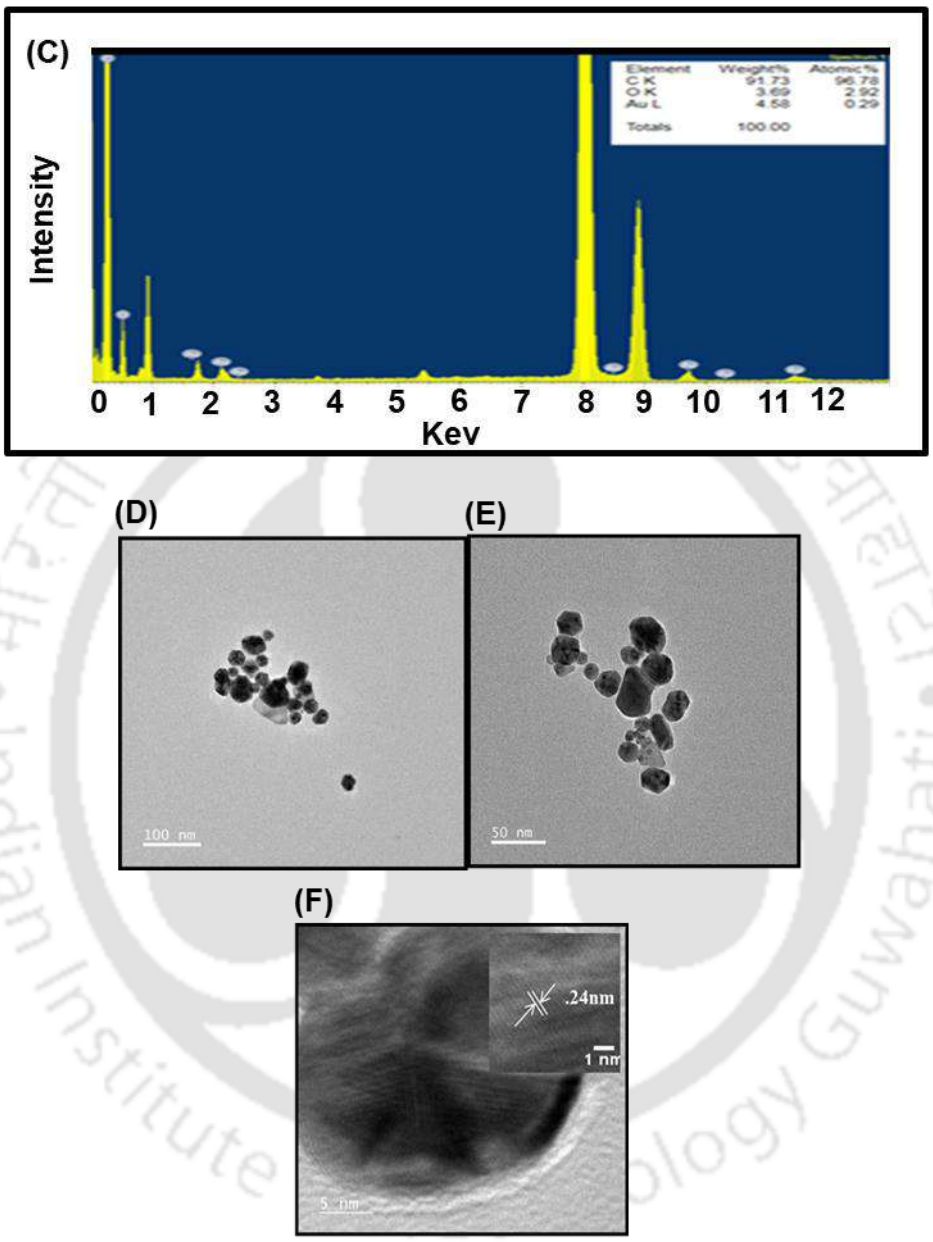

Figure 4.3: (C) Elemental analysis using EDX of the CD-AuNp depicting varied peaks for C, O, and Au. TEM images of CD-AuNp which exhibited a triangular-like morphology at (D) 100 nm, (E) 50 nm, (F) the HR-TEM images of the CD-AuNp with the fringe spacing shown around 0.24 nm.

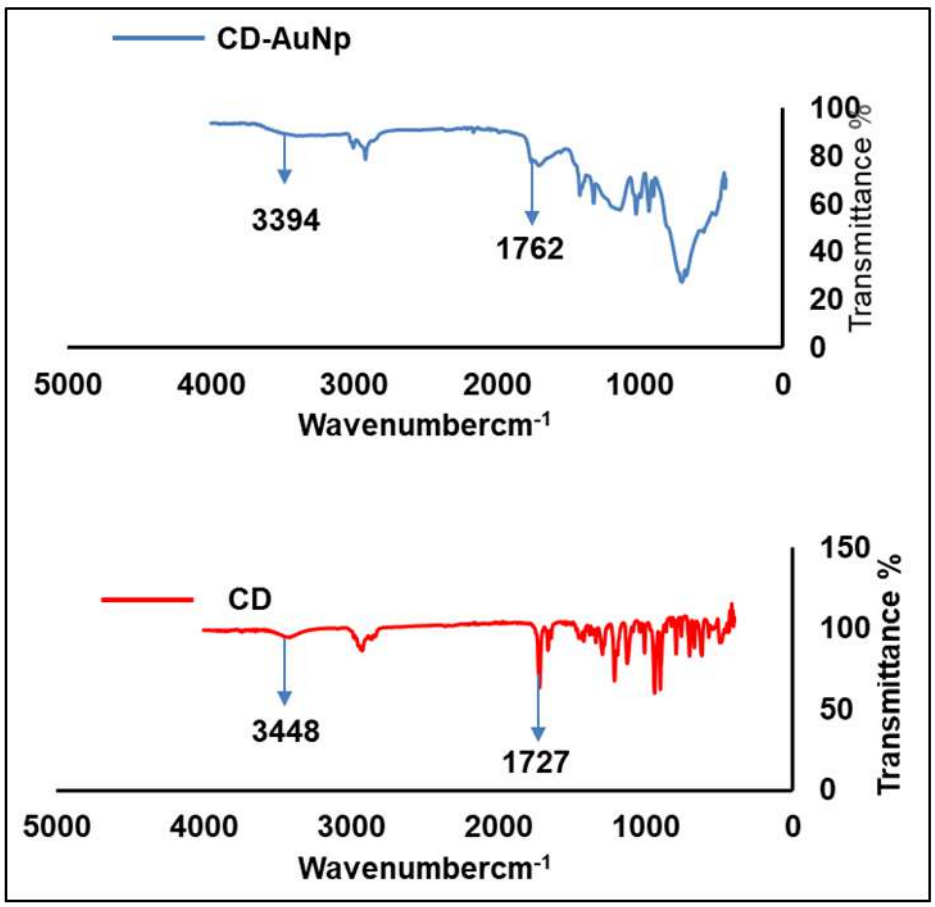

Figure 4.4: FT-IR spectrum of CD expressed a carbonyl group at 1727 cm^{-1} and an OH peak at 3448cm^{-1}. CD-AuNp showed damped OH peak (3394 cm^{-1}) and a shifted and supressed carbonyl peak at1762 cm^{-1}

FT-IR spectrum of CD showed a peak at 3448.7cm^{-1} which is the finger print peak for OH group. The peaks at 1727.21cm^{-1} and 1664.63 $cm^{-1}$are corresponds to CO group. After the bio reduction with the phytochemical, there is a clear suppression of keto group, also a shift in peak and damping for OH group, which is a clear indication of the reduction of Au^{3+} ions with the keto groups of coronarin D. As a result, the keto group may get oxidised to hydroxyl group (Figure 4.4).

4.6.2 Anti-proliferation effect of CD-AuNp complex

Further, we tested the anti-proliferative effect of CD-AuNp complex in TNBC cells. MTT assay on MDA-MB-231 cell line unveiled the anti-proliferative effect of CD-AuNp and CD, and was shown in Figure 4.5A. CD-AuNp have shown remarkable reduction in proliferation in comparison with CD , 7% more reduction at 10µg/ml, 42% reduction at 20µg/ml and 22% proliferation decrease at 50µg/ml. In addition, CD-AuNp showed 83% reduction in proliferation compared with control. For CD-AuNp IC_{50} was 18µg/ml compared to CD 34µg/ml for CD alone. Colony formation potential is important for cancer cells, implying a single cell's ability to survive in independent colonies. It is evident that, CD-AuNp reduced the clonogenic potential of MDA-MB-231 cells significantly, while CD alone didn't show much effect. CD-AuNp induced 68% reduction in survival fraction, at the same time CD induced only 9% reduction at 5µg/ml. In addition, CD-AuNps at 15µg/ml produced 96% reduction, CD induced only 18% reduction in survival fraction in comparison with control. Altogether, CD-AuNp expressed superior anti-proliferative property in MDA-MB-231 cells compared to phytochemical CD (Fig 4.5B and C).

4.6.3 Effect of CD-AuNp complex on cell viability

PI-FACS was performed to evaluate the effect of CD-AuNp complex on the cell viability of TNBC cell line. CD induced 27% cell death while CD-AuNp induced 77% cell death compared to control at 25µg/ml. Our studies revealed that CD-AuNp induced 50% more cell death in comparison with the phytochemical CD (Figure 4.6 A-D).

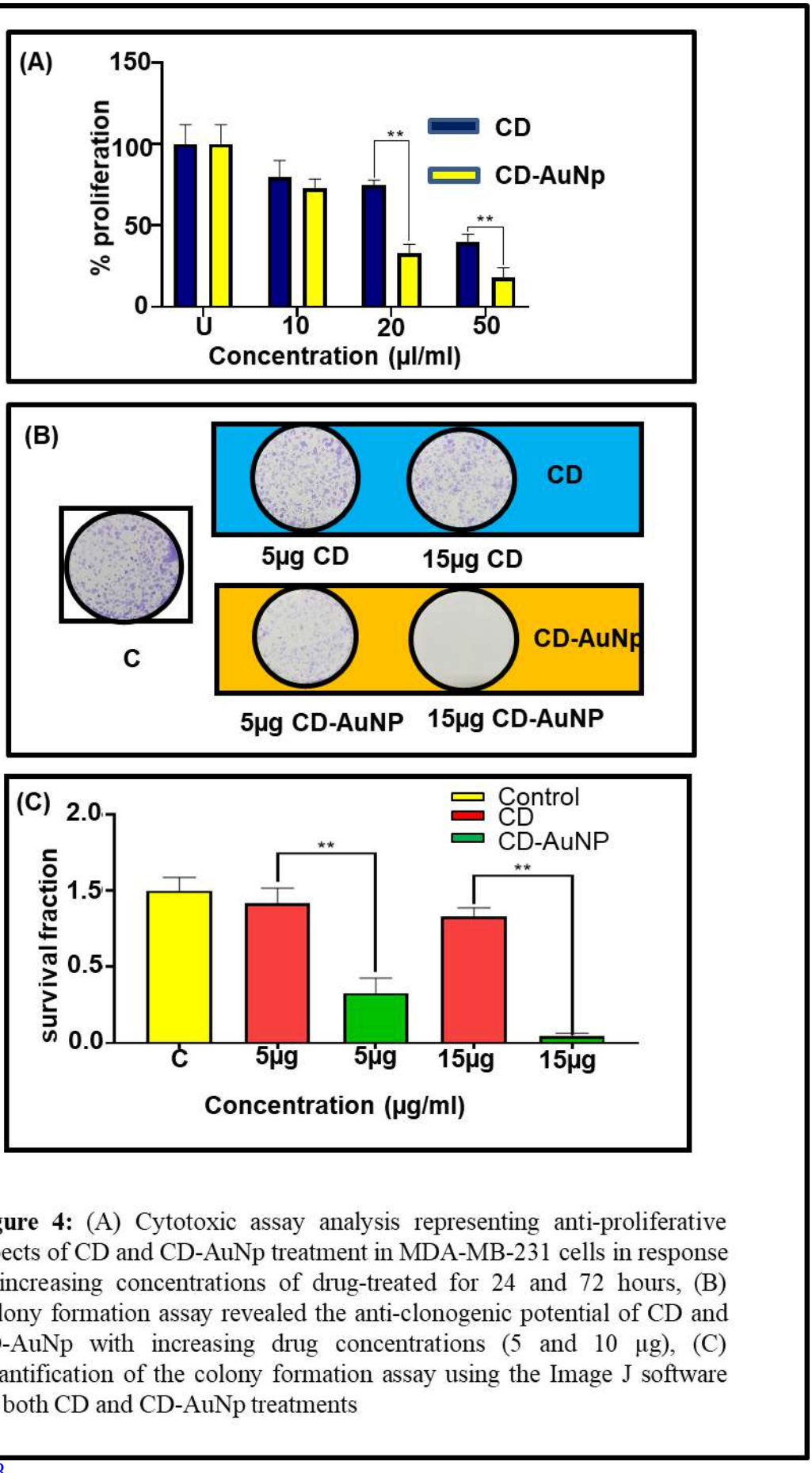

Figure 4: (A) Cytotoxic assay analysis representing anti-proliferative aspects of CD and CD-AuNp treatment in MDA-MB-231 cells in response to increasing concentrations of drug-treated for 24 and 72 hours, (B) Colony formation assay revealed the anti-clonogenic potential of CD and CD-AuNp with increasing drug concentrations (5 and 10 µg), (C) Quantification of the colony formation assay using the Image J software for both CD and CD-AuNp treatments

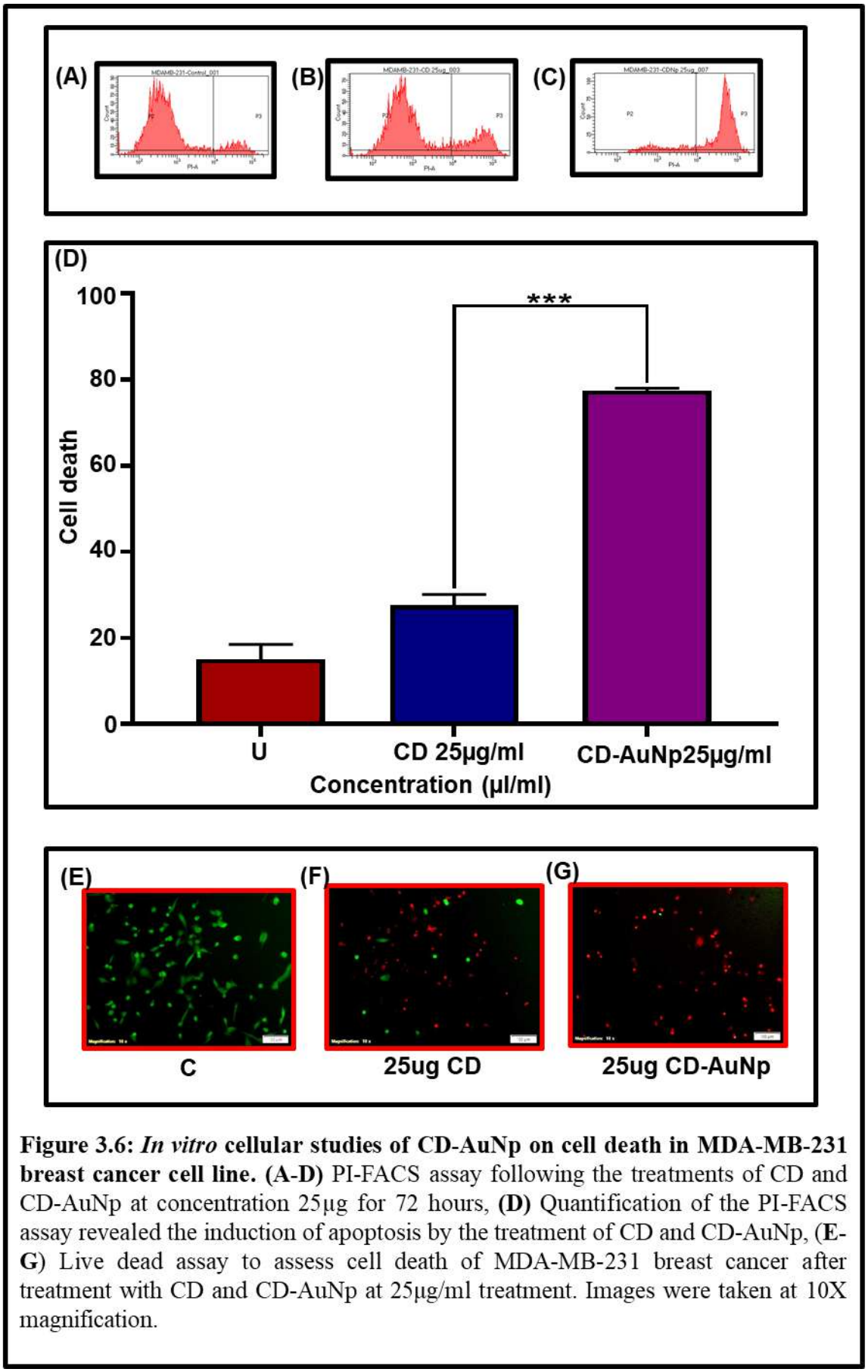

Figure 3.6: *In vitro* cellular studies of CD-AuNp on cell death in MDA-MB-231 breast cancer cell line. (A-D) PI-FACS assay following the treatments of CD and CD-AuNp at concentration 25µg for 72 hours, **(D)** Quantification of the PI-FACS assay revealed the induction of apoptosis by the treatment of CD and CD-AuNp, (**E-G**) Live dead assay to assess cell death of MDA-MB-231 breast cancer after treatment with CD and CD-AuNp at 25µg/ml treatment. Images were taken at 10X magnification.

In addition, live and dead assay revealed that at 25µg/ml CD-AuNps induced more cell death than CD at the same concentration. Overall, CD-AuNp exhibit significant cytotoxic effect in comparison with CD on MDA-MB-231 TNBC cell line (Figure 4.6 E-G).

4.7 Discussion

In the present study, we prepared CD-AuNp using CD as a reducing agent. Primary evidence for the formation of AuNps was the colour change to yellow to purple. Metal nanoparticles like gold exhibit SPR and absorbs visible light (Eustis et al., 2005). UV-visible spectra confirmed the formation of AuNps with an absorption peak at 535nm. Further, XRD spectrum confirmed the formation of AuNps with fingerprint peaks at3 8.1°, 44.4°, 64.5°,77.5°, and 81°. These peaks are corresponding to (111), (200, (220), (311) and (222) planes in FCC gold. SAED pattern further verified the formation of polycrystalline CD-AuNp with diffraction rings (111), (200, (220) and (311) from inner to outer side. Additionally, EDX pattern showed peaks for C, O and Au, verifying the presence of phytochemical along with the gold. EDX peaks at 2KeV represent crystalline AuNps (Baruah et al., 2018; Rajeshkumar, 2016). The morphology of CD-AuNP was verified by TEM images. TEM image exhibited circular-shaped CD-AuNp of below 50nm, which is suitable for therapeutic applications (Haume et al., 2016). Furthermore, FT-IR specta clearly showed the shift in the carbonyl group in CD-AuNp towards 1762cm^{-1}, there is also a suppression of carbonyl peak. Considering the hydroxyl peak, there is a shift including damping, in CD-AuNp (3393cm^{-1}) compared to CD (3448cm^{-1}). This suggests the involvement of carbonyl group in the bioreduction of $HAuCl_4$, and after the reduction process

carbonyl group also get oxidised to OH group. Hence, structural characterizations validated the successful reduction of $HAuCl_4$ into AuNps. It also verified the presence of CD along with AuNps. Further, anti-proliferative activity of CD-AuNp was analysed using MTT assay. MTT assay induced notable amount of reduction in proliferation, when treated with CD and CD-AuNp. At 50µg/ml CD-and CD-AuNp showed 61 and 83% reduction in proliferation in comparison with control. In addition, colony formation assay also substantiated the reduction in survival fraction induced by CD-AuNp. When treated with 15µg/ml, CD-AuNps produced 96% reduction; however, CD induced only 18% reduction in survival fraction in comparison with control. This result evidenced the superior anti-cancer potential of CD-AuNp over CD. Cytotoxicity of CD-AuNp and was verified by PI-FACS and live and dead assay. In PI-FACS, MDA-MB-231 cells were treated with 25µg/ml of CD and CD-AuNp respectively. It was observed that CD and CD-AuNp induced 27% and 77% cell death respectively. Higher cytotoxic potential of CD-AuNp over CD was upheld by the live and dead assay. This microscopic assay showed large amount dead cells in CD-AuNp treated cells compared to CD. Therefore, therapeutic potential of CD-AuNp was confirmed by these *in-vitro* studies in MDA-MB-231 cells.

4.8 Conclusion

This is the first report of the synthesis and potential of AuNps using CD as a precursor. AuNps were synthesised using CD as a reducing agent by direct reduction method. Structural characterization using XRD, UV-vis, EDX, TEM and FT-IR confirmed the formation of highly crystalline and pure AuNps also confirmed the presence of phytochemical coronarin D in the sample. Our in-vitro studies verified the potential

of CD-AuNp in reduction of proliferation, clonogenic potential and in cytotoxicity compared to CD in MDAMB-231 BC cells. Hence CD-AuNp could be used as a potential anti-cancer agent for the treatment of TNBC after validating these results using animal models.

CHAPTER 5

Synthesis, Characterization and Biological Activities of EAZD-AuNp

5.1 Epoxy azadiradone

Neem (*Azadiracta indica*) is a well-known traditional medicine since ancient days; almost all parts of this plant are using for medicinal purpose. Majority of triterpenoids isolated from neem are tetranortriterpenoids (limonoids) (Tan and Luo, 2011). Neem limonoids are classified into two groups based on chemical tructure, 1) basic/ring-intact limonoids possessing 4,4,8-trimethyl17-furanylsteroidal skeleton, includes azadirone, azadiradione, gedunin; 2) C-seco limonoids with rearranged framework generated through C-ring opening, includes, salannin, nimbin, azadirachtin (Haldar et al., 2013; Tan and Luo, 2011). Even though neem derived EAZD is explored very little for its medicinal properties, it is already been tested for its anti-feedant and anti-inflammatory properties (Govindachari et al., 2000; Halder et al., 2018). Couple of anti-cancer studies also reported on EAZD. EAZD inhibits PI3K/Akt pathway, induces apoptosis and suppresses migration of BC cells (MDA-MB-231 and MCF-7). In addition, EAZD also induces anti-cancer, anti-proliferative and anti-migratory activities in head and neck squamous cell carcinoma.

Currently, the efficacy of limonoids are limited by their poor bioavailability and other pharmacokinetic issues (Roy et al., 2021). To improve the performance of these compounds, AuNps were introduced along with the phytochemicals in our study.

In this study, we prepared gold nanoparticles using EAZD as a reducing agent. EAZD-AuNp were used to target cancer cells passively through EPR effect as its size ranges from 10-50nm. This is the first report on EAZD based AuNps for TNBC treatment.

(A)

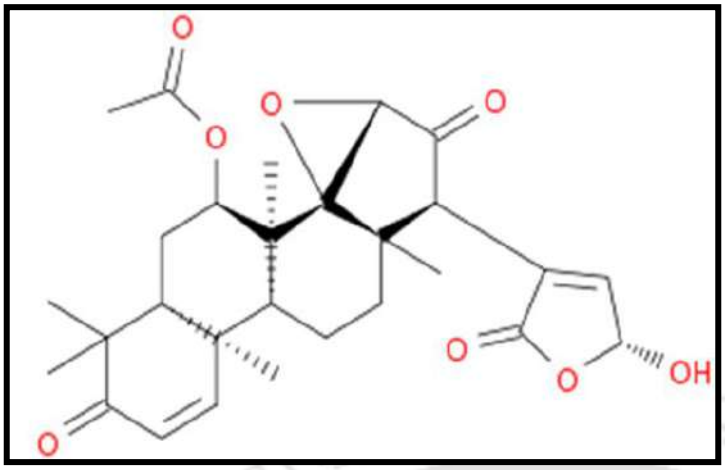

(B)

Figure 5.1 (A) Chemical structure of EAZD (B) Neem tree

5.2 Materials used

EAZD was kindly provided by Dr. Mangalam S. Nair (Chemical Sciences and Technology Division, CSIR- National Institute for Interdisciplinary Science and Technology (CSIR-NIIST), Thiruvananthapuram, Kerala, India. All other cell culture materials were same as in previous chapters.

5.3 Method of preparation

A stock solution of 2mM EAZD was prepared in DMSO and 0.41mM gold chloride was prepared in milli Q water separately. Then 1ml of EAZD was added drop wise in to 1ml of gold chloride solution with simultaneous stirring and heating at 50^{o}C. When EAZD was added to gold chloride solution, a white turbidity appeared. Further, the solution was heated again for 30 minutes while stirring. The colour of the solution changed to purple which indicated that the reduction reaction is completed.

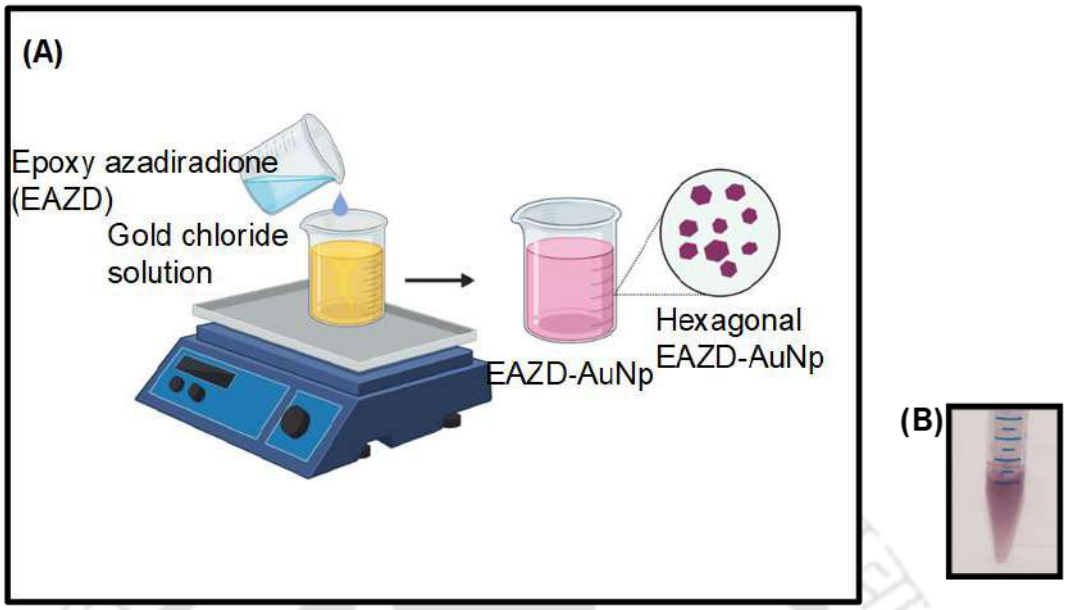

Figure 5.2 Method of preparation of EAZD-AuNp

5.4 Characterization of EAZD-AuNp

5.4.1 Structural characterization of EAZD-AuNp.

As discussed in previous chapters, structural characterizations for confirming the formation of AuNp.

5.4.2 *In-vitro* analysis of EAZD-AuNp on MDA-MB-231 cells.

All in-vitro studies were carried out using the same protocol as discussed in chapter 2. However, as EZAD is more potent than other compounds we have used 1 to10µg/ml of EZAD and EAZD-AuNp.

5.5 Statistical Analysis

Statistical analysis was performed as discussed in the previous chapter, with the software.

5.6 Results

5.6.1 Synthesis and Characterization of EAZD-AuNp

In the present study, we prepared AuNps by mixing 0.41mM gold chloride and 2mM EAZD. After heating and stirring for 30 minutes colour of the solution changed to purple, due to the LSPR) exhibited by AuNps. LSPR was confirmed experimentally by UV-visible spectra. UV spectra showed an absorption peak at 525nm (Figure 5.5A). XRD finger print peaks for AuNps were obtained at 38.1°, 44.4°,64.5°, 77.5°,61.2°, corresponds to (111), (200), (220), (311), (222) FCC planes, respectively. The absence of any additional peaks endorses the absence of impurity. Peak corresponds to (111) plane is more intense compared to others, implies (111) plane is more dominant than other planes in the sample (Philip D et al., 2009) (Figure 5.3B). Moreover, SAED pattern again confirmed the crystallinity of the sample. Diffraction rings from inner to outer can be indexed as (111), (200), (220), (311) and (222) reflections respectively of FCC gold (Figure 5.3 B) (Aromal et al., 2012).

An EDX spectrum was performed for the quantitative verification of the presence of EAZD along with AuNps. EDX showed peaks for Au, C and O and the high intense peak at 8KeV corresponds to Cu arising from copper grid. Peak at ~2KeV was typical for metallic AuNps in agreement with other reports (Fayaz et al., 2011). Carbon and oxygen peaks might have originated from the EAZD bound to the surface of the AuNps (Figure 5.3C).

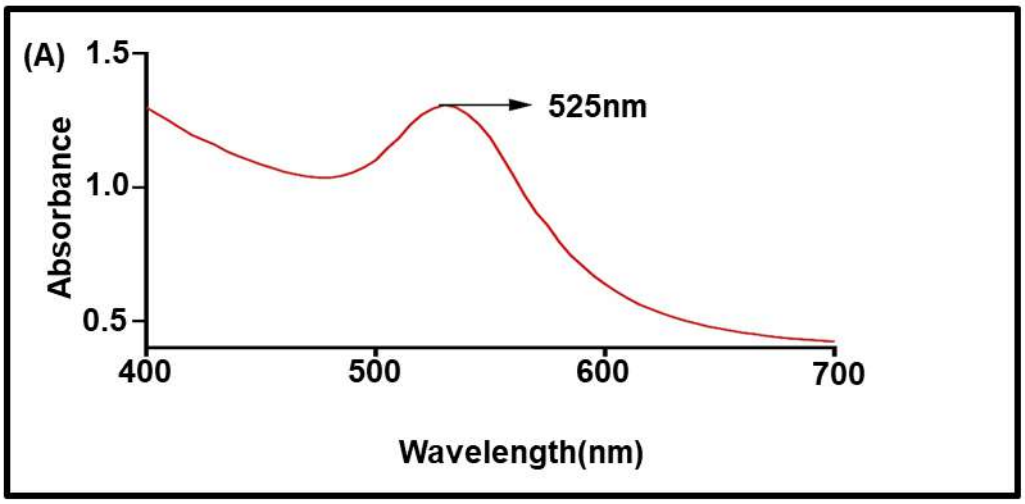

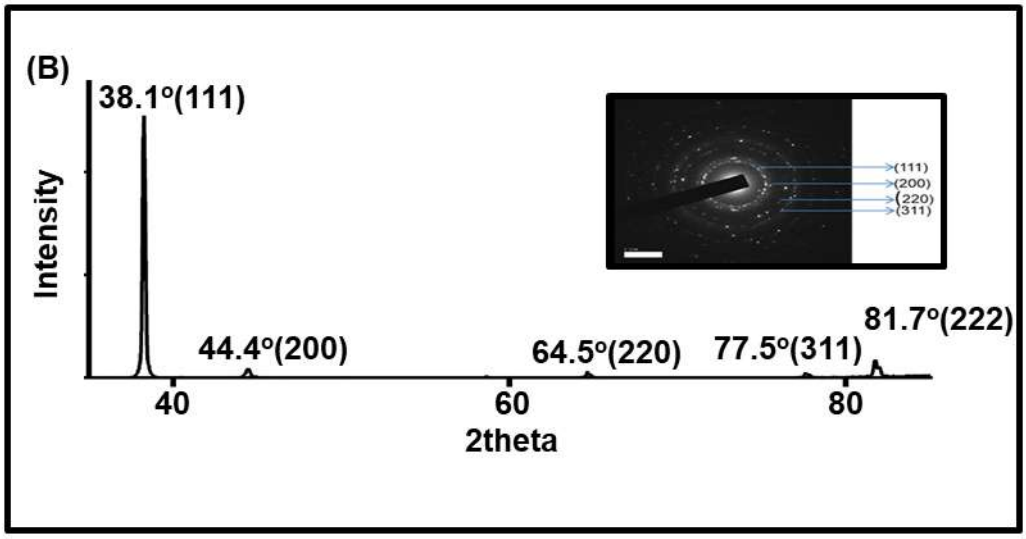

Figure 5.3: Characterization of EAZD-AuNp. (**A**) UV–vis spectrometric analysis of the EAZD-AuNp, which gives an absorbance peak at 525nm, (**B**) XRD analysis of EAZD-AuNp, where formation of gold nanoparticles is confirmed by five characteristic peaks corresponding to standard face centers cubic lattice. In addition, the SAED pattern of EAZD-AuNp shows four diffraction rings corresponding to four different crystal planes.

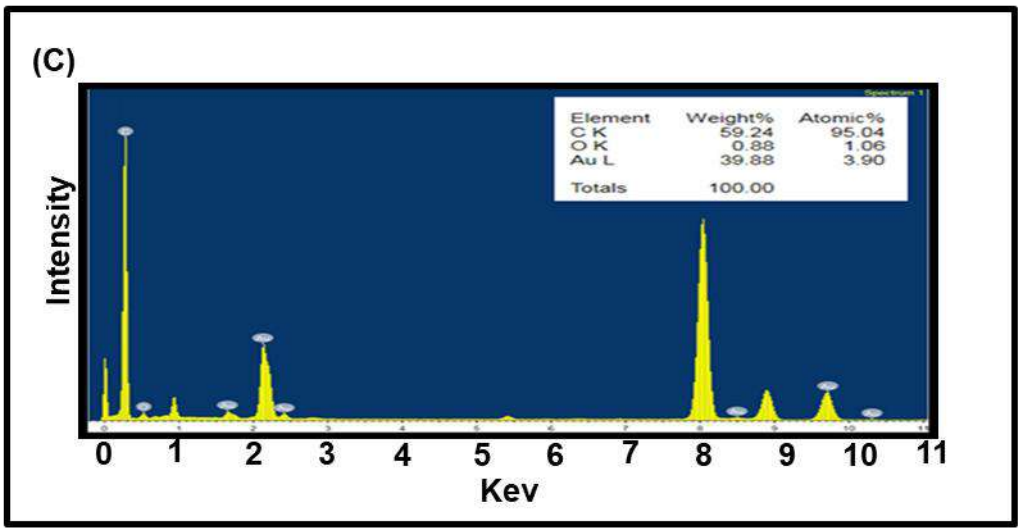

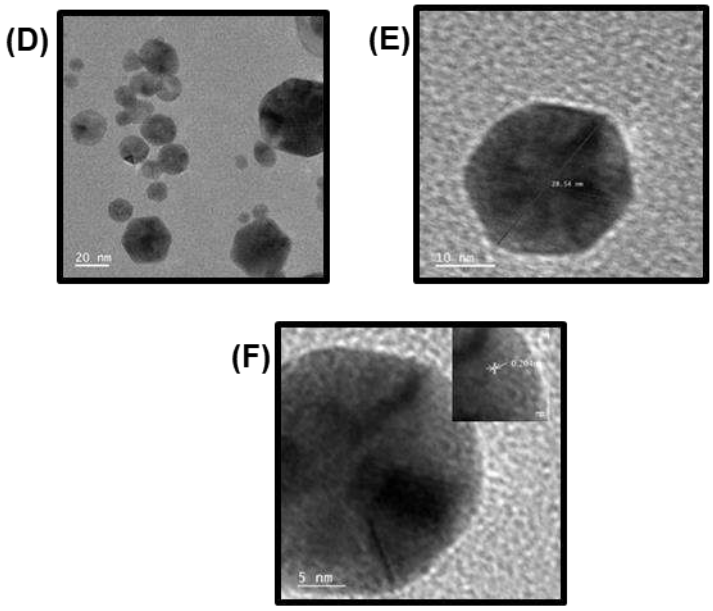

Figure 5.3: (C) Elemental analysis using EDX of the EAZD-AuNp revealing varied peaks for C, O, and Au. TEM images of EAZD-AuNp exhibited a triangular-like morphology at (D) 20 nm scale, (E) 10 nm scale, (F) the HR-TEM images of the EAZD-AuNp with the fringe spacing shown around 0.204 nm.

TEM was performed to analyse the surface morphology of the particles, since it is important to analyse the size and shape of the particles in biological studies. TEM images revealed that AuNps were in hexagonal shape. Though the particles are poly dispersed, they are in the 10-50nm size range and ideal for cellular administration. TEM analysis showed that nanoparticles are hexagonal and many reports showed that hexagonal-shaped AuNps possess significant anti-cancer properties (Mukherjee et al., 2012; Ohadi et al., 2020). Lattice spacing calculated from the HR-TEM image was 0.204nm correspond to (200) plane of AuNp (Figure 5.3D-F).

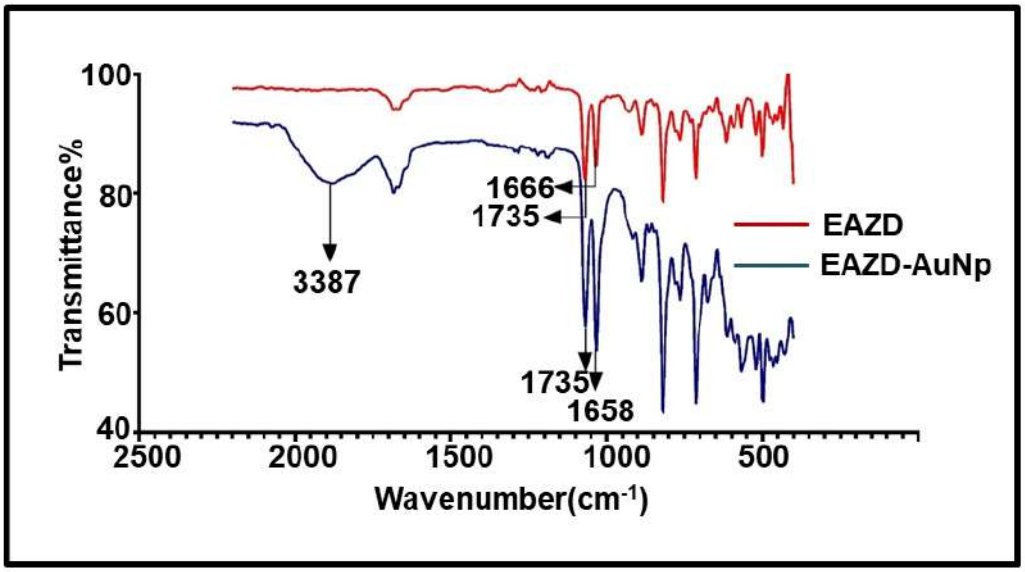

Figure 5.4: FT-IR graphs of EAZD-AuNp revealed peak shift at 1658cm-1 (CO group) from 1666cm-1 in EAZD, indicated the involvement of carbonyl group in the bio reduction.

FT-IR spectra of EAZD showed two carbonyl peaks at 1735cm^{-1} and 1666cm^{-1}. In AuNp one carbonyl peak got shifted to 1666cm^{-1} and hydroxyl group appeared at 3387cm^{-1}. After the bio reduction, the shift in peak at 1666cm^{-1} towards lower

frequency was attributed to the involvement of carbonyl group with nanoparticles. Presence of OH peak in EAZD-AuNp indicated that Au^{3+} ions were reduced with carbonyl group of EAZD and the carbonyl group got oxidised to OH group (Figure 5.4) (Kasthuri et al., 2009a).

5.6.2 Anti-proliferation effect of EAZD-AuNp complex.

Next to structural characterization, we moved to anti-proliferative studies of EAZD-AuNp. Though EAZD alone was not showing any effect up to 10µg/ml, EAZD-AuNp showed significant reduction in proliferation with increased concentration of drug. EAZD-AuNp showed 39%, 61% and 89% reduction at 1, 5 and10µg/ml respectively compared to the control. IC_{50} for EAZD-AuNp was 6µg/ml (Fig 5.5A).

Clonogenic potential is crucial for cancer cells, since it measures the ability of single cell to survive and reproduce to form colonies. It is noteworthy that EAZD and EAZD-AuNp have significantly reduced colony formation compared to control. Interestingly, most of the EAZD-AuNp treated cells were unable to form colonies. In clonogenic potential, EAZD-AuNp showed 60% and 38% higher reduction at 5µg/ml and 10µg/ml accordingly, compared to bare EAZD (Figure 5.5B and C).

5.6.3 Effect of EAZD-AuNp complex on cell viability.

Further, PI-FACS was performed to check the cell viability of EAZD-AuNp on ~~TNBC~~ cells. EAZD induced 13% and 44% cell death, while EAZD-AuNp treated cells showed 28% and 61% cell death at 5g/ml and 15µg/ml, respectively compared to control. Our studies revealed that EAZD-AuNp induced 13% and 17% more cell death at 5g/ml and 15µg/ml compared to the phytochemical counterpart (Fig 5.6A-F).

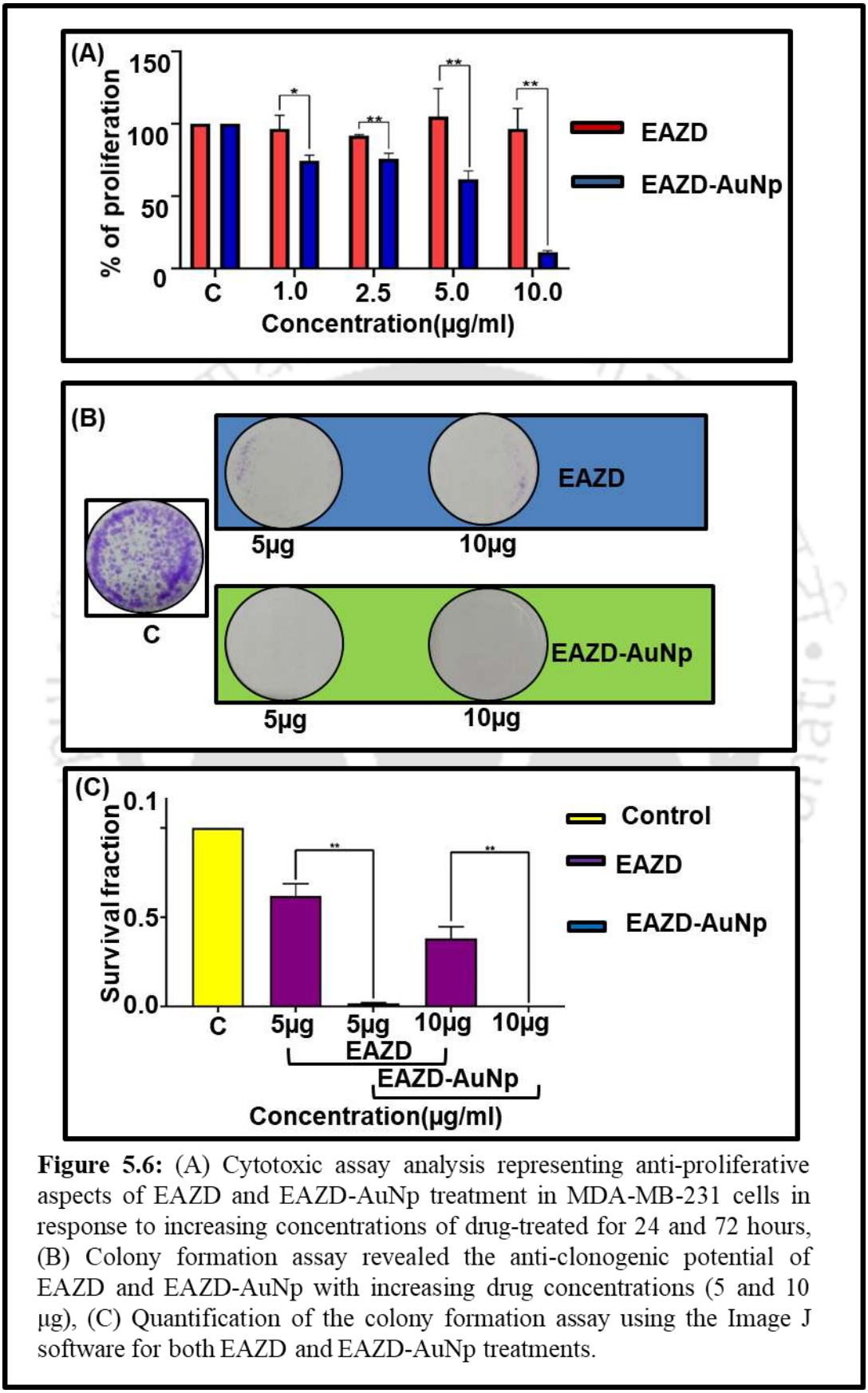

Figure 5.6: (A) Cytotoxic assay analysis representing anti-proliferative aspects of EAZD and EAZD-AuNp treatment in MDA-MB-231 cells in response to increasing concentrations of drug-treated for 24 and 72 hours, (B) Colony formation assay revealed the anti-clonogenic potential of EAZD and EAZD-AuNp with increasing drug concentrations (5 and 10 µg), (C) Quantification of the colony formation assay using the Image J software for both EAZD and EAZD-AuNp treatments.

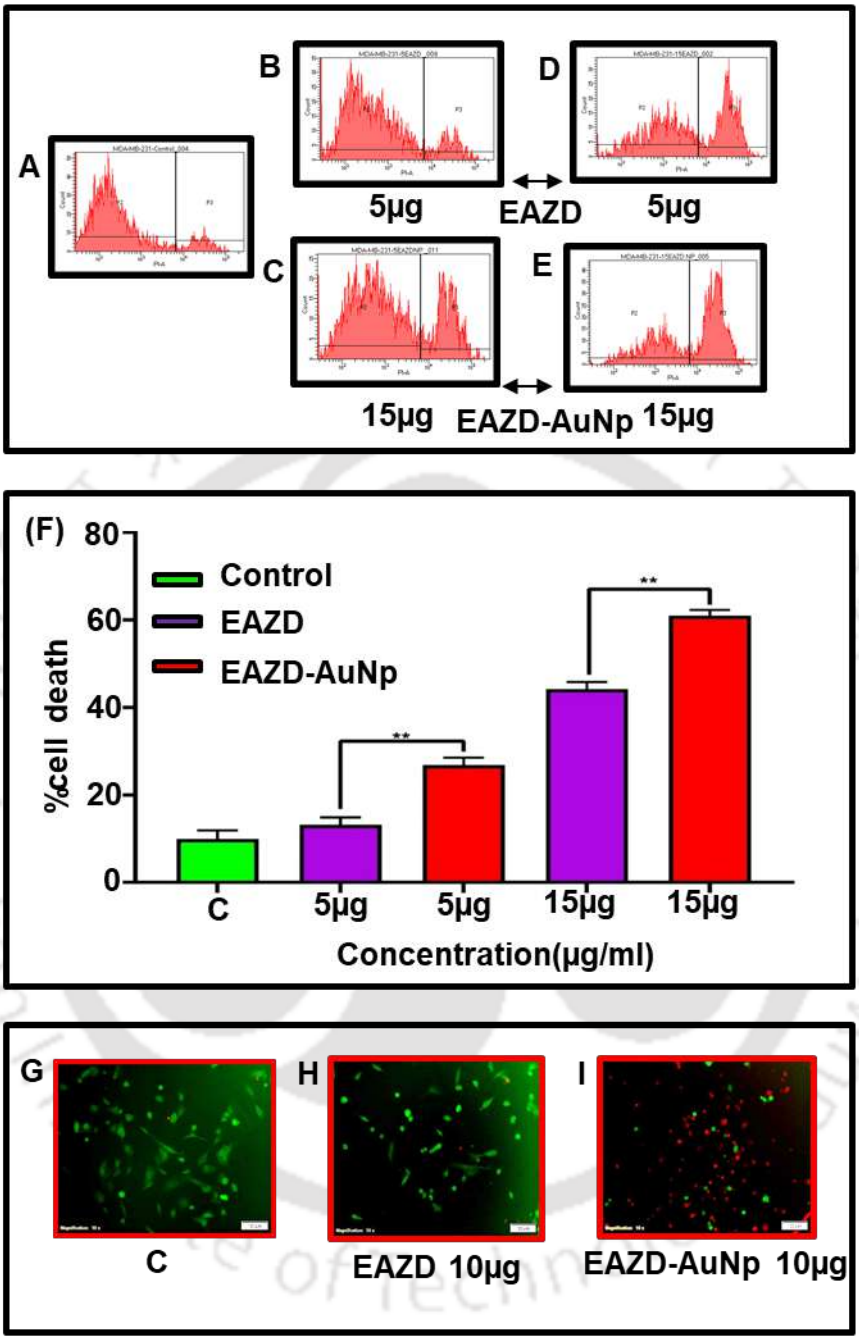

Figure 5: (A-D) PI-FACS assay following the treatments of EAZD and EAZD-AuNp at concentration 5µg and 15µg for 72 hours, (D) Quantification of the PI-FACS assay revealed the induction of apoptosis by the treatment of EAZD and EAZD-AuNp, (E-G) Live dead assay to assess cell death of MDA-MB-231 breast cancer after treatment with EAZD and EAZD-AuNp at 10µg treatment. Images were taken at 10X magnification.

Effect of EAZD-AuNp on the cell viability of TNBC cells was further confirmed by live and dead assay. EAZD-AuNp induced more cell death in comparison with EA at 10µg/ml. Altogether, EAZD-AuNp displayed remarkable cytotoxic effect compared to EAZD and control (Fig 5.6G-I).

5.7 Discussion

Here, we prepared AuNps using EAZD as a precursor. This is the first report on the preparation of AuNps using EAZD. Formation of AuNps were primarily evidenced by the colour change of the colloidal solution from yellow to purple. The colour change was attributed to localised LSPR of AuNps, which depends on the size and shape of the nanoparticles (Shabaninezhad and Ramakrishna, 2019). LSPR peak for AuNps was experimentally confirmed by UV-visible spectroscopy, showed an absorption peak at 525nm in agreement with other reports (Creighton and Eadon, 1991; Kumar et al., 2007) (Figure 2A). Further XRD spectrum verified characteristic AuNps peaks at 38.1°,44.4°, 64.5°,77.5°,81.7° corresponds to (111), (200, (220), (311) and (222) planes respectively (Basavegowda et al., 2014). The SAED pattern displayed the diffraction rings from inner to outer, indexed as (111), (200), and (220), reflections, corresponding to FCC gold. The typical SAED pattern with bright circular rings also confirmed the polycrystalline nature of the AuNps (Smitha et al., 2009). To further validate the formation of AuNps, EDX pattern was analysed, which showed peaks for C, O, and Au. Peak around 2 KeV was an indication of the presence of crystalline AuNps in the sample, carbon and oxygen peaks were originated from phytochemical (Ahmad et al., 2015; Kabeerdass et al., 2022). It is widely accepted that, the shape and size of nanoparticle play an important role in their biological

activities (Haume et al., 2016; Sztandera et al., 2018). Hence, the morphology of nanoparticles was analysed using TEM, and revealed the hexagonal shape of EAZD-AuNp. Besides, FT-IR spectra showed a shift in carbonyl group peak towards lower frequency (1658cm^{-1}) after the bio reduction of $HAuCl_4$ with EAZD, indicated the involvement of carbonyl group in the reduction process. Also the presence of OH group in EAZD-AuNp (3387cm^{-1}) indicated the oxidation of carbonyl group in to OH after the reduction of Au^{3+}.

Further, to evaluate the therapeutic potential of this novel nano bio complex, we analysed the cytotoxicity and cell viability of EAZD-AuNp in MDAMB-231 breast cancer cells. MTT assay showed significant reduction in proliferation compared to EAZD, even at 10µg/ml EAZD-AuNp induced 89% reduction in proliferation, with a very low IC_{50} of 6µg/ml. Moreover, EAZD-AuNp reduced the clonogenic potential of MDAMB-231 cells dramatically, not even a single colony survived in drug treated well at 10µg/ml. PI-FACS results showed 61% cell death in EAZD-AuNp treated cells (15µg/ml), moreover live and dead assay results validated the cytotoxicity of the EAZD-AuNp. These results points to the therapeutic potential of hexagonal EAZD-AuNp, there by this nano-bio combination could be a better counterpart for cancer treatment in future.

5.8 Conclusion

The present study has reported the preparation of AuNps using EAZD and investigated its anticancer activities in MDA-MB-231 cells. Hexagonal EAZD-AuNp complex (<50nm) were prepared using a single step direct reduction method via green synthesis approach. Characterization by UV-visible spectroscopy, XRD, EDX, and

FT-IR confirmed the formation of highly crystalline and extremely pure AuNps. Also, *in-vitro* studies disclosed the anti-cancer activity of hexagonal shaped EAZD-AuNps by reducing proliferation, clonogenic potential, and inducing cell death compared to the phytochemical EAZD alone in MDA-MB-231 cell line. Eventually, EAZD-AuNp developed in this study is a propitious therapeutic agent for various applications. However, the *in-vivo* parameters of EAZD-AuNp such as transport, safety, efficacy, toxicity and accumulation of AuNps in the biological system need to be analysed for further validation of these findings.

CHAPTER 6

Discussion, Conclusion and Future Aspects

6.1 Discussion and conclusion

Prevalence of TNBC in India is proclaimed to be higher than the Western population, with highest number of patients (n=1951) and maximum prevalence rate (27.9%) during the period 2004 to 2014 (Thakur et al., 2018). TNBC constitutes 15-20% of breast cancer cases globally, primarily afflicting younger women. TNBC remains untreated mainly due to the lack of hormone receptors, aggressiveness and late-stage diagnosis (Thakur et al., 2018). Although novel therapeutic approaches have increased the overall survival time of patients, clinical outcomes remain inadequate at advanced stages of the disease. Natural compounds derived from medicinal plants have been explored for their immense therapeutic and pharmacological activities (Babu et al., 2003; Kunnumakkara et al., 2018; Kunnumakkara et al., 2007; Monisha et al., 2016; Padmavathi et al., 2015; Padmavathi et al., 2017; Singh et al., 2019). A plethora of studies have elucidated that phytochemicals derived from a variety of medicinal plants have been shown to lower, various cancer-related risk factors with minimum toxicity to normal cells (Banik et al., 2020; Bordoloi et al., 2016; Bordoloi et al., 2019; Henamayee et al., 2020; Khatoon et al., 2020; Muralimanoharan et al., 2009; Parama et al., 2020). The increasing evidence suggests that, phytochemicals when used in conjunction with conventional anticancer treatments, attenuate the chemoresistance of tumors leading to apoptosis (Bishayee et al., 2013; Bordoloi et al., 2016; Bordoloi and Kunnumakkara, 2018; Patra et al., 2021; Saha et al., 2013; Sikdar et al., 2014). Contemporary TNBC research is focused on combinatorial therapies owing to their highly heterogeneous nature. Likewise, phyto-nano conjunctional therapies introduces a new era of cancer treatment in the present century.

In the current study, we selected four phytochemicals EF, EA, CD and EAZD based on their structure and availability. Presence of functional groups in the phytochemical is a crucial factor for reducing $HAuCl_4$ in to Au^0; since, carbonyl and hydroxyl group have been showed involvement in the bio reduction of gold chloride in previously reported studies (Behera and Ram, 2014; Gomes et al., 2015; Mata et al., 2009; Singh et al., 2010).

As we hypothesised, these eminent phytochemicals successfully reduced gold chloride into AuNps via direct reduction method. Formation of EF-AuNp, EA-AuNp, CD-AuNp and EAZD-AuNp were confirmed by UV-visible spectroscopy, XRD, EDX, TEM and FT-IR. SPR, the fundamental property of AuNps, was confirmed by UV-visible spectroscopy (Alkilany and Murphy, 2010a; Eustis et al., 2005). All four phyto-nano complexes exhibited UV-peak in the visible region of the electromagnetic spectrum. EF-AuNp, EA-AuNp, CD-AuNp and EAZD AuNp showed their UV-visible peak at 560nm, 530nm,535nm and 525nm, respectively. XRD, the powerful tool in characterising crystalline materials, undoubtedly confirmed the formation of AuNps. All four complexes showed four finger print peaks for AuNps in XRD spectrum. CD-AuNp and EAZD-AuNp nanoparticles showed a very intense (111) peak compared to other planes, which in turn, indicated the predominant growth of AuNps in a particular plane, in powder XRD. Less amount of sample also contributed to the preferred orientation of AuNps in (111) plane (Dohrmann et al., 2009). In addition, such high intense peak at 38^o was reported for gold nanoparticles of various shapes (Fragoon et al., 2012). Moreover, one unassigned peak at 58^o, indicates the crystallisation of bio-organic phase on the surface of nanoparticles in EF-AuNp and

CD-AuNp, which has been reported in the bio-reduction of AuNps previously (Juibari et al., 2015; Kumari and Philip, 2013). Furthermore, SAED pattern confirms the poly crystalline nature of every phyto-nano complexes. SAED revealed four diffraction rings in AuNps corresponding to crystal planes (111), (200), (220), and (311). Usually, in SAED diffraction rings are indexed from inner to outer side (Chen et al., 2010; Halder et al., 2018).

Next to SAED, EDX was performed to quantitatively examine elemental composition of phyto-nanocomplexes. All four phyto-nano complexes showed C, O and Au peaks in EDX spectrum. Thereby, EDX data confirmed the presence of AuNps along with phytochemicals. EDX also showed very strong peaks for copper and carbon, originated from carbon-coated copper grid (Halder et al., 2018; Khan et al., 2013; Zhao et al., 2019). Morphology of phyto-nano complexes were studied using TEM analysis. Even though, shape of the nanoparticles was different, all nanoparticles were in the size range of 10-50nm (the typical size range for a nano drug). Looking into the shapes of nanoparticles, EF-AuNps were in triangular shape, while EA-AuNp, CD-AuNp and EAZD-AuNp showed mixed, spherical and hexagonal shapes respectively. These different shapes of each nanoparticle may be due to the peculiar property of corresponding phytochemical. As a continuation of TEM, HR-TEM revealed the crystalline fringe spacing in each phyto-nano complexes. Fringe spacing for EF-AuNp, EA-AuNp, CD-AuNp and EAZD-AuNp were corresponding to (220), (111), (111), and (200) planes, respectively. All these structural characterization tools, undoubtedly verified the bio reduction of the $HAuCl_4$ by the selected phytochemicals.

FT-IR analysis of every single phytochemical and phyto-nano complex was performed to analyse the mechanism of formation of AuNps. In general, every phyto-nano complexes showed a shift and suppression in the carbonyl group and a shift in the hydroxyl group. Even though there was no hydroxyl group in the chemical structure of EAZD, yet after the bio reduction, FT-IR spectra showed one hydroxyl peak. Based on these findings, involvement of carbonyl and hydroxyl group in the bio reduction could be clearly evidenced. As mentioned in the literatures, carbonyl group has high affinity towards the reduction of $HAuCl_4$, and after the reduction reaction, it gets oxidised to hydroxyl group (Basha et al., 2010; Halder et al., 2018; Kasthuri et al., 2009a; Khan et al., 2013; Sreelakshmi et al., 2013; Zhao et al., 2019).

Further, we proceed to the *in-vitro* analysis of these unique phyto-nano complexes in the MDA-MB-231 cell line. MTT, colony formation, PI-FACS and live and dead assays were performed to verify the anticancer potential of these complexes. *In-vitro* studies revealed that 'phyto-nano complex' showed better anticancer performance than their phytochemical counterpart. Despite that, EAZD-AuNp expressed exceptionally superior performance over other nanoparticles.

Primarily, we carried out MTT assay to verify the anti-proliferative effect of phyto-nano complexes. At 50µg/ml, EF-AuNp, EA-AuNp and CD-AuNp induced 98%, 96% and 83% reduction in proliferation, respectively compared to control. Notably, EAZD-AuNp induced 89% decrease in proliferation at 10µg/ml. In addition, Ic50 for EF-AuNp, EA-AuNp, CD-AuNp and EAZD-AuNp were 18µg/ml, 15µg/ml, 18µg/ml and 6µg/ml, respectively. This clearly evidenced the better anti-proliferative effect of EAZD-AuNp than other complexes. Next to MTT, we carried colony formation assay.

The results revealed that phyto-nano complexes exhibited significant reduction in the clonogenic potential of MDA-MB-231. Quantitatively, EF-AuNp and CD-AuNp showed 89% and 98% reduction in survival fraction compared to control at 15µg/ml. Likewise, EA-AuNp and EAZD-AuNp exhibited 89 and 100% reduction in survival fraction at 10µg/ml. Interestingly, a remarkable reduction in survival fraction was exhibited by EAZD-AuNp, which decreased the survival fraction to 0% (none of the colonies survived). Further, PI-FACS was performed to verify the cytotoxic potential of phyto-nano complexes. The complexes expressed significant cytotoxic potential in MDA-MB-2321 cells. MDA-MB-231 cells were treated with 50µg/ml, EF-AuNp and EA-AuNp, each for analysing the cell death. Both of these showed 75% cell death. Likewise, CD-AuNp and EAZD-AuNp were induced 77% and 61% cell death at 25 and 15µg/ml, respectively. PI-FACS result also substantiated the superior cytotoxic efficacy of EAZD-AuNp, which induced 61% cell death at a comparatively lower concentration of 15µg/ml. Similarly, live and dead assay also verified the result obtained from PI-FACS, which proved the cytotoxic effect of each phyto-nano complex. EF-AuNp, EA-AuNp, CD-AuNp and EAZD-AuNp showed significant amount of dead cells in the microscope when treated with 75, 25, 25, and 10µg/ml, respectively.

The “shape of nanoparticle” can explain the inimitable performance of EAZD-AuNp as an anticancer agent. As discussed in chapter 1, when the hexagonal nanoparticles interact with the cellular surface, total parallel component of kinetic energy accumulates to the cutting wear. This particular phenomenon is known as “angle of attack concept” (Buzea et al., 2007; Neilson and Gilchrist, 1968). These peculiar

shaped EAZD-AuNp interact with the cell surface involving in small angle attack and results in greater internalisation. In a particular Study, Tian F et al proved the high mass internalisation of hexagonal AuNps compared to triangular ones in calu-3 cells. Furthermore, triangular nanoparticles exhibited 20 times more internalisation than spherical nanoparticles in HeLa cells (Nambara et al., 2016). Precisely, the remarkable efficacy of EAZD-AuNp in MDA-MB-231 cells could be due to the anomalous hexagonal shape. As some exceptional cases were reported in some studies, this structural superiority of hexagonal nanoparticles has to be further validated in *in-vivo* studies.

Collectively, based on the *in-vitro* analysis, superior anticancer efficacy of EAZD-AuNp was undoubtedly authenticated. It is also noted that, the current platinum based chemotherapeutic drug cisplatin reported an IC50 of 7.8µM or 2.3µg/ml in MDA-MB-231 cells. Even though, IC50 of EAZD-AuNp was 6 µg/ml, this naturally origin phyto-nano complex could be effectively bypass the adverse side effects of chemo drugs. In addition, 10-50nm sized EAZD-AuNp complex could target tumor cells selectively via EPR effect. Such passive targeting also supposed to minimize the detrimental outcome of conventional chemotherapeutic agents. Conclusively, EAZD-AuNp is a meritorious complex for further *in-vivo* studies. However, studies that validate the molecular pathways, bioavailability and intoxication in the biological system should get warranted for all four phyto-nano complexes. Thus, the current study gives an insight into phyto-nano combinatorial therapies for the next-generation cancer treatment strategies in combination with or without other treatment modalities.

6.2 Limitations and future prospects of the study

Present study is an attempt towards succeeding era of highly efficacious cancer therapeutics, as phyto-nano combinatorial therapies are the up-and-coming area of focus in cancer research. Here, we impeccably proved the anticancer potential of four selected phytochemicals in conjugation with AuNps. Nevertheless, some limitations are need to be elucidated in the future. Primarily, in this study, only four phytochemicals were selected for evaluation. Since the nature is an eminent source of therapeutic agents, quite a few are still under cover. Hence, a detailed investigation incorporating more phytochemicals is recommended.

Second, the mechanism of action of phytochemicals is unpredictable in different cancer cells. Sometimes, a single phytochemical targets different pathways in different cell lines to induce cell death. Mostly, they also target multiple pathways rather than a single pathway. Hence it is important to analyse the involvement of different molecular pathways in the mechanism of action of phyto-nano complexes.

Third, non-toxicity, bioavailability and specific targeting ability are the most important features of a therapeutic drug. Even though >10nm AuNps are non-toxic, toxicity of AuNps to normal cells is still debatable. Therefore, non-toxic nature of phyto-nano complexes should be evaluated *in-vivo*. Current study also anticipated high bioavailability for phyto-nano complexes, owing to its peculiar size and shape. In addition, most importantly, phyto-nano complexes should be able to target tumor cells specifically, owing to their EPR effect. Therefore, it is indispensable to validate the bioavailability and tumor-specific targeting ability of each phyto-nano complexes *in vivo*.

Ahmad, A., F. Syed, A. Shah, Z. Khan, K. Tahir, A.U. Khan, and Q. Yuan. 2015. Silver and gold nanoparticles from Sargentodoxa cuneata: synthesis, characterization and antileishmanial activity. *Rsc Advances*. 5:73793-73806.

Ahmed, S.A., D. Parama, E. Daimari, S. Girisa, K. Banik, C. Harsha, U. Dutta, and A.B. Kunnumakkara. 2021. Rationalizing the therapeutic potential of apigenin against cancer. *Life Sci*. 267:118814.

Ahmed, T., W. N Setzer, S. Fazel Nabavi, I. Erdogan Orhan, N. Braidy, E. Sobarzo-Sanchez, and S. Mohammad Nabavi. 2016. Insights into effects of ellagic acid on the nervous system: a mini review. *Current Pharmaceutical Design*. 22:1350-1360.

Akram, M., M. Iqbal, M. Daniyal, and A.U. Khan. 2017. Awareness and current knowledge of breast cancer. *Biological research*. 50:1-23.

Al-Sader, H., H. Abdul-Jabar, Z. Allawi, and Y. Haba. 2009. Alcohol and breast cancer: the mechanisms explained. *Journal of Clinical Medicine Research*. 1:125.

Alberg, A.J., D.R. Shopland, and K.M. Cummings. 2014. The 2014 Surgeon General's report: commemorating the 50th Anniversary of the 1964 Report of the Advisory Committee to the US Surgeon General and updating the evidence on the health consequences of cigarette smoking. *American journal of epidemiology*. 179:403-412.

Ali, S.M., M.Z. Hoemann, J. Aubé, G.I. Georg, L.A. Mitscher, and L.R. Jayasinghe. 1997. Butitaxel Analogues: Synthesis and Structure− Activity Relationships. *Journal of medicinal chemistry*. 40:236-241.

Alkilany, A.M., and C.J. Murphy. 2010a. Toxicity and cellular uptake of gold nanoparticles: what we have learned so far? *Journal of nanoparticle research*. 12:2313-2333.

Alkilany, A.M., and C.J. Murphy. 2010b. Toxicity and cellular uptake of gold nanoparticles: what we have learned so far? *J Nanopart Res*. 12:2313-2333.

Amalraj, A., K. Varma, J. Jacob, C. Divya, A.B. Kunnumakkara, S.J. Stohs, and S. Gopi. 2017. A Novel Highly Bioavailable Curcumin Formulation Improves Symptoms and Diagnostic Indicators in Rheumatoid Arthritis Patients: A Randomized, Double-Blind, Placebo-Controlled, Two-Dose, Three-Arm, and Parallel-Group Study. *J Med Food*. 20:1022-1030.

Anderson, T., F. Alexander, J. Lamb, A. Smith, and A. Forrest. 2000. Pathology characteristics that optimize outcome prediction of a breast screening trial. *British journal of cancer*. 83:487-492.

Aqil, F., R. Munagala, J. Jeyabalan, and M.V. Vadhanam. 2013. Bioavailability of phytochemicals and its enhancement by drug delivery systems. *Cancer letters*. 334:133-141.

Aromal, S.A., K.D. Babu, and D. Philip. 2012. Characterization and catalytic activity of gold nanoparticles synthesized using ayurvedic arishtams. *Spectrochimica Acta Part A: Molecular and Biomolecular Spectroscopy*. 96:1025-1030.

Assi, H.A., K.E. Khoury, H. Dbouk, L.E. Khalil, T.H. Mouhieddine, and N.S. El Saghir. 2013. Epidemiology and prognosis of breast cancer in young women. *Journal of thoracic disease*. 5:S2.

Aswathy, M., K. Banik, D. Parama, P. Sasikumar, C. Harsha, A.G. Joseph, D.R. Sherin, M.K. Thanathu, A.B. Kunnumakkara, and R.K. Vasu. 2021. Exploring the Cytotoxic Effects of the Extracts and Bioactive Triterpenoids from Dillenia indica against Oral Squamous Cell Carcinoma: A Scientific Interpretation and Validation of Indigenous Knowledge. *ACS Pharmacol Transl Sci*. 4:834-847.

Babu, B., H. Jayram, M. Nair, K. Ajaikumar, and J. Padikkala. 2003. Free radical scavenging, antitumor and anticarcinogenic activity of gossypin. *Journal of experimental & clinical cancer research: CR*. 22:581-589.

Band, P.R., N.D. Le, R. Fang, and M. Deschamps. 2002. Carcinogenic and endocrine disrupting effects of cigarette smoke and risk of breast cancer. *The Lancet*. 360:1044-1049.

Banik, K., A.M. Ranaware, C. Harsha, T. Nitesh, S. Girisa, V. Deshpande, L. Fan, S.P. Nalawade, G. Sethi, and A.B. Kunnumakkara. 2020. Piceatannol: A natural stilbene for the prevention and treatment of cancer. *Pharmacological research*. 153:104635.

Barbieri, R., E. Coppo, A. Marchese, M. Daglia, E. Sobarzo-Sánchez, S.F. Nabavi, and S.M. Nabavi. 2017. Phytochemicals for human disease: An update on plant-derived compounds antibacterial activity. *Microbiological research*. 196:44-68.

Barton, V.N., N.C. D'Amato, M.A. Gordon, H.T. Lind, N.S. Spoelstra, B.L. Babbs, R.E. Heinz, A. Elias, P. Jedlicka, and B.M. Jacobsen. 2015. Multiple molecular subtypes of triple-negative breast cancer critically rely on androgen

receptor and respond to enzalutamide in vivo. *Molecular cancer therapeutics*. 14:769-778.

Baruah, D., M. Goswami, R.N.S. Yadav, A. Yadav, and A.M. Das. 2018. Biogenic synthesis of gold nanoparticles and their application in photocatalytic degradation of toxic dyes. *Journal of Photochemistry and Photobiology B: Biology*. 186:51-58.

Basavegowda, N., A. Idhayadhulla, and Y.R. Lee. 2014. Phyto-synthesis of gold nanoparticles using fruit extract of Hovenia dulcis and their biological activities. *Industrial Crops and Products*. 52:745-751.

Baselga, J., J. Albanell, M.A. Molina, and J. Arribas. 2001. Mechanism of action of trastuzumab and scientific update. *In* Seminars in oncology. Vol. 28. Elsevier. 4-11.

Basha, S.K., K. Govindaraju, R. Manikandan, J.S. Ahn, E.Y. Bae, and G. Singaravelu. 2010. Phytochemical mediated gold nanoparticles and their PTP 1B inhibitory activity. *Colloids and Surfaces B: Biointerfaces*. 75:405-409.

Bayraktar, S., A.M. Gutierrez-Barrera, D. Liu, T. Tasbas, U. Akar, J.K. Litton, E. Lin, C.T. Albarracin, F. Meric-Bernstam, and A.M. Gonzalez-Angulo. 2011. Outcome of triple-negative breast cancer in patients with or without deleterious BRCA mutations. *Breast cancer research and treatment*. 130:145-153.

Behera, M., and S. Ram. 2014. Inquiring the mechanism of formation, encapsulation, and stabilization of gold nanoparticles by poly (vinyl pyrrolidone) molecules in 1-butanol. *Applied Nanoscience*. 4:247-254.

Bergin, A.R.T., and S. Loi. 2019. Triple-negative breast cancer: recent treatment advances. *F1000Res*. 8.

Bindhu, M., and M. Umadevi. 2014. Silver and gold nanoparticles for sensor and antibacterial applications. *Spectrochimica Acta Part A: Molecular and Biomolecular Spectroscopy*. 128:37-45.

Bishayee, K., A. Paul, S. Ghosh, S. Sikdar, A. Mukherjee, R. Biswas, N. Boujedaini, and A.R. Khuda-Bukhsh. 2013. Condurango-glycoside-A fraction of Gonolobus condurango induces DNA damage associated senescence and apoptosis via ROS-dependent p53 signalling pathway in HeLa cells. *Mol Cell Biochem*. 382:173-183.

Boice Jr, J.D., D. Preston, F.G. Davis, and R.R. Monson. 1991. Frequent chest X-ray fluoroscopy and breast cancer incidence among tuberculosis patients in Massachusetts. *Radiation research*. 125:214-222.

Boissonneault, G.A., C.E. Elson, and M.W. Pariza. 1986. Net energy effects of dietary fat on chemically induced mammary carcinogenesis in F344 rats. *Journal of the National Cancer institute*. 76:335-338.

Bordoloi, D., K. Banik, R. Vikkurthi, K.K. Thakur, G. Padmavathi, B.L. Sailo, S. Girisa, A. Chinnathambi, T.A. Alahmadi, S.A. Alharbi, C. Buhrmann, M. Shakibaei, and A.B. Kunnumakkara. 2020. Inflection of Akt/mTOR/STAT-3 cascade in TNF-α induced protein 8 mediated human lung carcinogenesis. *Life Sci*. 262:118475.

Bordoloi, D., N. K Roy, J. Monisha, G. Padmavathi, and A. B Kunnumakkara. 2016. Multi-targeted agents in cancer cell chemosensitization: What we learnt from curcumin thus far. *Recent patents on anti-cancer drug discovery*. 11:67-97.

Bordoloi, D., and A.B. Kunnumakkara. 2018. The potential of curcumin: a multitargeting agent in cancer cell chemosensitization. *In* Role of nutraceuticals in cancer chemosensitization. Elsevier. 31-60.

Bordoloi, D., J. Monisha, M. Roy, G. Padmavathi, K. Banik, C. Harsha, H. Wang, A.P. Kumar, F. Arfuso, and A.B. Kunnumakkara. 2019. An investigation on the therapeutic potential of butein, a tretrahydroxychalcone against human oral squamous cell carcinoma. *Asian Pacific journal of cancer prevention: APJCP*. 20:3437.

Bosch, A., P. Eroles, R. Zaragoza, J.R. Viña, and A. Lluch. 2010. Triple-negative breast cancer: molecular features, pathogenesis, treatment and current lines of research. *Cancer treatment reviews*. 36:206-215.

Brasky, T.M., Y. Li, D.J. Jaworowicz, N. Potischman, C.B. Ambrosone, A.D. Hutson, J. Nie, P.G. Shields, M. Trevisan, and C.B. Rudra. 2013. Pregnancy-related characteristics and breast cancer risk. *Cancer Causes & Control*. 24:1675-1685.

Buhrmann, C., A.B. Kunnumakkara, A. Kumar, M. Samec, P. Kubatka, B.B. Aggarwal, and M. Shakibaei. 2021. Multitargeting Effects of Calebin A on Malignancy of CRC Cells in Multicellular Tumor Microenvironment. *Front Oncol*. 11:650603.

Burstein, M.D., A. Tsimelzon, G.M. Poage, K.R. Covington, A. Contreras, S.A. Fuqua, M.I. Savage, C.K. Osborne, S.G. Hilsenbeck, and J.C. Chang. 2015. Comprehensive Genomic Analysis Identifies Novel Subtypes and Targets of Triple-Negative Breast CancerIdentification of Four Unique Subtypes of TNBCs. *Clinical Cancer Research*. 21:1688-1698.

Buzea, C., I.I. Pacheco, and K. Robbie. 2007. Nanomaterials and nanoparticles: sources and toxicity. *Biointerphases*. 2:MR17-MR71.

Byrne, C., G. Ursin, C.F. Martin, J.D. Peck, E.B. Cole, D. Zeng, E. Kim, M.D. Yaffe, N.F. Boyd, and G. Heiss. 2017. Mammographic density change with estrogen and progestin therapy and breast cancer risk. *JNCI: Journal of the National Cancer Institute*. 109.

Byrski, T., J. Gronwald, T. Huzarski, E. Grzybowska, M. Budryk, M. Stawicka, T. Mierzwa, M. Szwiec, R. Wiśniowski, and M. Siolek. 2010. Pathologic complete response rates in young women with BRCA1-positive breast cancers after neoadjuvant chemotherapy. *Journal of Clinical Oncology*. 28:375-379.

Calle, E.E., and R. Kaaks. 2004. Overweight, obesity and cancer: epidemiological evidence and proposed mechanisms. *Nature Reviews Cancer*. 4:579-591.

Cao, L., and Y. Niu. 2020. Triple negative breast cancer: special histological types and emerging therapeutic methods. *Cancer Biol Med*. 17:293-306.

Carey, L.A., E.C. Dees, L. Sawyer, L. Gatti, D.T. Moore, F. Collichio, D.W. Ollila, C.I. Sartor, M.L. Graham, and C.M. Perou. 2007. The triple negative paradox: primary tumor chemosensitivity of breast cancer subtypes. *Clinical cancer research*. 13:2329-2334.

Cedervall, T., I. Lynch, M. Foy, T. Berggård, S.C. Donnelly, G. Cagney, S. Linse, and K.A. Dawson. 2007. Detailed identification of plasma proteins adsorbed on copolymer nanoparticles. *Angewandte Chemie International Edition*. 46:5754-5756.

Charafe-Jauffret, E., C. Ginestier, F. Iovino, J. Wicinski, N. Cervera, P. Finetti, M.-H. Hur, M.E. Diebel, F. Monville, and J. Dutcher. 2009. Breast cancer cell lines contain functional cancer stem cells with metastatic capacity and a distinct molecular signature. *Cancer research*. 69:1302-1313.

Chaturvedi, V.K., A. Singh, V.K. Singh, and M.P. Singh. 2019. Cancer Nanotechnology: A New Revolution for Cancer Diagnosis and Therapy. *Curr Drug Metab*. 20:416-429.

Chen, H., W. Lu, Y. Zhang, X. Zhu, J. Zhou, and Y. Chen. 2019. A Bayesian network meta-analysis of the efficacy of targeted therapies and chemotherapy for treatment of triple-negative breast cancer. *Cancer medicine*. 8:383-399.

Chen, J.-C., M.-C. Hsieh, S.-H. Lin, C.-C. Lin, Y.-T. Hsi, Y.-S. Lo, Y.-C. Chuang, M.-J. Hsieh, and M.-K. Chen. 2017. Coronarin D induces reactive oxygen species-mediated cell death in human nasopharyngeal cancer cells through inhibition of p38 MAPK and activation of JNK. *Oncotarget*. 8:108006.

Chen, R., J. Wu, H. Li, G. Cheng, Z. Lu, and C.-M. Che. 2010. Fabrication of gold nanoparticles with different morphologies in HEPES buffer. *Rare Metals*. 29:180-186.

Chimnoi, N., S. Pisutjaroenpong, L. Ngiwsara, D. Dechtrirut, D. Chokchaichamnankit, N. Khunnawutmanotham, C. Mahidol, and S.

Techasakul. 2008. Labdane diterpenes from the rhizomes of Hedychium coronarium. *Natural Product Research*. 22:1249-1256.

Chin, Y.R., T. Yoshida, A. Marusyk, A.H. Beck, K. Polyak, and A. Toker. 2014. Targeting Akt3 Signaling in Triple-Negative Breast CancerAkt3 in Triple-Negative Breast Cancer. *Cancer research*. 74:964-973.

Chithrani, B.D., A.A. Ghazani, and W.C. Chan. 2006. Determining the size and shape dependence of gold nanoparticle uptake into mammalian cells. *Nano letters*. 6:662-668.

Cho, E., W.Y. Chen, D.J. Hunter, M.J. Stampfer, G.A. Colditz, S.E. Hankinson, and W.C. Willett. 2006. Red meat intake and risk of breast cancer among premenopausal women. *Archives of internal medicine*. 166:2253-2259.

Choudhari, A.S., P.C. Mandave, M. Deshpande, P. Ranjekar, and O. Prakash. 2020. Phytochemicals in cancer treatment: From preclinical studies to clinical practice. *Frontiers in pharmacology*. 10:1614.

Choudhury, B., R. Kandimalla, R. Bharali, J. Monisha, A.B. Kunnumakara, K. Kalita, and J. Kotoky. 2016. Anticancer activity of Garcinia morella on T-cell murine lymphoma via apoptotic induction. *Frontiers in pharmacology*. 7:3.

Clegg, N.J., J. Wongvipat, J.D. Joseph, C. Tran, S. Ouk, A. Dilhas, Y. Chen, K. Grillot, E.D. Bischoff, and L. Cai. 2012. ARN-509: A Novel Antiandrogen for Prostate Cancer TreatmentDevelopment of Antiandrogen ARN-509. *Cancer research*. 72:1494-1503.

Clichici, S., L. David, B. Moldovan, I. Baldea, D. Olteanu, M. Filip, A. Nagy, V. Luca, C. Crivii, and P. Mircea. 2020a. Hepatoprotective effects of silymarin

coated gold nanoparticles in experimental cholestasis. *Materials Science and Engineering: C*. 115:111117.

Clichici, S., L. David, B. Moldovan, I. Baldea, D. Olteanu, M. Filip, A. Nagy, V. Luca, C. Crivii, P. Mircea, G. Katona, and G.A. Filip. 2020b. Hepatoprotective effects of silymarin coated gold nanoparticles in experimental cholestasis. *Mater Sci Eng C Mater Biol Appl*. 115:111117.

Cohen, L.A., K. Choi, and C.-X. Wang. 1988. Influence of dietary fat, caloric restriction, and voluntary exercise on N-nitrosomethylurea-induced mammary tumorigenesis in rats. *Cancer research*. 48:4276-4283.

Connor, E.E., J. Mwamuka, A. Gole, C.J. Murphy, and M.D. Wyatt. 2005. Gold nanoparticles are taken up by human cells but do not cause acute cytotoxicity. *Small*. 1:325-327.

Conway, K., S.N. Edmiston, L. Cui, S.S. Drouin, J. Pang, M. He, C.-K. Tse, J. Geradts, L. Dressler, and E.T. Liu. 2002. Prevalence and spectrum of p53 mutations associated with smoking in breast cancer. *Cancer research*. 62:1987-1995.

Corti, C., K. Venetis, E. Sajjadi, L. Zattoni, G. Curigliano, and N. Fusco. 2022. CAR-T cell therapy for triple-negative breast cancer and other solid tumors: preclinical and clinical progress. *Expert Opinion on Investigational Drugs*:1-13.

Cozza, G., P. Bonvini, E. Zorzi, G. Poletto, M.A. Pagano, S. Sarno, A. Donella-Deana, G. Zagotto, A. Rosolen, and L.A. Pinna. 2006. Identification of ellagic acid as

potent inhibitor of protein kinase CK2: a successful example of a virtual screening application. *Journal of medicinal chemistry*. 49:2363-2366.

Creighton, J.A., and D.G. Eadon. 1991. Ultraviolet–visible absorption spectra of the colloidal metallic elements. *Journal of the Chemical Society, Faraday Transactions*. 87:3881-3891.

Cui, Y., and T.E. Rohan. 2006. Vitamin D, calcium, and breast cancer risk: a review. *Cancer Epidemiology Biomarkers & Prevention*. 15:1427-1437.

Cunha, F.V.M., A.G. Coelho, P.S.d.S. Azevedo, A.A. da Silva, F.d.A. Oliveira, and L.C.C. Nunes. 2019. Systematic review and technological prospection: ethyl ferulate, a phenylpropanoid with antioxidant and neuroprotective actions. *Expert Opinion on Therapeutic Patents*. 29:73-83.

Daimary, U.D., D. Parama, V. Rana, K. Banik, A. Kumar, C. Harsha, and A.B. Kunnumakkara. 2021. Emerging roles of cardamonin, a multitargeted nutraceutical in the prevention and treatment of chronic diseases. *Curr Res Pharmacol Drug Discov*. 2:100008.

De Laurentiis, M., D. Cianniello, R. Caputo, B. Stanzione, G. Arpino, S. Cinieri, V. Lorusso, and S. De Placido. 2010. Treatment of triple negative breast cancer (TNBC): current options and future perspectives. *Cancer treatment reviews*. 36:S80-S86.

Dent, R., W.M. Hanna, M. Trudeau, E. Rawlinson, P. Sun, and S.A. Narod. 2009. Pattern of metastatic spread in triple-negative breast cancer. *Breast cancer research and treatment*. 115:423-428.

Dent, R., M. Trudeau, K.I. Pritchard, W.M. Hanna, H.K. Kahn, C.A. Sawka, L.A. Lickley, E. Rawlinson, P. Sun, and S.A. Narod. 2007. Triple-negative breast cancer: clinical features and patterns of recurrence. *Clinical cancer research*. 13:4429-4434.

Desmedt, C., B. Haibe-Kains, P. Wirapati, M. Buyse, D. Larsimont, G. Bontempi, M. Delorenzi, M. Piccart, and C. Sotiriou. 2008. Biological processes associated with breast cancer clinical outcome depend on the molecular subtypes. *Clinical cancer research*. 14:5158-5165.

Di Cello, F., V.L. Flowers, H. Li, B. Vecchio-Pagán, B. Gordon, K. Harbom, J. Shin, R. Beaty, W. Wang, and C. Brayton. 2013. Cigarette smoke induces epithelial to mesenchymal transition and increases the metastatic ability of breast cancer cells. *Molecular cancer*. 12:1-11.

Ding, Z., K. Sigdel, L. Yang, Y. Liu, M. Xuan, X. Wang, Z. Gu, J. Wu, and H. Xie. 2020. Nanotechnology-based drug delivery systems for enhanced diagnosis and therapy of oral cancer. *J Mater Chem B*. 8:8781-8793.

Dohrmann, R., K. Rüping, M. Kleber, K. Ufer, and R. Jahn. 2009. Variation of preferred orientation in oriented clay mounts as a result of sample preparation and composition. *Clays and Clay Minerals*. 57:686-694.

Dorgan, J.F., M.E. Reichman, J.T. Judd, C. Brown, C. Longcope, A. Schatzkin, W.S. Campbell, C. Franz, L. Kahle, and P.R. Taylor. 1994. The relation of reported alcohol ingestion to plasma levels of estrogens and androgens in premenopausal women (Maryland, United States). *Cancer Causes & Control*. 5:53-60.

Doval, D.C., A. Sharma, R. Sinha, K. Kumar, A.K. Dewan, H. Chaturvedi, U. Batra, V. Talwar, S.K. Gupta, and S. Singh. 2015. Immunohistochemical profile of breast cancer patients at a tertiary care hospital in New Delhi, India. *Asian Pacific Journal of Cancer Prevention*. 16:4959-4964.

Dreaden, E.C., A.M. Alkilany, X. Huang, C.J. Murphy, and M.A. El-Sayed. 2012. The golden age: gold nanoparticles for biomedicine. *Chemical Society Reviews*. 41:2740-2779.

Eisenhauer, E.A., W. ten Bokkel Huinink, K.D. Swenerton, L. Gianni, J. Myles, M. Van der Burg, I. Kerr, J.B. Vermorken, K. Buser, and N. Colombo. 1994. European-Canadian randomized trial of paclitaxel in relapsed ovarian cancer: high-dose versus low-dose and long versus short infusion. *Journal of clinical Oncology*. 12:2654-2666.

Elbialy, N., M. Abdelhamid, and T. Youssef. 2010. Low power argon laser-induced thermal therapy for subcutaneous Ehrlich carcinoma in mice using spherical gold nanoparticles. *Journal of biomedical nanotechnology*. 6:687-693.

Emens, L.A., C. Cruz, J.P. Eder, F. Braiteh, C. Chung, S.M. Tolaney, I. Kuter, R. Nanda, P.A. Cassier, and J.-P. Delord. 2019. Long-term clinical outcomes and biomarker analyses of atezolizumab therapy for patients with metastatic triple-negative breast cancer: a phase 1 study. *JAMA oncology*. 5:74-82.

Eroles, P., A. Bosch, J.A. Pérez-Fidalgo, and A. Lluch. 2012. Molecular biology in breast cancer: intrinsic subtypes and signaling pathways. *Cancer treatment reviews*. 38:698-707.

Escobar, P.F., J.R. Lurain, D.K. Singh, K. Bozorgi, and D.A. Fishman. 2003. Treatment of high-risk gestational trophoblastic neoplasia with etoposide, methotrexate, actinomycin D, cyclophosphamide, and vincristine chemotherapy☆. *Gynecologic oncology*. 91:552-557.

Esserman, L., C. Perou, M. Cheang, A. DeMichele, L. Carey, L. Van't Veer, J. Gray, E. Petricoin, K. Conway, and N. Hylton. 2009. Breast cancer molecular profiles and tumor response of neoadjuvant doxorubicin and paclitaxel: the I-SPY TRIAL (CALGB 150007/150012, ACRIN 6657). *Journal of Clinical Oncology*. 27:LBA515-LBA515.

Eustis, S., and M.A. el-Sayed. 2006. Why gold nanoparticles are more precious than pretty gold: noble metal surface plasmon resonance and its enhancement of the radiative and nonradiative properties of nanocrystals of different shapes. *Chem Soc Rev*. 35:209-217.

Eustis, S., H.-Y. Hsu, and M.A. El-Sayed. 2005. Gold nanoparticle formation from photochemical reduction of Au3+ by continuous excitation in colloidal solutions. A proposed molecular mechanism. *The Journal of Physical Chemistry B*. 109:4811-4815.

Evtyugin, D.D., S. Magina, and D.V. Evtuguin. 2020. Recent advances in the production and applications of ellagic acid and its derivatives. A review. *Molecules*. 25:2745.

Fan, M., J. Zhang, Z. Wang, B. Wang, Q. Zhang, C. Zheng, T. Li, C. Ni, Z. Wu, and Z. Shao. 2014. Phosphorylated VEGFR2 and hypertension: potential

biomarkers to indicate VEGF-dependency of advanced breast cancer in anti-angiogenic therapy. *Breast cancer research and treatment*. 143:141-151.

Fayaz, A.M., M. Girilal, S.A. Mahdy, S. Somsundar, R. Venkatesan, and P. Kalaichelvan. 2011. Vancomycin bound biogenic gold nanoparticles: a different perspective for development of anti VRSA agents. *Process biochemistry*. 46:636-641.

Feigelson, H.S., E.E. Calle, A.S. Robertson, P.A. Wingo, and M.J. Thun. 2001. Alcohol consumption increases the risk of fatal breast cancer (United States). *Cancer Causes & Control*. 12:895-902.

Fjällskog, M.-L., L. Frii, and J. Bergh. 1993. Is Cremophor EL, solvent for paclitaxel, cytotoxic? *The Lancet*. 342:873.

Fragoon, A., J. Li, J. Zhu, and J. Zhao. 2012. Biosynthesis of controllable size and shape gold nanoparticles by black seed (Nigella sativa) extract. *Journal of Nanoscience and Nanotechnology*. 12:2337-2345.

Fulford, L.G., J.S. Reis-Filho, K. Ryder, C. Jones, C.E. Gillett, A. Hanby, D. Easton, and S.R. Lakhani. 2007. Basal-like grade III invasive ductal carcinoma of the breast: patterns of metastasis and long-term survival. *Breast Cancer Research*. 9:1-11.

Ghosh, P., G. Han, M. De, C.K. Kim, and V.M. Rotello. 2008. Gold nanoparticles in delivery applications. *Advanced drug delivery reviews*. 60:1307-1315.

Giordano, S., A. Buzdar, and G. Hortobagyi. 2002. Male breast cancer. *Ann Intern Med*. 137:678-687.

Girisa, S., A. Kumar, V. Rana, D. Parama, U.D. Daimary, S. Warnakulasuriya, A.P. Kumar, and A.B. Kunnumakkara. 2021a. From Simple Mouth Cavities to Complex Oral Mucosal Disorders-Curcuminoids as a Promising Therapeutic Approach. *ACS Pharmacol Transl Sci*. 4:647-665.

Girisa, S., Q. Saikia, D. Bordoloi, K. Banik, J. Monisha, U.D. Daimary, E. Verma, K.S. Ahn, and A.B. Kunnumakkara. 2021b. Xanthohumol from Hop: Hope for cancer prevention and treatment. *IUBMB life*. 73:1016-1044.

Girisa, S., B. Shabnam, J. Monisha, L. Fan, C.E. Halim, F. Arfuso, K.S. Ahn, G. Sethi, and A.B. Kunnumakkara. 2019. Potential of Zerumbone as an Anti-Cancer Agent. *Molecules*. 24.

Godet, I., and D.M. Gilkes. 2017. BRCA1 and BRCA2 mutations and treatment strategies for breast cancer. *Integrative cancer science and therapeutics*. 4.

Goldhirsch, A., J.N. Ingle, R. Gelber, A. Coates, B. Thürlimann, and H.-J. Senn. 2009. Thresholds for therapies: highlights of the St Gallen International Expert Consensus on the primary therapy of early breast cancer 2009. *Annals of oncology*. 20:1319-1329.

Goldhirsch, A., E.P. Winer, A. Coates, R. Gelber, M. Piccart-Gebhart, B. Thürlimann, H.-J. Senn, K.S. Albain, F. André, and J. Bergh. 2013. Personalizing the treatment of women with early breast cancer: highlights of the St Gallen International Expert Consensus on the Primary Therapy of Early Breast Cancer 2013. *Annals of oncology*. 24:2206-2223.

Golombek, S.K., J.-N. May, B. Theek, L. Appold, N. Drude, F. Kiessling, and T. Lammers. 2018. Tumor targeting via EPR: Strategies to enhance patient responses. *Advanced drug delivery reviews*. 130:17-38.

Gomes, J.F., A.C. Garcia, E.B. Ferreira, C. Pires, V.L. Oliveira, G. Tremiliosi-Filho, and L.H. Gasparotto. 2015. New insights into the formation mechanism of Ag, Au and AgAu nanoparticles in aqueous alkaline media: alkoxides from alcohols, aldehydes and ketones as universal reducing agents. *Physical Chemistry Chemical Physics*. 17:21683-21693.

Govindachari, T., G. Suresh, G. Gopalakrishnan, and S. Wesley. 2000. Insect antifeedant and growth regulating activities of neem seed oil–the role of major tetranortriterpenoids. *Journal of applied Entomology*. 124:287-291.

Grant, B.F. 1997. Prevalence and correlates of alcohol use and DSM-IV alcohol dependence in the United States: results of the National Longitudinal Alcohol Epidemiologic Survey. *Journal of studies on alcohol*. 58:464-473.

Grem, J., K. Tutsch, K. Simon, D. Alberti, J. Willson, D. Tormey, S. Swaminathan, and D. Trump. 1987. Phase I study of taxol administered as a short iv infusion daily for 5 days. *Cancer treatment reports*. 71:1179-1184.

Guarneri, V., and P. Conte. 2009. Metastatic breast cancer: therapeutic options according to molecular subtypes and prior adjuvant therapy. *The oncologist*. 14:645-656.

Gucalp, A., S. Tolaney, S.J. Isakoff, J.N. Ingle, M.C. Liu, L.A. Carey, K. Blackwell, H. Rugo, L. Nabell, and A. Forero. 2013. Phase II Trial of Bicalutamide in Patients with Androgen Receptor–Positive, Estrogen Receptor–Negative

Metastatic Breast CancerBicalutamide in AR (+) ER/PgR (−) Metastatic Breast Cancer. *Clinical cancer research*. 19:5505-5512.

Gunn, A.R., B. Banos-Pinero, P. Paschke, L. Sanchez-Pulido, A. Ariza, J. Day, M. Emrich, D. Leys, C.P. Ponting, and I. Ahel. 2016. The role of ADP-ribosylation in regulating DNA interstrand crosslink repair. *Journal of Cell Science*. 129:3845-3858.

Gupta, S.C., S. Prasad, A.K. Tyagi, A.B. Kunnumakkara, and B.B. Aggarwal. 2017. Neem (Azadirachta indica): An indian traditional panacea with modern molecular basis. *Phytomedicine*. 34:14-20.

Hadi, M.A., M.A. Hassali, A.A. Shafie, and A. Awaisu. 2010. Evaluation of breast cancer awareness among female university students in Malaysia. *Pharmacy practice*. 8:29.

Haffty, B.G., Q. Yang, M. Reiss, T. Kearney, S.A. Higgins, J. Weidhaas, L. Harris, W. Hait, and D. Toppmeyer. 2006. Locoregional relapse and distant metastasis in conservatively managed triple negative early-stage breast cancer. *Journal of clinical oncology*. 24:5652-5657.

Haldar, S., P.B. Phapale, S.P. Kolet, and H.V. Thulasiram. 2013. Expedient preparative isolation, quantification and characterization of limonoids from Neem fruits. *Analytical Methods*. 5:5386-5391.

Halder, A., S. Das, D. Ojha, D. Chattopadhyay, and A. Mukherjee. 2018. Highly monodispersed gold nanoparticles synthesis and inhibition of herpes simplex virus infections. *Materials Science and Engineering: C*. 89:413-421.

Hamada, H., K. Ishihara, N. Masuoka, K. Mikuni, and N. Nakajima. 2006. Enhancement of water-solubility and bioactivity of paclitaxel using modified cyclodextrins. *Journal of bioscience and bioengineering*. 102:369-371.

Han, Y., X. Yu, S. Li, Y. Tian, and C. Liu. 2020. New perspectives for resistance to PARP inhibitors in triple-negative breast cancer. *Frontiers in Oncology*. 10:578095.

Harlow, S.D., and G.M. Matanoski. 1991. The association between weight, physical activity, and stress and variation in the length of the menstrual cycle. *American journal of epidemiology*. 133:38-49.

Hauck, T.S., A.A. Ghazani, and W.C. Chan. 2008. Assessing the effect of surface chemistry on gold nanorod uptake, toxicity, and gene expression in mammalian cells. *Small*. 4:153-159.

Haume, K., S. Rosa, S. Grellet, M.A. Śmiałek, K.T. Butterworth, A.V. Solov'yov, K.M. Prise, J. Golding, and N.J. Mason. 2016. Gold nanoparticles for cancer radiotherapy: a review. *Cancer nanotechnology*. 7:1-20.

He, X., and H. Lu. 2014. Graphene-supported tunable extraordinary transmission. *Nanotechnology*. 25:325201.

Heim, E., L. Valach, and L. Schaffner. 1997. Coping and psychosocial adaptation: Longitudinal effects over time and stages in breast cancer. *Psychosomatic Medicine*. 59:408-418.

Henamayee, S., K. Banik, B.L. Sailo, B. Shabnam, C. Harsha, S. Srilakshmi, N. Vgm, S.H. Baek, K.S. Ahn, and A.B. Kunnumakkara. 2020. Therapeutic emergence

of rhein as a potential anticancer drug: A review of its molecular targets and anticancer properties. *Molecules*. 25:2278.

Henson, D.E., L. Ries, L.S. Freedman, and M. Carriaga. 1991. Relationship among outcome, stage of disease, and histologic grade for 22,616 cases of breast cancer. The basis for a prognostic index. *Cancer*. 68:2142-2149.

Ho, M.Y., and J.R. Mackey. 2014. Presentation and management of docetaxel-related adverse effects in patients with breast cancer. *Cancer management and research*. 6:253.

Holmes, M.D., W.Y. Chen, D. Feskanich, C.H. Kroenke, and G.A. Colditz. 2005. Physical activity and survival after breast cancer diagnosis. *Jama*. 293:2479-2486.

Howe, G.R., and J. McLaughlin. 1996. Breast cancer mortality between 1950 and 1987 after exposure to fractionated moderate-dose-rate ionizing radiation in the Canadian fluoroscopy cohort study and a comparison with breast cancer mortality in the atomic bomb survivors study. *Radiation research*. 145:694-707.

Hsieh, M.-Y., M.-J. Hsieh, Y.-S. Lo, C.-C. Lin, Y.-C. Chuang, M.-K. Chen, and M.-C. Chou. 2020. Modulating effect of Coronarin D in 5-fluorouracil resistance human oral cancer cell lines induced apoptosis and cell cycle arrest through JNK1/2 signaling pathway. *Biomedicine & Pharmacotherapy*. 128:110318.

Hsu, C.-T., Y.-F. Huang, C.-P. Hsieh, C.-C. Wu, and T.-S. Shen. 2018. JNK inactivation induces polyploidy and drug-resistance in coronarin D-treated osteosarcoma cells. *Molecules*. 23:2121.

Hubalek, M., T. Czech, and H. Müller. 2017. Biological subtypes of triple-negative breast cancer. *Breast Care*. 12:8-14.

Iancu, G., D. Serban, C.D. Badiu, C. Tanasescu, M.S. Tudosie, C. Tudor, D.O. Costea, A. Zgura, R. Iancu, and D. Vasile. 2022. Tyrosine kinase inhibitors in breast cancer. *Experimental and Therapeutic Medicine*. 23:1-10.

Igene, H. 2008. Global health inequalities and breast cancer: an impending public health problem for developing countries. *The breast journal*. 14:428-434.

Inic, Z., M. Zegarac, M. Inic, I. Markovic, Z. Kozomara, I. Djurisic, I. Inic, G. Pupic, and S. Jancic. 2014. Difference between luminal A and luminal B subtypes according to Ki-67, tumor size, and progesterone receptor negativity providing prognostic information. *Clinical Medicine Insights: Oncology*. 8:CMO. S18006.

Innes, K.E., and T.E. Byers. 2004. First pregnancy characteristics and subsequent breast cancer risk among young women. *International journal of cancer*. 112:306-311.

ITOKAWA, H., H. MORITA, K. TAKEYA, and M. MOTIDOME. 1988. Diterpenes from rhizomes of Hedychium coronarium. *Chemical and pharmaceutical bulletin*. 36:2682-2684.

Iyer, A.K., G. Khaled, J. Fang, and H. Maeda. 2006. Exploiting the enhanced permeability and retention effect for tumor targeting. *Drug discovery today*. 11:812-818.

Jacquillat, C., M. Weil, F. Baillet, C. Borel, G. Auclerc, M. De Maublanc, M. Housset, G. Forget, L. Thill, and C. Soubrane. 1990. Results of neoadjuvant

chemotherapy and radiation therapy in the breast-conserving treatment of 250 patients with all stages of infiltrative breast cancer. *Cancer*. 66:119-129.

Jain, S., D.G. Hirst, and J.M. O'Sullivan. 2012. Gold nanoparticles as novel agents for cancer therapy. *Br J Radiol*. 85:101-113.

Jain, V., H. Kumar, H.V. Anod, P. Chand, N.V. Gupta, S. Dey, and S.S. Kesharwani. 2020. A review of nanotechnology-based approaches for breast cancer and triple-negative breast cancer. *J Control Release*. 326:628-647.

Jaman, M., and M. Sayeed. 2018. Ellagic acid, sulforaphane, and ursolic acid in the prevention and therapy of breast cancer: current evidence and future perspectives. *Breast Cancer*. 25:517-528.

Jiang, W., B. Kim, J.T. Rutka, and W.C. Chan. 2008. Nanoparticle-mediated cellular response is size-dependent. *Nature nanotechnology*. 3:145-150.

Johnson, K.C. 2005. Accumulating evidence on passive and active smoking and breast cancer risk. *International journal of cancer*. 117:619-628.

Johnson, K.C., A.B. Miller, N.E. Collishaw, J.R. Palmer, S.K. Hammond, A.G. Salmon, K.P. Cantor, M.D. Miller, N.F. Boyd, and J. Millar. 2011. Active smoking and secondhand smoke increase breast cancer risk: the report of the Canadian Expert Panel on Tobacco Smoke and Breast Cancer Risk (2009). *Tobacco control*. 20:e2-e2.

Juibari, M.M., L.P. Yeganeh, S. Abbasalizadeh, R. Azarbaijani, S.H. Mousavi, M. Tabatabaei, G.S. Jouzani, and G.H. Salekdeh. 2015. Investigation of a hot-spring extremophilic Ureibacillus thermosphaericus strain Thermo-BF for

extracellular biosynthesis of functionalized Gold nanoparticles. *Bionanoscience*. 5:233-241.

Kabeerdass, N., S. Kandasamy, G. Albasher, O. Alamri, N. Alsultan, S. Thangaswamy, and M. Mathanmohun. 2022. Limonia acidissima leaf mediated gold nanoparticles synthesis and their antimicrobial and wound healing properties. *Materials Letters*. 314:131893.

Kaikini, A.A., S. Muke, V. Peshattiwar, S. Bagle, V. Dighe, and S. Sathaye. 2021. Ethyl ferulate, a lipophilic phenylpropanoid, prevents diabetes-associated renal injury in rats by amelioration of hyperglycemia-induced oxidative stress via activation of nuclear factor erythroid 2-related factor 2. *Journal of Food Biochemistry*. 45:e13607.

Kakarala, M., L. Rozek, M. Cote, S. Liyanage, and D.E. Brenner. 2010. Breast cancer histology and receptor status characterization in Asian Indian and Pakistani women in the US-a SEER analysis. *BMC cancer*. 10:1-8.

Kalashgrani, M.Y., and N. Javanmardi. 2022. Multifunctional Gold nanoparticle: As novel agents for cancer treatment. *Advances in Applied NanoBio-Technologies*:1-6.

Kamani, M., U. Akgor, and M. Gültekin. 2022. Review of the literature on combined oral contraceptives and cancer.

Kaomongkolgit, R., K. Jamdee, S. Wongnoi, N. Chimnoi, and S. Techasakul. 2012. Antifungal activity of coronarin D against Candida albicans. *Oral surgery, oral medicine, oral pathology and oral radiology*. 114:61-66.

Kasthuri, J., S. Veerapandian, and N. Rajendiran. 2009a. Biological synthesis of silver and gold nanoparticles using apiin as reducing agent. *Colloids and Surfaces B: Biointerfaces*. 68:55-60.

Kasthuri, J., S. Veerapandian, and N. Rajendiran. 2009b. Biological synthesis of silver and gold nanoparticles using apiin as reducing agent. *Colloids Surf B Biointerfaces*. 68:55-60.

Kawai, M., K.E. Malone, M.T.C. Tang, and C.I. Li. 2014. Active smoking and the risk of estrogen receptor-positive and triple-negative breast cancer among women ages 20 to 44 years. *Cancer*. 120:1026-1034.

Kelly, K.L., E. Coronado, L.L. Zhao, and G.C. Schatz. 2003. The optical properties of metal nanoparticles: the influence of size, shape, and dielectric environment. Vol. 107. ACS Publications. 668-677.

Kennecke, H., R. Yerushalmi, R. Woods, M.C.U. Cheang, D. Voduc, C.H. Speers, T.O. Nielsen, and K. Gelmon. 2010. Metastatic behavior of breast cancer subtypes. *Journal of clinical oncology*. 28:3271-3277.

Kenney, L.B., Y. Yasui, P.D. Inskip, S. Hammond, J.P. Neglia, A.C. Mertens, A.T. Meadows, D. Friedman, L.L. Robison, and L. Diller. 2004. Breast cancer after childhood cancer: a report from the Childhood Cancer Survivor Study. *Annals of internal medicine*. 141:590-597.

Khan, M.A., V.K. Jain, M. Rizwanullah, J. Ahmad, and K. Jain. 2019. PI3K/AKT/mTOR pathway inhibitors in triple-negative breast cancer: a review on drug discovery and future challenges. *Drug Discovery Today*. 24:2181-2191.

Khan, M.M., S. Kalathil, T.H. Han, J. Lee, and M.H. Cho. 2013. Positively charged gold nanoparticles synthesized by electrochemically active biofilm—a biogenic approach. *Journal of Nanoscience and Nanotechnology*. 13:6079-6085.

Khatoon, E., K. Banik, C. Harsha, B.L. Sailo, K.K. Thakur, A.D. Khwairakpam, R. Vikkurthi, T.B. Devi, S.C. Gupta, and A.B. Kunnumakkara. 2020. Phytochemicals in cancer cell chemosensitization: Current knowledge and future perspectives. *In* Seminars in Cancer Biology. Elsevier.

Khlebtsov, N., and L. Dykman. 2011. Biodistribution and toxicity of engineered gold nanoparticles: a review of in vitro and in vivo studies. *Chemical Society Reviews*. 40:1647-1671.

Kohno, M., K. Musashi, H.O. Ikeda, T. Horibe, A. Matsumoto, and K. Kawakami. 2020. Oral administration of ferulic acid or ethyl ferulate attenuates retinal damage in sodium iodate-induced retinal degeneration mice. *Scientific reports*. 10:1-9.

Kourani, K., P. Jain, A. Kumar, A.K. Jangid, G. Swaminathan, V.R. Durgempudi, J. Jose, R. Reddy, D. Pooja, H. Kulhari, and L.D. Kumar. 2022. Inulin coated Mn(3)O(4) nanocuboids coupled with RNA interference reverse intestinal tumorigenesis in Apc knockout murine colon cancer models. *Nanomedicine*. 40:102504.

Krishnamurthy, S., A. Esterle, N.C. Sharma, and S.V. Sahi. 2014. Yucca-derived synthesis of gold nanomaterial and their catalytic potential. *Nanoscale Res Lett*. 9:627.

KS, U.S., K. Govindaraju, D. Prabhu, C. Arulvasu, V. Karthick, and N. Changmai. 2016. Anti-proliferative effect of biogenic gold nanoparticles against breast cancer cell lines (MDA-MB-231 & MCF-7). *Applied Surface Science*. 371:415-424.

Kubis, A. 1979. The cytotoxic effect of Tween 80 on Ehrlich ascites cancer cells in mice.

Kumar, A., A. Golani, and L.D. Kumar. 2020. EMT in breast cancer metastasis: an interplay of microRNAs, signaling pathways and circulating tumor cells. *Front. Biosci*. 25:979-1010.

Kumar, A., C. Harsha, D. Parama, S. Girisa, U.D. Daimary, X. Mao, and A.B. Kunnumakkara. 2021. Current clinical developments in curcumin-based therapeutics for cancer and chronic diseases. *Phytotherapy Research*. 35:6768-6801.

Kumar, A., A. Singam, G. Swaminathan, N. Killi, N.K. Tangudu, J. Jose, and L.D. Kumar. 2022. Combinatorial therapy using RNAi and curcumin nano-architectures regresses tumors in breast and colon cancer models. *Nanoscale*. 14:492-505.

Kumar, K.M., B.K. Mandal, M. Sinha, and V. Krishnakumar. 2012. Terminalia chebula mediated green and rapid synthesis of gold nanoparticles. *Spectrochimica Acta Part A: Molecular and Biomolecular Spectroscopy*. 86:490-494.

Kumar, S.S., C.S. Kumar, J. Mathiyarasu, and K.L. Phani. 2007. Stabilized gold nanoparticles by reduction using 3, 4-ethylenedioxythiophene-

polystyrenesulfonate in aqueous solutions: nanocomposite formation, stability, and application in catalysis. *Langmuir*. 23:3401-3408.

Kumari, M.M., and D. Philip. 2013. Facile one-pot synthesis of gold and silver nanocatalysts using edible coconut oil. *Spectrochimica Acta Part A: Molecular and Biomolecular Spectroscopy*. 111:154-160.

Kunnumakkara, A.B., K. Banik, D. Bordoloi, C. Harsha, B.L. Sailo, G. Padmavathi, N.K. Roy, S.C. Gupta, and B.B. Aggarwal. 2018. Googling the Guggul (Commiphora and Boswellia) for prevention of chronic diseases. *Frontiers in pharmacology*. 9:686.

Kunnumakkara, A.B., D. Bordoloi, G. Padmavathi, J. Monisha, N.K. Roy, S. Prasad, and B.B. Aggarwal. 2017. Curcumin, the golden nutraceutical: multitargeting for multiple chronic diseases. *Br J Pharmacol*. 174:1325-1348.

Kunnumakkara, A.B., A.S. Nair, K.S. Ahn, M.K. Pandey, Z. Yi, M. Liu, and B.B. Aggarwal. 2007. Gossypin, a pentahydroxy glucosyl flavone, inhibits the transforming growth factor beta-activated kinase-1-mediated NF-κB activation pathway, leading to potentiation of apoptosis, suppression of invasion, and abrogation of osteoclastogenesis. *Blood, The Journal of the American Society of Hematology*. 109:5112-5121.

Kunnumakkara, A.B., V. Rana, D. Parama, K. Banik, S. Girisa, S. Henamayee, K.K. Thakur, U. Dutta, P. Garodia, and S.C. Gupta. 2021. COVID-19, cytokines, inflammation, and spices: How are they related? *Life sciences*. 284:119201.

Lakhani, S.R., M.J. Van De Vijver, J. Jacquemier, T.J. Anderson, P.P. Osin, L. McGuffog, and D.F. Easton. 2002. The pathology of familial breast cancer:

predictive value of immunohistochemical markers estrogen receptor, progesterone receptor, HER-2, and p53 in patients with mutations in BRCA1 and BRCA2. *Journal of clinical oncology*. 20:2310-2318.

Lalloo, F., J. Varley, D. Ellis, A. Moran, L. O'Dair, P. Pharoah, D.G.R. Evans, and E.O.B.C.S. Group. 2003. Prediction of pathogenic mutations in patients with early-onset breast cancer by family history. *The Lancet*. 361:1101-1102.

Law, D.J. 1922. Synthetic tannins: Their synthesis, industrial products and application. By Georg Grasser. Translated by FGA Enna. Pp. vi+ 143.(London: Crosby Lockwood and Son. 1922.) Price 12s. net. Wiley Online Library.

Lee, J., D.K. Chatterjee, M.H. Lee, and S. Krishnan. 2014. Gold nanoparticles in breast cancer treatment: promise and potential pitfalls. *Cancer letters*. 347:46-53.

Lehmann, B.D., J.A. Bauer, X. Chen, M.E. Sanders, A.B. Chakravarthy, Y. Shyr, and J.A. Pietenpol. 2011. Identification of human triple-negative breast cancer subtypes and preclinical models for selection of targeted therapies. *The Journal of clinical investigation*. 121:2750-2767.

Lewinska, A., J. Adamczyk-Grochala, E. Kwasniewicz, A. Deregowska, and M. Wnuk. 2017. Diosmin-induced senescence, apoptosis and autophagy in breast cancer cells of different p53 status and ERK activity. *Toxicology Letters*. 265:117-130.

Li, D., W. Zhang, A.A. Sahin, and W.N. Hittelman. 1999. DNA adducts in normal tissue adjacent to breast cancer: a review. *Cancer detection and prevention*. 23:454-462.

Li, Y., H. Zhang, Y. Merkher, L. Chen, N. Liu, S. Leonov, and Y. Chen. 2022. Recent advances in therapeutic strategies for triple-negative breast cancer. *Journal of Hematology & Oncology*. 15:1-30.

Liedtke, C., C. Mazouni, K.R. Hess, F. André, A. Tordai, J.A. Mejia, W.F. Symmans, A.M. Gonzalez-Angulo, B. Hennessy, and M. Green. 2008. Response to neoadjuvant therapy and long-term survival in patients with triple-negative breast cancer. *Journal of clinical oncology*. 26:1275-1281.

Lim, Z.Z., J.E. Li, C.T. Ng, L.Y. Yung, and B.H. Bay. 2011. Gold nanoparticles in cancer therapy. *Acta Pharmacol Sin*. 32:983-990.

Lin, H.W., M.J. Hsieh, C.B. Yeh, K.C. Hsueh, Y.H. Hsieh, and S.F. Yang. 2018. Coronarin D induces apoptotic cell death through the JNK pathway in human hepatocellular carcinoma. *Environmental toxicology*. 33:946-954.

Lin, M.-c., and M.-c. Yin. 2013. Preventive effects of ellagic acid against doxorubicin-induced cardio-toxicity in mice. *Cardiovascular toxicology*. 13:185-193.

Lin, S.-X., J. Chen, M. Mazumdar, D. Poirier, C. Wang, A. Azzi, and M. Zhou. 2010. Molecular therapy of breast cancer: progress and future directions. *Nature Reviews Endocrinology*. 6:485-493.

Linos, E., W.C. Willett, E. Cho, and L. Frazier. 2010. Adolescent Diet in Relation to Breast Cancer Risk among Premenopausal WomenAdolescent Diet and Breast Cancer. *Cancer epidemiology, biomarkers & prevention*. 19:689-696.

Liu, Q.-s., R. Deng, S. Li, X. Li, K. Li, G. Kebaituli, X. Li, and R. Liu. 2017. Ellagic acid protects against neuron damage in ischemic stroke through regulating the ratio of Bcl-2/Bax expression. *Applied physiology, nutrition, and metabolism*. 42:855-860.

Liu, Q., X. Liang, M. Liang, R. Qin, F. Qin, and X. Wang. 2020. Ellagic acid ameliorates renal ischemic-reperfusion injury through NOX4/JAK/STAT signaling pathway. *Inflammation*. 43:298-309.

Liu, Y.T., M.J. Hsieh, J.T. Lin, G. Chen, C.C. Lin, Y.S. Lo, Y.C. Chuang, Y.T. Hsi, M.K. Chen, and M.C. Chou. 2019. Coronarin D induces human oral cancer cell apoptosis though upregulate JNK1/2 signaling pathway. *Environmental toxicology*. 34:513-520.

Lo, Y.-L., C.-S. Wang, Y.-C. Chen, T.-Y. Wang, Y.-H. Chang, C.-J. Chen, and C.-P. Yang. 2020. Mitochondrion-directed nanoparticles loaded with a natural compound and a microRNA for promoting cancer cell death via the modulation of tumor metabolism and mitochondrial dynamics. *Pharmaceutics*. 12:756.

Longley, D., and P. Johnston. 2005. Molecular mechanisms of drug resistance. *The Journal of Pathology: A Journal of the Pathological Society of Great Britain and Ireland*. 205:275-292.

Longmire, M., P.L. Choyke, and H. Kobayashi. 2008. Clearance properties of nano-sized particles and molecules as imaging agents: considerations and caveats.

Lorenzo, J.M., P.E. Munekata, P. Putnik, D.B. Kovačević, V. Muchenje, and F.J. Barba. 2019. Sources, chemistry, and biological potential of ellagitannins and ellagic acid derivatives. *Studies in Natural Products Chemistry*. 60:189-221.

Losso, J.N., R.R. Bansode, A. Trappey II, H.A. Bawadi, and R. Truax. 2004. In vitro anti-proliferative activities of ellagic acid. *The Journal of nutritional biochemistry*. 15:672-678.

Lundell, M., A. Mattsson, P. Karlsson, E. Holmberg, A. Gustafsson, and L.-E. Holm. 1999. Breast cancer risk after radiotherapy in infancy: a pooled analysis of two Swedish cohorts of 17,202 infants. *Radiation research*. 151:626-632.

Macacu, A., P. Autier, M. Boniol, and P. Boyle. 2015. Active and passive smoking and risk of breast cancer: a meta-analysis. *Breast cancer research and treatment*. 154:213-224.

Malhotra, G.K., X. Zhao, H. Band, and V. Band. 2010. Histological, molecular and functional subtypes of breast cancers. *Cancer biology & therapy*. 10:955-960.

Maqbool, M., F. Bekele, and G. Fekadu. 2022. Treatment Strategies Against Triple-Negative Breast Cancer: An Updated Review. *Breast Cancer: Targets and Therapy*. 14:15.

Mastropaolo, D., A. Camerman, Y. Luo, G.D. Brayer, and N. Camerman. 1995. Crystal and molecular structure of paclitaxel (taxol). *Proceedings of the National Academy of Sciences*. 92:6920-6924.

Mata, Y., E. Torres, M. Blazquez, A. Ballester, F. González, and J. Munoz. 2009. Gold (III) biosorption and bioreduction with the brown alga Fucus vesiculosus. *Journal of hazardous materials*. 166:612-618.

Mathew, A., V. Gajalakshmi, B. Rajan, V. Kanimozhi, P. Brennan, B. Mathew, and P. Boffetta. 2008. Anthropometric factors and breast cancer risk among urban and rural women in South India: a multicentric case–control study. *British Journal of Cancer*. 99:207-213.

Mattsson, A., B.-I. Rudén, P. Hall, N. Wilking, and L.E. Rutqvist. 1993. Radiation-induced breast cancer: long-term follow-up of radiation therapy for benign breast disease. *JNCI: Journal of the National Cancer Institute*. 85:1679-1685.

Mazurakova, A., M. Samec, L. Koklesova, K. Biringer, E. Kudela, R.K. Al-Ishaq, M. Pec, F.A. Giordano, D. Büsselberg, and P. Kubatka. 2022. Anti-prostate cancer protection and therapy in the framework of predictive, preventive and personalised medicine—comprehensive effects of phytochemicals in primary, secondary and tertiary care. *EPMA Journal*:1-26.

McPherson, K., C. Steel, and J. Dixon. 2000. ABC of breast diseases: breast cancer—epidemiology, risk factors, and genetics. *BMJ: British Medical Journal*. 321:624.

Metcalfe, K., A. Finch, A. Poll, D. Horsman, C. Kim-Sing, J. Scott, R. Royer, P. Sun, and S. Narod. 2009. Breast cancer risks in women with a family history of breast or ovarian cancer who have tested negative for a BRCA1 or BRCA2 mutation. *British journal of cancer*. 100:421-425.

Michels, K.B., A.P. Mohllajee, E. Roset-Bahmanyar, G.P. Beehler, and K.B. Moysich. 2007. Diet and breast cancer: a review of the prospective observational studies. *Cancer: Interdisciplinary International Journal of the American Cancer Society*. 109:2712-2749.

Momenimovahed, Z., and H. Salehiniya. 2019. Epidemiological characteristics of and risk factors for breast cancer in the world. *Breast Cancer: Targets and Therapy*. 11:151.

Monisha, J., G. Padmavathi, N.K. Roy, A. Deka, D. Bordoloi, A. Anip, and A. B Kunnumakkara. 2016. NF-κB blockers gifted by mother nature: Prospectives in cancer cell chemosensitization. *Current pharmaceutical design*. 22:4173-4200.

Montazeri, A., J. Sadighi, F. Farzadi, F. Maftoon, M. Vahdaninia, M. Ansari, A. Sajadian, M. Ebrahimi, S. Haghighat, and I. Harirchi. 2008. Weight, height, body mass index and risk of breast cancer in postmenopausal women: a case-control study. *BMC cancer*. 8:1-7.

Mukherjee, S., V. Sushma, S. Patra, A.K. Barui, M.P. Bhadra, B. Sreedhar, and C.R. Patra. 2012. Green chemistry approach for the synthesis and stabilization of biocompatible gold nanoparticles and their potential applications in cancer therapy. *Nanotechnology*. 23:455103.

Muralimanoharan, S.B., A. Kunnumakkara, B. Shylesh, K.H. Kulkarni, X. Haiyan, H. Ming, B.B. Aggarwal, G. Rita, and A.P. Kumar. 2009. Butanol fraction containing berberine or related compound from Nexrutine® inhibits NFκB

signaling and induces apoptosis in prostate cancer cells. *The Prostate*. 69:494-504.

Mushtaq, S., B.H. Abbasi, B. Uzair, and R. Abbasi. 2018. Natural products as reservoirs of novel therapeutic agents. *EXCLI journal*. 17:420.

Nair, A., A. Amalraj, J. Jacob, A.B. Kunnumakkara, and S. Gopi. 2019. Non-curcuminoids from turmeric and their potential in cancer therapy and anticancer drug delivery formulations. *Biomolecules*. 9:13.

Nambara, K., K. Niikura, H. Mitomo, T. Ninomiya, C. Takeuchi, J. Wei, Y. Matsuo, and K. Ijiro. 2016. Reverse size dependences of the cellular uptake of triangular and spherical gold nanoparticles. *Langmuir*. 32:12559-12567.

Nanda, R., L.Q. Chow, E.C. Dees, R. Berger, S. Gupta, R. Geva, L. Pusztai, K. Pathiraja, G. Aktan, and J.D. Cheng. 2016. Pembrolizumab in patients with advanced triple-negative breast cancer: phase Ib KEYNOTE-012 study. *Journal of Clinical oncology*. 34:2460.

Nazari, S.S., and P. Mukherjee. 2018. An overview of mammographic density and its association with breast cancer. *Breast cancer*. 25:259-267.

Neamatallah, T., N. El-Shitany, A. Abbas, B.G. Eid, S. Harakeh, S. Ali, and S. Mousa. 2020. Nano ellagic acid counteracts cisplatin-induced upregulation in OAT1 and OAT3: a possible nephroprotection mechanism. *Molecules*. 25:3031.

Neilson, J., and A. Gilchrist. 1968. Erosion by a stream of solid particles. *wear*. 11:111-122.

Nel, A., T. Xia, L. Madler, and N. Li. 2006. Toxic potential of materials at the nanolevel. *science*. 311:622-627.

Neuman, H.B., M. Morrogh, M. Gonen, K.J. Van Zee, M. Morrow, and T.A. King. 2010. Stage IV breast cancer in the era of targeted therapy: does surgery of the primary tumor matter? *Cancer: Interdisciplinary International Journal of the American Cancer Society*. 116:1226-1233.

Newman, D.J., and G.M. Cragg. 2016. Natural products as sources of new drugs from 1981 to 2014. *Journal of natural products*. 79:629-661.

Nishimura, R., T. Osako, Y. Okumura, M. Hayashi, Y. Toyozumi, and N. Arima. 2010. Ki-67 as a prognostic marker according to breast cancer subtype and a predictor of recurrence time in primary breast cancer. *Experimental and therapeutic medicine*. 1:747-754.

O'Reilly, E.A., L. Gubbins, S. Sharma, R. Tully, M.H.Z. Guang, K. Weiner-Gorzel, J. McCaffrey, M. Harrison, F. Furlong, and M. Kell. 2015. The fate of chemoresistance in triple negative breast cancer (TNBC). *BBA clinical*. 3:257-275.

Ohadi, M., H. Forootanfar, G. Dehghannoudeh, T. Eslaminejad, A. Ameri, M. Shakibaie, and A. Najafi. 2020. Biosynthesis of gold nanoparticles assisted by lipopeptide biosurfactant derived from Acinetobacter junii B6 and evaluation of its antibacterial and cytotoxic activities. *BioNanoScience*. 10:899-908.

Okobia, M.N., C.H. Bunker, F.E. Okonofua, and U. Osime. 2006. Knowledge, attitude and practice of Nigerian women towards breast cancer: a cross-sectional study. *World journal of surgical oncology*. 4:1-9.

Osguthorpe, D., and A. Hagler. 2011. Mechanism of androgen receptor antagonism by bicalutamide in the treatment of prostate cancer. *Biochemistry*. 50:4105-4113.

Padmavathi, G., S.R. Rathnakaram, J. Monisha, D. Bordoloi, N.K. Roy, and A.B. Kunnumakkara. 2015. Potential of butein, a tetrahydroxychalcone to obliterate cancer. *Phytomedicine*. 22:1163-1171.

Padmavathi, G., N.K. Roy, D. Bordoloi, F. Arfuso, S. Mishra, G. Sethi, A. Bishayee, and A.B. Kunnumakkara. 2017. Butein in health and disease: A comprehensive review. *Phytomedicine*. 25:118-127.

Paik, S., S. Shak, G. Tang, C. Kim, J. Baker, M. Cronin, F.L. Baehner, M.G. Walker, D. Watson, and T. Park. 2004. A multigene assay to predict recurrence of tamoxifen-treated, node-negative breast cancer. *New England Journal of Medicine*. 351:2817-2826.

Palmer, J.R., L.L. Adams-Campbell, D.A. Boggs, L.A. Wise, and L. Rosenberg. 2007. A prospective study of body size and breast cancer in black women. *Cancer Epidemiology Biomarkers & Prevention*. 16:1795-1802.

Pan, Y., A. Leifert, D. Ruau, S. Neuss, J. Bornemann, G. Schmid, W. Brandau, U. Simon, and W. Jahnen-Dechent. 2009. Gold nanoparticles of diameter 1.4 nm trigger necrosis by oxidative stress and mitochondrial damage. *small*. 5:2067-2076.

Pang, M., X. Xie, Y. Zhang, K.V. Laster, K. Liu, and D.J. Kim. 2022. Ethyl ferulate suppresses esophageal squamous cell carcinoma tumor growth through inhibiting the mTOR signaling pathway. *Frontiers in Oncology*. 11:780011.

Parama, D., M. Boruah, K. Yachna, V. Rana, K. Banik, C. Harsha, K.K. Thakur, U. Dutta, A. Arya, and X. Mao. 2020. Diosgenin, a steroidal saponin, and its analogs: Effective therapies against different chronic diseases. *Life sciences*. 260:118182.

Parker, J., A. Prat, M. Cheang, M. Lenburg, S. Paik, and C. Perou. 2009. Breast cancer molecular subtypes predict response to anthracycline/taxane-based chemotherapy. *Cancer Res*. 69:2019.

Parsa, P., M. Kandiah, N.M. Zulkefli, and H.A. Rahman. 2008. Knowledge and behavior regarding breast cancer screening among female teachers in Selangor, Malaysia. *Asian Pacific journal of cancer prevention*. 9:221-228.

Pascual, J., and N. Turner. 2019. Targeting the PI3-kinase pathway in triple-negative breast cancer. *Annals of Oncology*. 30:1051-1060.

Patra, S., B. Pradhan, R. Nayak, C. Behera, K.C. Panda, S. Das, M. Jena, and S.K. Bhutia. 2021. Apoptosis and autophagy modulating dietary phytochemicals in cancer therapeutics: Current evidences and future perspectives. *Phytother Res*. 35:4194-4214.

Pearson, A., E. Smyth, I.S. Babina, M.T. Herrera-Abreu, N. Tarazona, C. Peckitt, E. Kilgour, N.R. Smith, C. Geh, and C. Rooney. 2016. High-level clonal FGFR amplification and response to FGFR inhibition in a translational clinical trial. *Cancer discovery*. 6:838-851.

Pharoah, P.D., N.E. Day, S. Duffy, D.F. Easton, and B.A. Ponder. 1997. Family history and the risk of breast cancer: a systematic review and meta-analysis. *International journal of cancer*. 71:800-809.

Philip, D. 2010. Green synthesis of gold and silver nanoparticles using Hibiscus rosa sinensis. *Physica E: Low-Dimensional Systems and Nanostructures*. 42:1417-1424.

Piccart, M.J., M. Gore, W.T.B. Huinink, A. Van Oosterom, J. Verweij, J. Wanders, H. Frankli, M. Bayssas, and S. Kaye. 1995. Docetaxel: an active new drug for treatment of advanced epithelial ovarian cancer. *JNCI: Journal of the National Cancer Institute*. 87:676-681.

Pierce, J.P., L. Natarajan, B.J. Caan, B.A. Parker, E.R. Greenberg, S.W. Flatt, C.L. Rock, S. Kealey, W.K. Al-Delaimy, and W.A. Bardwell. 2007. Influence of a diet very high in vegetables, fruit, and fiber and low in fat on prognosis following treatment for breast cancer: the Women's Healthy Eating and Living (WHEL) randomized trial. *Jama*. 298:289-298.

Preston, D.L., A. Mattsson, E. Holmberg, R. Shore, N.G. Hildreth, and J.D. Boice Jr. 2002. Radiation effects on breast cancer risk: a pooled analysis of eight cohorts. *Radiation research*. 158:220-235.

Rajeshkumar, S. 2016. Anticancer activity of eco-friendly gold nanoparticles against lung and liver cancer cells. *Journal of Genetic Engineering and Biotechnology*. 14:195-202.

Rakha, E.A., M.E. El-Sayed, A.H. Lee, C.W. Elston, M.J. Grainge, Z. Hodi, R.W. Blamey, and I.O. Ellis. 2008a. Prognostic significance of Nottingham histologic grade in invasive breast carcinoma. *Journal of clinical oncology*. 26:3153-3158.

Rakha, E.A., M.E. El-Sayed, D.G. Powe, A.R. Green, H. Habashy, M.J. Grainge, J.F. Robertson, R. Blamey, J. Gee, and R.I. Nicholson. 2008b. Invasive lobular carcinoma of the breast: response to hormonal therapy and outcomes. *European journal of cancer*. 44:73-83.

Rakha, E.A., S.E. Elsheikh, M.A. Aleskandarany, H.O. Habashi, A.R. Green, D.G. Powe, M.E. El-Sayed, A. Benhasouna, J.-S. Brunet, and L.A. Akslen. 2009. Triple-negative breast cancer: distinguishing between basal and nonbasal subtypes. *Clinical Cancer Research*. 15:2302-2310.

Rakha, E.A., J.S. Reis-Filho, F. Baehner, D.J. Dabbs, T. Decker, V. Eusebi, S.B. Fox, S. Ichihara, J. Jacquemier, and S.R. Lakhani. 2010. Breast cancer prognostic classification in the molecular era: the role of histological grade. *Breast cancer research*. 12:1-12.

Rampurwala, M., K.B. Wisinski, and R. O'Regan. 2016. Role of the androgen receptor in triple-negative breast cancer. *Clinical advances in hematology & oncology: H&O*. 14:186.

Reuk-ngam, N., N. Chimnoi, N. Khunnawutmanotham, and S. Techasakul. 2014. Antimicrobial activity of coronarin D and its synergistic potential with antibiotics. *BioMed research international*. 2014.

Reynolds, P. 2013. Smoking and breast cancer. *Journal of mammary gland biology and neoplasia*. 18:15-23.

Ríos, J.-L., R.M. Giner, M. Marín, and M.C. Recio. 2018. A pharmacological update of ellagic acid. *Planta medica*. 84:1068-1093.

Robson, M., S.-A. Im, E. Senkus, B. Xu, S.M. Domchek, N. Masuda, S. Delaloge, W. Li, N. Tung, and A. Armstrong. 2017. Olaparib for metastatic breast cancer in patients with a germline BRCA mutation. *New England Journal of Medicine*. 377:523-533.

Román, M., M.J. Quintana, J. Ferrer, M. Sala, and X. Castells. 2017. Cumulative risk of breast cancer screening outcomes according to the presence of previous benign breast disease and family history of breast cancer: supporting personalised screening. *British journal of cancer*. 116:1480-1485.

Romieu, I. 2011. Diet and breast cancer. *Salud publica de Mexico*. 53:430-439.

Ronckers, C.M., C.A. Erdmann, and C.E. Land. 2004. Radiation and breast cancer: a review of current evidence. *Breast Cancer Research*. 7:1-12.

Rosenberg, L., D.A. Boggs, T.N. Bethea, L.A. Wise, L.L. Adams-Campbell, and J.R. Palmer. 2013. A prospective study of smoking and breast cancer risk among African-American women. *Cancer Causes & Control*. 24:2207-2215.

Ross, J.S., and J.A. Fletcher. 1998. The HER-2/neu oncogene in breast cancer: prognostic factor, predictive factor, and target for therapy. *Stem cells*. 16:413-428.

Ross, J.S., E.A. Slodkowska, W.F. Symmans, L. Pusztai, P.M. Ravdin, and G.N. Hortobagyi. 2009. The HER-2 receptor and breast cancer: ten years of targeted anti–HER-2 therapy and personalized medicine. *The oncologist*. 14:320-368.

Ross, R.K., A. Paganini-Hill, P.C. Wan, and M.C. Pike. 2000. Effect of hormone replacement therapy on breast cancer risk: estrogen versus estrogen plus progestin. *Journal of the National Cancer Institute*. 92:328-332.

Rouzier, R., C.M. Perou, W.F. Symmans, N. Ibrahim, M. Cristofanilli, K. Anderson, K.R. Hess, J. Stec, M. Ayers, and P. Wagner. 2005. Breast cancer molecular subtypes respond differently to preoperative chemotherapy. *Clinical cancer research*. 11:5678-5685.

Roy, A., S. Datta, K.S. Bhatia, P. Jha, and R. Prasad. 2021. Role of plant derived bioactive compounds against cancer. *South African Journal of Botany*.

Roy, N.K., D. Parama, K. Banik, D. Bordoloi, A.K. Devi, K.K. Thakur, G. Padmavathi, M. Shakibaei, L. Fan, G. Sethi, and A.B. Kunnumakkara. 2019. An Update on Pharmacological Potential of Boswellic Acids against Chronic Diseases. *Int J Mol Sci*. 20.

Saha, S.K., S. Sikdar, A. Mukherjee, K. Bhadra, N. Boujedaini, and A.R. Khuda-Bukhsh. 2013. Ethanolic extract of the Goldenseal, Hydrastis canadensis, has demonstrable chemopreventive effects on HeLa cells in vitro: Drug-DNA interaction with calf thymus DNA as target. *Environ Toxicol Pharmacol*. 36:202-214.

Scapagnini, G., D.A. Butterfield, C. Colombrita, R. Sultana, A. Pascale, and V. Calabrese. 2004. Ethyl ferulate, a lipophilic polyphenol, induces HO-1 and protects rat neurons against oxidative stress. *Antioxidants & redox signaling*. 6:811-818.

Schettino, M.R., M.A. Hernández-Valero, R. Moguel, R.A. Hajek, and L.A. Jones. 2006. Assessing breast cancer knowledge, beliefs, and misconceptions among Latinas in Houston, Texas. *Journal of Cancer Education*. 21.

Schneider, B.P., E.P. Winer, W.D. Foulkes, J. Garber, C.M. Perou, A. Richardson, G.W. Sledge, and L.A. Carey. 2008. Triple-negative breast cancer: risk factors to potential targets. *Clinical Cancer Research*. 14:8010-8018.

Seidman, H., M.H. Mushinski, S.K. Gelb, and E. Silverberg. 1985. Probabilities of eventually developing or dying of cancer--United States, 1985. *CA: A Cancer Journal for Clinicians*. 35:36-56.

Shabaninezhad, M., and G. Ramakrishna. 2019. Theoretical investigation of size, shape, and aspect ratio effect on the LSPR sensitivity of hollow-gold nanoshells. *The Journal of chemical physics*. 150:144116.

Shah, S.P., A. Roth, R. Goya, A. Oloumi, G. Ha, Y. Zhao, G. Turashvili, J. Ding, K. Tse, and G. Haffari. 2012. The clonal and mutational evolution spectrum of primary triple-negative breast cancers. *Nature*. 486:395-399.

Shankar, S.S., A. Rai, B. Ankamwar, A. Singh, A. Ahmad, and M. Sastry. 2004. Biological synthesis of triangular gold nanoprisms. *Nat Mater*. 3:482-488.

Sharma, B., A. Kalwar, N. Sharma, A. Kapoor, and N. Kumar. 2013. Five year retrospective survival analysis of triple negative breast cancer in North-West India. *Indian Journal of Cancer*. 50:330.

Sharma, M., J.D. Sharma, A. Sarma, S. Ahmed, A.C. Kataki, R. Saxena, and D. Sharma. 2014. Triple negative breast cancer in people of North East India: Critical insights gained at a regional cancer centre. *Asian Pacific Journal of Cancer Prevention*. 15:4507-4511.

Shen, M., H. Pan, Y. Chen, Y.H. Xu, W. Yang, and Z. Wu. 2020. A review of current progress in triple-negative breast cancer therapy. *Open Medicine*. 15:1143-1149.

Shi, J., P.W. Kantoff, R. Wooster, and O.C. Farokhzad. 2017. Cancer nanomedicine: progress, challenges and opportunities. *Nature reviews cancer*. 17:20-37.

Shiyanbola, O.O., R.F. Arao, D.L. Miglioretti, B.L. Sprague, J.M. Hampton, N.K. Stout, K. Kerlikowske, D. Braithwaite, D.S. Buist, and K.M. Egan. 2017. Emerging Trends in Family History of Breast Cancer and Associated RiskTrends in Family History of Breast Cancer. *Cancer epidemiology, biomarkers & prevention*. 26:1753-1760.

Sikdar, S., A. Mukherjee, S. Ghosh, and A.R. Khuda-Bukhsh. 2014. Condurango glycoside-rich components stimulate DNA damage-induced cell cycle arrest and ROS-mediated caspase-3 dependent apoptosis through inhibition of cell-proliferation in lung cancer, in vitro and in vivo. *Environmental Toxicology and Pharmacology*. 37:300-314.

Sikov, W.M., D.S. Dizon, R. Strenger, R.D. Legare, K.P. Theall, T.A. Graves, J.S. Gass, T.A. Kennedy, and M.A. Fenton. 2009. Frequent pathologic complete responses in aggressive stages II to III breast cancers with every-4-week carboplatin and weekly paclitaxel with or without trastuzumab: a Brown University Oncology Group Study. *Journal of Clinical Oncology*. 27:4693-4700.

Silver, D.P., A.L. Richardson, A.C. Eklund, Z.C. Wang, Z. Szallasi, Q. Li, N. Juul, C.-O. Leong, D. Calogrias, and A. Buraimoh. 2010. Efficacy of neoadjuvant

Cisplatin in triple-negative breast cancer. *Journal of clinical oncology*. 28:1145.

Silverman, J.A., and S.R. Deitcher. 2013. Marqibo®(vincristine sulfate liposome injection) improves the pharmacokinetics and pharmacodynamics of vincristine. *Cancer chemotherapy and pharmacology*. 71:555-564.

Singh, A.K., M. Talat, D. Singh, and O. Srivastava. 2010. Biosynthesis of gold and silver nanoparticles by natural precursor clove and their functionalization with amine group. *Journal of Nanoparticle Research*. 12:1667-1675.

Singh, Y.P., S. Girisa, K. Banik, S. Ghosh, P. Swathi, M. Deka, G. Padmavathi, J. Kotoky, G. Sethi, and L. Fan. 2019. Potential application of zerumbone in the prevention and therapy of chronic human diseases. *Journal of Functional Foods*. 53:248-258.

Singletary, S.E. 2003. Rating the risk factors for breast cancer. *Annals of surgery*. 237:474.

Smith-Warner, S.A., D. Spiegelman, S.-S. Yaun, P.A. Van Den Brandt, A.R. Folsom, R.A. Goldbohm, S. Graham, L. Holmberg, G.R. Howe, and J.R. Marshall. 1998. Alcohol and breast cancer in women: a pooled analysis of cohort studies. *Jama*. 279:535-540.

Smitha, S., D. Philip, and K. Gopchandran. 2009. Green synthesis of gold nanoparticles using Cinnamomum zeylanicum leaf broth. *Spectrochimica Acta Part A: Molecular and Biomolecular Spectroscopy*. 74:735-739.

Son, Y., Y. An, J. Jung, S. Shin, I. Park, J. Gwak, B.G. Ju, Y.H. Chung, M. Na, and S. Oh. 2019. Protopine isolated from Nandina domestica induces apoptosis

and autophagy in colon cancer cells by stabilizing p53. *Phytotherapy Research*. 33:1689-1696.

Song, Y., Q. Tian, Z. Huang, D. Fan, Z. She, X. Liu, X. Cheng, B. Yu, and Y. Deng. 2014. Self-assembled micelles of novel amphiphilic copolymer cholesterol-coupled F68 containing cabazitaxel as a drug delivery system. *International journal of nanomedicine*. 9:2307.

Sonnenschein, E., P. Toniolo, M.B. Terry, P.F. Bruning, I. Kato, K.L. Koenig, and R.E. Shore. 1999. Body fat distribution and obesity in pre-and postmenopausal breast cancer. *International journal of epidemiology*. 28:1026-1031.

Sparano, J.A., R.J. Gray, D.F. Makower, K.I. Pritchard, K.S. Albain, D.F. Hayes, C.E. Geyer Jr, E.C. Dees, E.A. Perez, and J.A. Olson Jr. 2015. Prospective validation of a 21-gene expression assay in breast cancer. *New England Journal of Medicine*. 373:2005-2014.

Spector, N.L., and K.L. Blackwell. 2009. Understanding the mechanisms behind trastuzumab therapy for human epidermal growth factor receptor 2–positive breast cancer. *Journal of Clinical Oncology*. 27:5838-5847.

Sreelakshmi, C., N. Goel, K. Datta, A. Addlagatta, R. Ummanni, and B. Reddy. 2013. Green synthesis of curcumin capped gold nanoparticles and evaluation of their cytotoxicity. *Nanoscience and Nanotechnology Letters*. 5:1258-1265.

Stadel, B., L. Webster, G. Rubin, J. Schlesselman, P. Wingo, Cancer, and S.H.S. Group. 1985. Oral contraceptives and breast cancer in young women. *The Lancet*. 326:970-973.

Stefansson, O.A., J.G. Jonasson, O.T. Johannsson, K. Olafsdottir, M. Steinarsdottir, S. Valgeirsdottir, and J.E. Eyfjord. 2009. Genomic profiling of breast tumours in relation to BRCAabnormalities and phenotypes. *Breast Cancer Research*. 11:1-14.

Storm, H.H., M. Andersson, J.D. Boice Jr, M. Blettner, M. Stovall, H.T. Mouridsen, P. Dombernowsky, C. Rose, A. Jacobsen, and M. Pedersen. 1992. Adjuvant radiotherapy and risk of contralateral breast cancer. *JNCI: Journal of the National Cancer Institute*. 84:1245-1250.

Su, Z., D. Xiao, F. Xie, L. Liu, Y. Wang, S. Fan, X. Zhou, and S. Li. 2021. Antibody–drug conjugates: Recent advances in linker chemistry. *Acta Pharmaceutica Sinica B*.

Suarasan, S., A. Campu, A. Vulpoi, M. Banciu, and S. Astilean. 2022. Assessing the Efficiency of Triangular Gold Nanoparticles as NIR Photothermal Agents In Vitro and Melanoma Tumor Model. *International Journal of Molecular Sciences*. 23:13724.

Sun, Y.-N., C.-D. Wang, X.-M. Zhang, L. Ren, and X.-H. Tian. 2011. Shape dependence of gold nanoparticles on in vivo acute toxicological effects and biodistribution. *Journal of nanoscience and nanotechnology*. 11:1210-1216.

Sun, Y.-S., Z. Zhao, Z.-N. Yang, F. Xu, H.-J. Lu, Z.-Y. Zhu, W. Shi, J. Jiang, P.-P. Yao, and H.-P. Zhu. 2017. Risk factors and preventions of breast cancer. *International journal of biological sciences*. 13:1387.

Sung, H., J. Ferlay, R.L. Siegel, M. Laversanne, I. Soerjomataram, A. Jemal, and F. Bray. 2021. Global cancer statistics 2020: GLOBOCAN estimates of

incidence and mortality worldwide for 36 cancers in 185 countries. *CA: a cancer journal for clinicians*. 71:209-249.

Swaminathan, G., A. Shigna, A. Kumar, V.V. Byroju, V.R. Durgempudi, and L. Dinesh Kumar. 2021. RNA interference and nanotechnology: A promising alliance for next generation cancer therapeutics. *Frontiers in Nanotechnology*. 3:42.

Sztandera, K., M. Gorzkiewicz, and B. Klajnert-Maculewicz. 2018. Gold nanoparticles in cancer treatment. *Molecular pharmaceutics*. 16:1-23.

Tan, Q.-G., and X.-D. Luo. 2011. Meliaceous limonoids: chemistry and biological activities. *Chemical reviews*. 111:7437-7522.

Tehard, B., and F. Clavel-Chapelon. 2006. Several anthropometric measurements and breast cancer risk: results of the E3N cohort study. *International journal of obesity*. 30:156-163.

Terry, P.D., and M. Goodman. 2006. Is the association between cigarette smoking and breast cancer modified by genotype? A review of epidemiologic studies and meta-analysis. *Cancer Epidemiology Biomarkers & Prevention*. 15:602-611.

Thakur, K.K., D. Bordoloi, and A.B. Kunnumakkara. 2018. Alarming burden of triple-negative breast cancer in India. *Clinical breast cancer*. 18:e393-e399.

Thakur, K.K., A. Kumar, K. Banik, E. Verma, E. Khatoon, C. Harsha, G. Sethi, S.C. Gupta, and A.B. Kunnumakkara. 2021. Long noncoding RNAs in triple-negative breast cancer: A new frontier in the regulation of tumorigenesis. *Journal of cellular physiology*. 236:7938-7965.

Thakur, P., R.K. Seam, M.K. Gupta, M. Gupta, M. Sharma, and V. Fotedar. 2017. Breast cancer risk factor evaluation in a Western Himalayan state: A case–control study and comparison with the Western World. *South Asian journal of cancer*. 6:106-109.

Thakur, V., and R.V. Kutty. 2019. Recent advances in nanotheranostics for triple negative breast cancer treatment. *Journal of Experimental & Clinical Cancer Research*. 38:1-22.

Thipe, V.C., K.P. Amiri, P. Bloebaum, A.R. Karikachery, M. Khoobchandani, K.K. Katti, S.S. Jurisson, and K.V. Katti. 2019. Development of resveratrol-conjugated gold nanoparticles: Interrelationship of increased resveratrol corona on anti-tumor efficacy against breast, pancreatic and prostate cancers. *International journal of nanomedicine*. 14:4413.

Tian, F., M.J. Clift, A. Casey, P. Del Pino, B. Pelaz, J. Conde, H.J. Byrne, B. Rothen-Rutishauser, G. Estrada, and J.M. De La Fuente. 2015. Investigating the role of shape on the biological impact of gold nanoparticles in vitro. *Nanomedicine*. 10:2643-2657.

Tian, Y.-F., C.-H. Chu, M.-H. Wu, C.-L. Chang, T. Yang, Y.-C. Chou, G.-C. Hsu, C.-P. Yu, J.-C. Yu, and C.-A. Sun. 2007. Anthropometric measures, plasma adiponectin, and breast cancer risk. *Endocrine-related cancer*. 14:669-677.

Turkevich, J., P.C. Stevenson, and J. Hillier. 1951. A study of the nucleation and growth processes in the synthesis of colloidal gold. *Discussions of the Faraday Society*. 11:55-75.

Turner, M., V.B. Golovko, O.P. Vaughan, P. Abdulkin, A. Berenguer-Murcia, M.S. Tikhov, B.F. Johnson, and R.M. Lambert. 2008. Selective oxidation with dioxygen by gold nanoparticle catalysts derived from 55-atom clusters. *Nature*. 454:981-983.

Turner, N., M.B. Lambros, H.M. Horlings, A. Pearson, R. Sharpe, R. Natrajan, F.C. Geyer, M. van Kouwenhove, B. Kreike, and A. Mackay. 2010. Integrative molecular profiling of triple negative breast cancers identifies amplicon drivers and potential therapeutic targets. *Oncogene*. 29:2013-2023.

Uzma, M., N. Sunayana, V.B. Raghavendra, C.S. Madhu, R. Shanmuganathan, and K. Brindhadevi. 2020. Biogenic synthesis of gold nanoparticles using Commiphora wightii and their cytotoxic effects on breast cancer cell line (MCF-7). *Process Biochemistry*. 92:269-276.

Vagia, E., D. Mahalingam, and M. Cristofanilli. 2020. The landscape of targeted therapies in TNBC. *Cancers*. 12:916.

Van De Rijn, M., C.M. Perou, R. Tibshirani, P. Haas, O. Kallioniemi, J. Kononen, J. Torhorst, G. Sauter, M. Zuber, and O.R. Köchli. 2002. Expression of cytokeratins 17 and 5 identifies a group of breast carcinomas with poor clinical outcome. *The American journal of pathology*. 161:1991-1996.

Van Gils, C.H., P.H. Peeters, H.B. Bueno-de-Mesquita, H.C. Boshuizen, P.H. Lahmann, F. Clavel-Chapelon, A. Thiébaut, E. Kesse, S. Sieri, and D. Palli. 2005. Consumption of vegetables and fruits and risk of breast cancer. *Jama*. 293:183-193.

Van Kiem, P., N.T.K. Thuy, H.L.T. Anh, N.X. Nhiem, C. Van Minh, P.H. Yen, N.K. Ban, D.T. Hang, B.H. Tai, and N. Van Tuyen. 2011. Chemical constituents of the rhizomes of Hedychium coronarium and their inhibitory effect on the pro-inflammatory cytokines production LPS-stimulated in bone marrow-derived dendritic cells. *Bioorganic & medicinal chemistry letters*. 21:7460-7465.

Vemuri, S.K., R.R. Banala, S. Mukherjee, P. Uppula, G. Subbaiah, G.R. AV, and T. Malarvilli. 2019. Novel biosynthesized gold nanoparticles as anti-cancer agents against breast cancer: Synthesis, biological evaluation, molecular modelling studies. *Materials Science and Engineering: C*. 99:417-429.

Verma, E., A. Kumar, U.D. Daimary, D. Parama, S. Girisa, G. Sethi, and A.B. Kunnumakkara. 2021. Potential of baicalein in the prevention and treatment of cancer: A scientometric analyses based review. *Journal of Functional Foods*. 86:104660.

Wang, C., S. Kar, X. Lai, W. Cai, F. Arfuso, G. Sethi, P.E. Lobie, B.C. Goh, L.H. Lim, and M. Hartman. 2018a. Triple negative breast cancer in Asia: An insider's view. *Cancer treatment reviews*. 62:29-38.

Wang, Z., L. Ma, M. Su, Y. Zhou, K. Mao, C. Li, G. Peng, C. Zhou, B. Shen, and J. Dou. 2018b. Baicalin induces cellular senescence in human colon cancer cells via upregulation of DEPP and the activation of Ras/Raf/MEK/ERK signaling. *Cell death & disease*. 9:1-17.

Watkins, E.J. 2019. Overview of breast cancer. *Journal of the American Academy of PAs*. 32:13-17.

Weiss, R.B., R. Donehower, P. Wiernik, T. Ohnuma, R. Gralla, D. Trump, J. Baker Jr, D. Van Echo, D. Von Hoff, and B. Leyland-Jones. 1990. Hypersensitivity reactions from taxol. *Journal of clinical oncology*. 8:1263-1268.

Wilkinson, L., and T. Gathani. 2022. Understanding breast cancer as a global health concern. *The British Journal of Radiology*. 95:20211033.

Wirapati, P., C. Sotiriou, S. Kunkel, P. Farmer, S. Pradervand, B. Haibe-Kains, C. Desmedt, M. Ignatiadis, T. Sengstag, and F. Schütz. 2008. Meta-analysis of gene expression profiles in breast cancer: toward a unified understanding of breast cancer subtyping and prognosis signatures. *Breast Cancer Research*. 10:1-11.

Wolf, I., S. Sadetzki, R. Catane, A. Karasik, and B. Kaufman. 2005. Diabetes mellitus and breast cancer. *The lancet oncology*. 6:103-111.

Wu, Y.-x., Y.-y. Wang, Z.-q. Gao, D. Chen, G. Liu, B.-b. Wan, F.-j. Jiang, M.-x. Wei, J. Zuo, and J. Zhu. 2021. Ethyl ferulate protects against lipopolysaccharide-induced acute lung injury by activating AMPK/Nrf2 signaling pathway. *Acta Pharmacologica Sinica*. 42:2069-2081.

Xie, J., Z. Yang, C. Zhou, J. Zhu, R.J. Lee, and L. Teng. 2016. Nanotechnology for the delivery of phytochemicals in cancer therapy. *Biotechnology advances*. 34:343-353.

Yang, X., D.L. Phillips, A.T. Ferguson, W.G. Nelson, J.G. Herman, and N.E. Davidson. 2001. Synergistic activation of functional estrogen receptor (ER)-α by DNA methyltransferase and histone deacetylase inhibition in human ER-α-negative breast cancer cells. *Cancer research*. 61:7025-7029.

Yanochko, G.M., and W. Eckhart. 2006. Type I insulin-like growth factor receptor over-expression induces proliferation and anti-apoptotic signaling in a three-dimensional culture model of breast epithelial cells. *Breast cancer research*. 8:1-13.

Yersal, O., and S. Barutca. 2014. Biological subtypes of breast cancer: Prognostic and therapeutic implications. *World journal of clinical oncology*. 5:412.

Yin, L., J.-J. Duan, X.-W. Bian, and S.-c. Yu. 2020. Triple-negative breast cancer molecular subtyping and treatment progress. *Breast Cancer Research*. 22:1-13.

Yousef, A.J.A. 2017. Male breast cancer: epidemiology and risk factors. *In* Seminars in oncology. Vol. 44. Elsevier. 267-272.

Yüce, A., A. Ateşşahin, A.O. Çeribaşı, and M. Aksakal. 2007. Ellagic acid prevents cisplatin-induced oxidative stress in liver and heart tissue of rats. *Basic & clinical pharmacology & toxicology*. 101:345-349.

Zhao, L., Y. Wang, Z. Li, Y. Deng, X. Zhao, and Y. Xia. 2019. Facile synthesis of chitosan-gold nanocomposite and its application for exclusively sensitive detection of Ag+ ions. *Carbohydrate polymers*. 226:115290.

Zheng, Z., L. Zhang, and X. Hou. 2022. Potential roles and molecular mechanisms of phytochemicals against cancer. *Food & Function*. 13:9208-9225.

Zhou, H., J. Liu, and Z. Chen. 2020. Coronarin D suppresses proliferation, invasion and migration of glioma cells via activating J

NK signaling pathway. *Pathology-Research and Practice*. 216:152789.

ABBREVIATIONS

BC:	Breast cancer
AAR:	Age Adjusted rate
ER:	Estrogen receptor
PR:	Progesterone receptor
HER2:	Human epidermal growth factor2
TNBC:	Triple negative breast cancer
VEGF-A:	Vascular endothelial growth factor A
EGFR:	Epidermal growth factor receptor
PARP:	Poly-ADP-ribose polymerase
mTOR:	Mammalian target of rapamycin
EPR:	Enhanced permeability and retention
LN:	Lymph node
SERMs:	Selective estrogen receptor modulators
AI:	Aromatase inhibitors
GATA3:	GATA Binding Protein 3
MKI67:	Marker of Proliferation Ki-67
GFR:	Glomerular filtration rate
pCR:	Pathological complete response
ADCC:	Antibody-dependent cell-mediated cytotoxicity
T-DM1:	Trastuzumab emtansine
EGF:	Epidermal growth factor
IHC:	Immunohistochemistry
FDA:	Food and drug administration
BRCA1/2:	Breast cancer gene 1 or 2
BL:	Basal like

IM:	Immunomodulatory
M:	Mesenchymal
MSL:	Mesenchymal stem like
AR:	Androgen receptor
LAR:	Luminal-AR
BLIS:	Basal-like immune-suppressed
BLIA:	basal-like immune-activated
MET:	Mesenchymal Epithelial Transition
EphA2:	Hepatocellular receptor tyrosine kinase class A2
NFκB:	Nuclear factor kappa B
STAT:	Signal transducer and activators
PDGF:	Platelet-derived growth factor
RNA:	Ribonucleic acid
BMI:	Body mass index
BBD:	Bladder bowl Dysfunction
VEGFR:	Vascular endothelial growth factor receptor
PI3K:	Phosphoinositide 3-kinase
AKT:	Ak strain transforming
PI3K:	Phosphoinositide 3-kinase
PD-L1:	Programmed death-ligand 1
PD-1	Programmed cell death protein-1
ACT:	Adoptive cell therapy
FGFR:	Fibroblast growth factor receptor inhibitor
ALDH1:	Aldehyde dehydrogenase 1
GSH:	glutathione

GST:	Glutathione-S-transferase
HCC:	hepatocellular carcinoma
MDA-MB	M.D. Anderson - Metastatic Breast
OP-B:	Ophiopogonin B
HCT:	Human colorectal carcinoma
MCF-7	Michigan Cancer Foundation-7
EF:	ethyl 4-hydroxy-3-methoxycinnamate
EA:	Ellagic acid
CD:	Coronarin D
EAZD:	Epoxy azadiradione
EF-AuNp:	Ethyl ferulate AuNp complex
EA-AuNp:	Ellagic acid AuNp complex
CD-AuNp:	Coronarin D AuNp complex
EAZD-AuNp:	Epoxy azadiradione AuNp complex
MTT:	3-(4, 5-dimethylthiazol-2-yl)-2, 5-diphenyl tetrazolium bromide
NCCS:	National Centre for Cell Sciences
DMEM:	Dulbecco's Modified Eagle Medium
PI:	Propidium iodide
XRD:	X-ray diffraction spectroscopy
EDX:	Energy dispersive X-ray analysis
SAED:	Selective area diffraction pattern
TEM:	Transmission electron spectroscopy
FT-IR:	Fourier Transform Infrared- Spectroscopy
FACS:	Fluorescence-activated cell sorting
HR-TEM:	High resolution transmission electron spectroscopy

ABBREVIATIONS

DMSO:	Dimethyl sulfoxide
FCC:	Face cantered cubic
SPR:	Surface plasmon resonance
LSPR:	Localised surface plasmon resonance
PBS:	Phosphate buffer saline
JNK:	Jun N-terminal Kinase

LIST OF FIGURES

characteristic peaks corresponding to standard face centers cubic lattice. In addition, the SAED pattern of EAZD-AuNp shows four diffraction rings corresponding to four different crystal planes. (C) Elemental analysis using EDX of the EAZD-AuNp revealing varied peaks for C, O, and Au. TEM images of EAZD-AuNp exhibited a triangular-like morphology at (D) 20 nm scale, (E) 10 nm scale, (F) the HR-TEM images of the EAZD-AuNp with the fringe spacing shown around 0.204 nm.

Figure 5.4: FT-IR graphs of EAZD-AuNp revealed peak shift at 1658cm-1 (CO group) from 1666cm-1 in EAZD, indicated the the involvement of carbonyl group in the bio reduction.

Figure 5.5: (A) Cytotoxic assay analysis representing anti-proliferative aspects of EA and EA-AuNp treatment in MDA-MB-231 cells in response to increasing concentrations of drug-treated for 24 and 72 hours, (B) Colony formation assay revealed the anti-clonogenic potential of EAZD and EAZD-AuNp with increasing drug concentrations (5 and 10 µg), (C) Quantification of the colony formation assay using the Image J software for both EAZD and EAZD-AuNp treatments.

Figure 5.6: (A-D) PI-FACS assay following the treatments of EA and EA-AuNp at concentration 5µg and 15µg for 72 hours, (D) Quantification of the PI-FACS assay revealed the induction of apoptosis by the treatment of EAZD and EAZD-AuNp, (E-G) Live dead assay to assess cell death of MDA-MB-231 breast cancer after treatment with EAZD and EAZD-AuNp at 10µg treatment. Images were taken at 10X magnification.

PUBLICATIONS

1. Jyothsna Unnikrishnan, Mangala Hegde, Aviral Kumar, Sosmitha Girisa, Priyadarshi Satpati, Ajaikumar B. Kunnumakkara (2022) **Phytofabrication and Characterization of Ethyl Ferulate Gold Nanoparticle and its Efficacy against Triple-Negative Breast Cancer Cells (Accepted in "Exploration of medicine")**

2. Jyothsna Unnikrishnan, Mangala Hegde, Sosmitha Girisa, Priyadarshi Satpati, Ajaikumar B. Kunnumakkara (2022) **Ellagic acid-gold nanoparticle complex as anticancer agent in TNBC cells (Communicated in "Exploration of targeted anti-tumor therapy").**

XXXXXXXXXXXX